# ULTRASONIC DESTRUCTION OF TRIHALOMETHANES:
# OPTIMIZATION OF SYSTEM PARAMETERS

by

## YONCA ERCÜMEN

**B. S. in Environmental Engineering, Yıldız Technical University, 1995**

**M. Sc. in Environmental Technology, Boğaziçi University, 1998**

**Submitted to the Institute of Environmental Sciences**

**In partial fulfillment of the requirements for the degree of**

**Doctor of Philosophy**

**Graduate Program in Environmental Technology**

**Boğaziçi University**

**2006**

# ACKNOWLEDGEMENTS

**ABSTRACT**

Disinfection of drinking waters is a major public health triumph of our age. However, while the pathogenic microorganisms provide the primary health risk from drinking water, chemical disinfection by-products also introduce an unintended health hazard. Trihalomethanes are the most common by-products of disinfection with chlorination. Due to their carcinogenic properties, removal of trihalomethanes from drinking water has become an important public health concern.

Research into the use of ultrasound in environmental protection has received a considerable amount of attention with the majority of investigations focusing on the harnessing of cavitational effects for the destruction of biological and chemical pollutants in water. Sonochemical removal of hydrophilic compounds has been investigated more than hydrophobic compounds.

In this study sonolytical removal of trihalomethanes from aqueous solutions has been investigated. Chloroform was selected as a model compound for the investigation of factors affecting sonolytical trihalomethanes removal. The sonolytical removal of chloroform was studied at three distinct frequencies and at different power densities. The effect of different sparging gases on chloroform removal was investigated using argon, air, nitrogen and oxygen. The effect of hydroxyl radical reactions on chloroform removal was investigated through the use of radical scavangers. The effect of trihalomethanes combinations on the removal rates of chloroform and bromoform were investigated. The results obtained from the model compound studies were compared with results obtained from tap water treatment studies. Finally, the effect of sonolysis on the acute toxicity of tap water was investigated using the Microtox test method.

# ÖZET

İçme sularının dezenfeksiyonu çağımızda elde edilmiş önemli bir halk sağlığı zaferidir. Ancak her ne kadar hastalık yapıcı microorganizmalar içme suyundan kaynaklanan birincil sağlık riskini oluşturmakta ise de, kimyasal dezenfeksiyon yan ürünleri beklenmeyen bir sağlık tehdidi oluşturmaktadır. Klorlama ile dezenfeksiyonun en sık karşılaşılan yan ürünleri trihalometanlardır. Kanserojen özellikleri sebebiyle trihalometanların içme sularından uzaklaştırılması önemli bir halk sağlığı konusu olmuştur.

Sesüstü dalgaların çevre koruması amacıyla kullanılmasına yönelik çalışmalar, özellikle sudaki biyolojik ve kimyasal kirleticilerin giderilmesi amacıyla kavitasyon etkisinin kontrol altına alınması üzerinde yoğunlaşmaktadır. Araştırmaların hidrofobik maddelerden çok hidrofilik maddelerin uzaklaştırılması üzerinde yoğunlaştığı görülmektedir.

Bu çalışmada trihalometanların sulu çözeltilerinden sesüstü dalgalar yardımıyla uzaklaştırılması incelenmiştir. Trihalometanların sesüstü dalgalar ile uzaklaştırılmasında etkili olan parametrelerin incelenmesinde model bileşik olarak kloroform kullanılmıştır. Kloroformun sonolitik yöntemle uzaklaştırılması üç ayrı frekansta ve değişik güç yoğunluklarında incelenmiştir. Farklı gazların kloroform giderilmesine etkisi argon, hava, azot ve oksijen kullanılarak incelenmiştir. Kloroform giderilmesinde hidroksil radikali reaksiyonlarının etkisi radikal tüketicisi maddeler yardımıyla incelenmiştir. Kloroform ve bromoform giderimine diğer trihalometanların etkisi ayrıca incelenmiştir. Model bileşik üzerinde yapılan çalışmalardan elde edilen sonuçlar çeşme suyu ile yapılan arıtma deneylerinde elde edilen sonuçlarla karşılaştırılmıştır. Son olarak sonolitik uygulamaların çeşme suyunun akut zehirliliği üzerindeki etkisi Microtox test yöntemi kullanılarak incelenmiştir.

# TABLE OF CONTENTS

# LIST OF TABLES

## LIST OF FIGURES

# LIST OF ABBREVIATIONS

| | |
|---|---|
| AOC | Assimilable organic carbon |
| AOT | Advanced oxidation techniques |
| BAA | Bromoacetic acid |
| CH | Chloral hydrate |
| DBA | Dibromoacetone |
| DBAN | Dibromoacetonitrile |
| DBPs | Disinfection byproducts |
| DCAA | Dichloroacetic acid |
| EC50 | Effective concentration, the concentration of a toxicant that affects 50% of the test organisms. |
| GC | Gas chromatography |
| IC | Inorganic carbon |
| ISTD | Internal standard |
| K | Equilibrium constant |
| k | Rate constant |
| MS | Mass spectrometry |
| NOM | Natural organic matter |
| NTU | Nephelometric turbidity unit |
| ORP | Oxidation-reduction potential |
| TC | Total carbon |
| TCAA | Trichloroacetic acid |
| THMs | Trihalomethanes |
| TOC | Total organic carbon |
| TOX | Total organic halide |
| TTHMs | Total trihalomethanes |
| USEPA | United States Environmental Protection Agency |
| UV | Ultraviolet |
| VOC | Volatile organic compounds |

# 1. INTRODUCTION

Drinking water disinfection was a major public health triumph of the 20th century. Before the widespread disinfection of drinking water, millions of people died from infectious waterborne diseases such as typhoid and cholera. However, following the use of chemical disinfection, starting in the early 1900s, deaths attributable to these waterborne pathogens virtually ceased in countries using disinfection. While pathogenic organisms provide the primary human health risk from drinking water, chemical disinfection by-products (DBPs) also introduce an unintended health hazard. Disinfectants, in addition to effectively killing harmful microorganisms, are powerful oxidants that oxidize organic matter naturally present in most surface waters (rivers, lakes, and many ground waters), forming DBPs. Reports of research results linking some DBPs to cancer formation in laboratory animals caused concern for these compounds and led to further studies conducted to determine the effect of DBPs on consumer health, collect information on their formation and various treatment/abatement possibilities. Chlorine is the most extensively used disinfectant in water treatment because of its efficiency, cost effectiveness and wide availability in various forms. It also has the advantage of leaving highly desirable residual disinfectant in the water that prevents microbial contamination before its use.

Power ultrasound, when applied to an elastic medium enhances chemical reactivity through the generation and destruction of cavitation bubbles. Like any wave, ultrasound is propagated through via a series of compression and rarefaction waves induced in the molecules of the medium through which it passes. At sufficiently high power, the rarefaction cycle may exceed the attractive forces of the molecules of liquid media and cavitation bubbles form. It is the fate of these cavities when they collapse in succeeding compression waves, which generates the energy for chemical and mechanical effects known as sonochemistry. The collapse is thought to generate very high local temperatures (around 5000 °C) and pressures (in excess of 1000 atm). In effect, sonication of a liquid produces a number of hot spots throughout the system. In these hot spots radicals of various origins form and subsequently undergo a series of radical reactions. Unlike other new technologies which require some special attribute of the system being activated such as the use of microwaves (requiring dipolar medium), electrochemistry (requiring

conducting medium) and photochemistry (requiring the presence of a chromophore) for chemical applications, ultrasound only requires the presence of a liquid to transmit its power.

Ultrasonic irradiation has been used for various industrial applications of enhancing reactions, synthesis, welding, disinfection, cleaning, catalysis etc. It is being used for environmental remediation for the removal of hydrophylic compounds, textiles dyes (Ince and Tezcanli-Guyer, 2004), phenolic wastes (Ince and Kidak, 2006), volatile compounds (Hoffmann, 1996) benzene, chlorobenzene etc. The application of ultrasonic irradiation for trihalomethanes (THM) removal is a new field which hasn't been studied in detail. THMs are volatile compounds found in micromolar concentrations in drinking water that can be expected to have low matrix-effect that may reduce efficiency, which may be a very successful application of ultrasonic applications in environmental remediation.

The objective of this study was to investigate the capacity of ultrasonic reaction systems as potential alternatives to the removal of trihalomethanes from chlorinated water. Chloroform was selected as a model compound to represent the THMs, and a significant fraction of the experimental work was carried out with chloroform solutions in deionized water to isolate the matrix effects in depicting reaction rate constants and optimizing system parameters. Three different ultrasonic generators and reactors each with varying energies and frequencies were used to investigate the effect of operational parameters known to influence ultrasonic treatment systems. The impacts of instrumental parameters such as power density, irradiation frequency and hydroxyl radical formation capacity, as well as operational parameters of initial solute concentration, purge gas type, effect of hydroxyl radical scavengers, and the presence of other trihalomethanes on the removal rate of chloroform were experimentally investigated. The parameters found were tested in drinking water samples. The effect of ultrasonic treatment on the acute toxicity of drinking water samples was also investigated

## 2. BACKGROUND

### 2.1 Disinfection

The purpose of disinfection is to prevent the spread of waterborne diseases. Communicable diseases were the curse of mankind since time immemorial. The intensity of the problem seems to heave been magnified as the density of the population increased. During the fourteenth century a plague known as "Black Death" swept over Europe killing 25 percent of the continent's population. An epidemic in London in the winter of 1664-1665 caused 70,000 deaths, 14 percent of the city's population. With the development of the industrial revolution, which attracted people to urban areas and caused them to live in more crowded conditions, the frequency of epidemics increased.

Disinfection refers to the selective destruction of disease-causing organisms. All the organisms are not destroyed during the process. This differentiates disinfection from sterilization, which is the destruction of all organisms. Disinfection in water and wastewater involves the exposure of disease-causing organisms in water to some destructive agent.

Four mechanisms have been proposed to explain the action of disinfectants; damage to the cell wall, alteration of cell permeability, alteration of the colloidal nature of the protoplasm, and inhibition of enzyme activity (Tchobanoglous and Burton, 1991).

Damage or destruction of the cell wall will result in cell lysis and death. Some agents such as penicillin inhibit the synthesis of cell wall. Agents such as phenolic compounds or detergents alter the permeability of cytoplasmic membrane. These substances destroy the selective permeability of the membrane and allow vital nutrients such as nitrogen and phosphorus to escape. Heat, radiation and highly acidic or alkaline agents alter the colloidal nature of the protoplasm. Heat coagulates the cell proteins, and acids and bases denature proteins, producing a lethal effect. Another mode of disinfection is the inhibition of enzyme activity. Oxidizing agents, such as chlorine, can alter the

chemical arrangement of enzymes and deactivate these vital proteins (Tchobanoglous and Burton, 1991).

### 2.1.1. Methods of Disinfection

Methods and means that have been used for disinfection include;

- The addition of chemicals
- The application of physical agents (such as heat and light)
- Mechanical means

2.1.1.1. The Addition of Chemicals. The exposure to chemical agents is the most common method used throughout the world (Tchobanoglous and Schroeder, 1985). Some desired properties of chemical disinfectants and the actual characteristics of a group of commonly used disinfectants are given in Table 2.1.

Table 2.1. Some desired properties of chemical disinfectants and the actual characteristics of a group of commonly used disinfectants (Tchobanoglous and Burton, 1991).

| Characteristic | Desired | Chlorine | Sodium hypochlorite | Ozone | UV Irradiation |
|---|---|---|---|---|---|
| Toxicity to microorganisms | High | High | High | High | High |
| Solubility | High | Slight | High | High | N/A |
| Stability in time | High | Stable | Slightly unstable | Unstable | Unstable |
| Nontoxic to higher forms of life | Nontoxic | Toxic | Toxic | Toxic | Toxic |
| Homogeneity | Homogenous | Homogenous | Homogenous | Homogenous | Homogenous |
| Toxicity at ambient temperatures | High | High | High | High | High |
| Corrosivity | Noncorrosive | Highly corrosive | Corrosive | Highly corrosive | N/A |
| Availability and cost | Low cost | Low cost | Moderately low | Moderately high cost | Moderately high cost |

N/A: Not Applicable

1) Chlorination

Chlorination is the most commonly used water disinfection method throughout the world. Chlorine is used in the form of free chlorine or as hypochlorites. In either form it acts as a potent oxidizing agent and often dissipates itself in side reactions so rapidly that little disinfection is accomplished until amounts in excess of the chlorine demand have been added.

Chlorine combines with water to form hypochlorous and hydrochloric acids.

$$Cl_2 + H_2O \Leftrightarrow HOCl + H^+ + Cl^- \qquad K = 4 \times 10^{-4} \text{ (at 25 °C)} \qquad (2.1)$$

In dilute solution and at pH levels above about four, the equilibrium shown above is displaced greatly to the right, and very little $Cl_2$ exists as such in solution. The hypochlorous acid formed is a weak acid and is poorly dissociated at pH levels below 6 (Sawyer and McCarty, 1978).

$$HOCl \Leftrightarrow H^+ + OCl^- \qquad K = 2.7 \times 10^{-8} \text{ (at 20 °C)} \qquad (2.2)$$
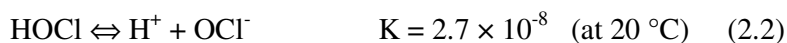
The hypochlorite ion forms hydrochloric acid and atomic oxygen.

$$OCl^- \Leftrightarrow Cl^- + O \qquad (2.3)$$

Hypochlorous acid and hypochlorite ions have distinctive behavior regarding disinfection. Whereas hypochlorous acid is readily reactive and is a stronger disinfectant than hypochlorite, hypochlorite achieves disinfection through the disinfectant properties of atomic oxygen. The disinfection properties of chlorine in water are based on the oxidizing power of free oxygen atoms and on chlorine substitution reactions. When enzymes come into contact with chlorine, one or more of the hydrogen atoms in the molecule are replaced by chlorine. This causes the entire enzyme structure to change shape or fall apart (Morris, 1975).

Being highly active oxidizers, chlorine and hypochlorous acid react with a wide variety of substances in water, including ammonia. Ammonium ion exists in equilibrium with ammonia and hydrogen ion.

$$NH_4^+ \Leftrightarrow NH_3 + H^+ \qquad\qquad K = 5.7 \times 10\text{ -10} \quad (2.4)$$

Chlorine and hypochlorous acid react with ammonia in water if available, to form monochloramines, dichloramines and trichloramines, depending upon the relative amounts of each and to some extent on the pH.

$$NH_3 + HOCl \rightarrow NH_2Cl + H_2O \qquad \text{(monochloramine)} \quad (2.5)$$

$$NH_2Cl + HOCl \rightarrow NHCl_2 + H_2O \qquad \text{(dichloramine)} \quad (2.6)$$

$$NHCl_2 + HOCl \rightarrow NCl_3 + H_2O \qquad \text{(trichloramine)} \quad (2.7)$$

With mole ratios of chlorine to ammonia up to 1:1, both mono- and dichloroamines are formed. The relative amounts of each are a function of the pH, which affects the relative rate of formation of the two species as well as the thermodynamic equilibrium between them. Greater proportions of dichloramine appear at lower pH values. Further increases in the mole ratio of chlorine to ammonia result in formation of some trichloramine and oxidation of part of the ammonia to $N_2$ or $NO_3^-$.

The mono- and dichloramines have significant disinfecting power and are therefore of interest. It has become common practice to refer to chlorine, hypochlorous acid and hypochlorite ion as free chlorine residuals, and the chloramines are called combined chlorine residuals. Research has shown that with free chlorine residuals, a lower pH, which favors the formation of HOCl over OCl⁻, is more effective for disinfection. Research has also shown that a greater concentration of combined chlorine residual than of free chlorine residual is required to achieve a given kill in a specified time. For these reasons it is important to know both the concentration and the kind of chlorine residual acting in order to evaluate any particular disinfection process. While free chlorine residuals have good disinfecting powers, they dissipate quickly in the distribution systems through other

oxidation reactions. For this reason, final treatment with ammonia is often practiced to convert free chlorine residuals to longer lasting combined chlorine residuals (Sawyer and McCarty, 1978).

Chlorination of water to the extent that all the ammonia is converted to $N_2$ or a higher oxidation state is referred to as "breakpoint chlorination", after which point all dissolved chlorine exists as free available hypochlorous acid or hypochlorite ion. The amount of chlorine required to reach breakpoint depends upon the amount of ammonia present.
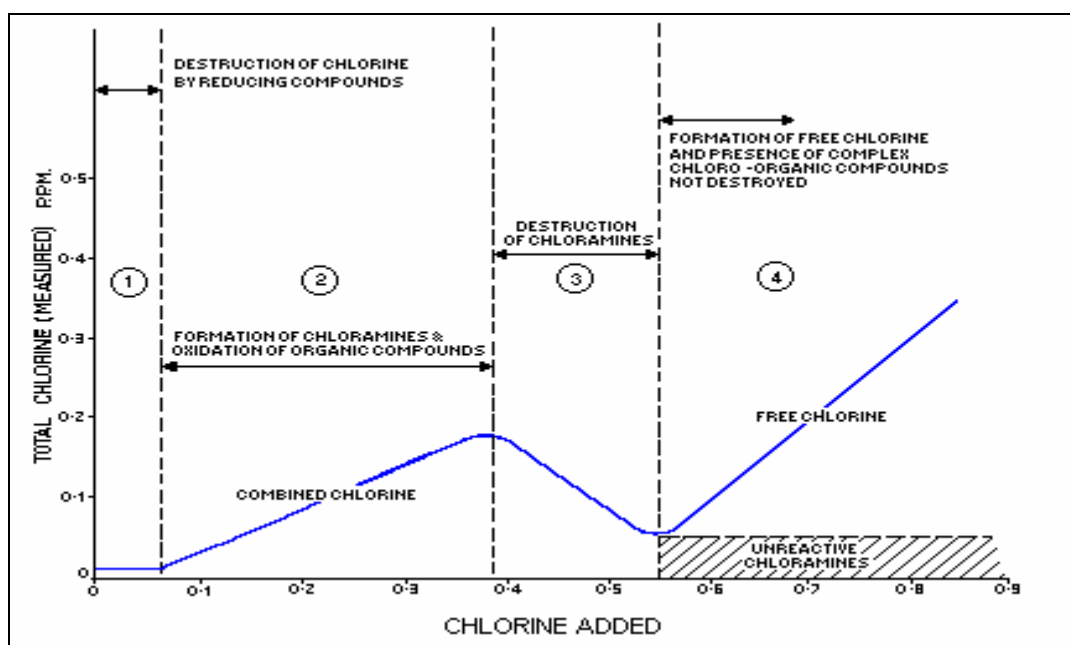


Figure 2.1. Breakpoint chlorination curve
(http://education.qld.gov.au/corporate/doem/forms/am-02b.doc)

For many years the addition of chlorine to drinking water was thought to be sufficient treatment for obtaining healthy drinking water. However chlorine can readily react with naturally occurring organic matter (NOM) in water to form disinfection by-products. Although sporadic reports of the presence of chloroform and other trihalomethanes in finished drinking water occurs before 1974, the reports of Rook, Bellar, Lichtenberg and Kroner clearly demonstrated that these contaminants were formed during the water treatment process as a result of chlorination (Rook, 1974). Trihalomethanes in

drinking water had more often than not escaped detection until 1974 because the analytical techniques used to measure the organic content of water were unable to detect them. Once discovered however, extensive research began to determine if their presence in drinking water was a hazard for consumers which led to the identification of other disinfection by-products (Symons et al., 1981). Hundreds of disinfection by-products have been identified and new compounds are still being discovered (Gong et al., 2005; Richardson, 2003). According to one estimation 77 per cent of organohalogen compounds formed during chlorination were trihalomethanes, 15 per cent were haloacetic acids, three per cent were halonitriles, four per cent were trichloro acetaldehyde hydrate and one per cent were other compounds (Biziuk and Przyjazny, 1996). The formation, occurrence and impact of these compounds are discussed further in section 2.2 of this study.

2) Ozonation

Ozone has been applied for water disinfection purposes for almost a century. A survey conducted in Switzerland among water works that apply ozonation techniques has shown that for 90 per cent of these plants the main reason for ozone usage was disinfection (Courbat et al., 1999).

Ozone is an excellent disinfectant and is able to inactivate even more resistant pathogenic microorganisms such as protozoa (e.g. Cryptosporidium parvum oocysts) where conventional disinfectants (i.e. chlorine) fail. However, the ozone exposure required to inactivate these microorganisms is quite high. This may lead to the formation of excess concentrations of undesired disinfection by-products, which are in particular aldehydes, carboxylic acids and ketones (Richardson et al., 1999). On the other hand, ozonation of bromide-containing waters can produce brominated DBPs including bromate ($BrO_3^-$), bromoform ($CHBr_3$), bromoacetic acids (BAA), dibromoacetone (DBA), and dibromoacetonitrile (DBAN). Ozonation of drinking water transforms natural organic matter into a more biodegradable form. This can cause significant bacterial regrowth in the distribution system, if biodegradable organic matter is not removed by subsequent treatment steps (Huang et al., 2005). Bromate, which is considered to be a potential human carcinogen, is particularly problematic because unlike many other organic by-products, it

is not biodegraded in biological filters which usually follow an ozonation step (von Gunten, 2003).

3) Other Chemical Disinfectants

Chlorine dioxide is about as effective an oxidizing agent as hypochlorous acid and is a particularly good disinfectant at high pH values. It does not combine with ammonia to produce chloramines nor does it combine with natural organic matter to form trihalomethanes. Another advantage of chlorine dioxide is that it is effective in the destruction of phenolic compounds that combine with other types of chlorine to create the undesirable taste-producing chlorinated phenols.

However, chlorine dioxide is an unstable gas and so is usually produced at the site where it is used. The more extensive use of chlorine dioxide in water treatment has been hampered by both the lack of suitable test for residual measurement and by its comparatively high cost (Sawyer and McCarty, 1978).

In aqueous systems where ammonia nitrogen and organic nitrogen compounds are present, chlorine reacts with both to form chloramines. Organic chloramines have poor germicidal properties, which makes their formation undesirable during chlorination (Donnermair and Blatchley, 2003)

Inorganic mono-, di- and trichloramines were also shown to demonstrate germicidal effects. Inorganic combined chlorine, predominantly in the form of monochloramine, is used in water treatment as a disinfectant. It generally is not as potent as free chlorine in terms of disinfection efficacy against planktonic organisms, but provides a relatively stable disinfecting residual that can be maintained over a relatively long period of time during and after chlorination.

2.1.1.2. The Application of Physical Agents.

1) Heat

Thermal disinfection of water is obtained by heating water to very high temperatures. It is mostly used in the beverage and dairy industry, but it is not a feasible means of disinfecting large quantities of wastewater because of the high cost. Water temperatures with a threshold of approximately $50^{o}$C considerably increase the inactivation rate of bacteria induced by thermal ways whereas the inactivation rate of viruses steadily increases with temperatures in the range of 20-50$^{o}$C. The recorded synergetic effects of solar radiation and thermal water treatment favour a combined use of these two water-treatment processes (Wegelin et al., 1994).

2) Ultraviolet Irradiation

Application of ultraviolet rays have been used successfully to sterilize small quantities of water. The efficiency of the process depends on the penetration of the rays into water. The contact geometry between the ultraviolet light source and water is extremely important because suspended matter, dissolved organic molecules and water itself, as well as the microorganisms, will absorb the radiation. It is therefore difficult to use ultraviolet irradiation in aqueous systems, especially when large amounts of particulate matter are present (Qualls and Johnson, 1983).

Disinfection of drinking water by ultraviolet radiation does not produce toxic chlorinated organic chemicals as does chlorination. The germicidal effectiveness of UV radiation is in the 180-320 nm region, with the optimum at 265 nm. A low-pressure mercury arc is effective for germicidal applications because 95% of the energy radiated by this source is at the 253.7 nm line. When microorganisms are subjected to UV radiation, they are not all inactivated at once, but a constant fraction of the present living number dies in each increment of time. With viruses inactivation usually occurs with one hit. However, with bacteria a shouldered survival curve is seen; meaning that more than one hit is necessary for inactivation, or that reactivation mechanisms are opposing the UV inactivation. Destruction of a microorganism is the result of UV radiation hitting one or

more targets such as DNA, RNA, or enzymes. Those microorganisms which are more resistant to inactivation are algae, gram-positive bacteria, and spore-forming bacteria. A microorganism may be spared if it is shaded by another particle during UV exposure. UV radiation can act as a catalyst in oxidation reactions with ozone or hydrogen peroxide to decrease the total inorganic carbon. The more turbid the water to be treated, the more radiation intensity is required. Lamps should not be immersed in the water. The decrease of radiation intensity with lamp age needs to be considered. One disadvantage of UV disinfection is that the destroyed organisms are not removed from the treated water. (Meulemans, 1987).

3) γ-Irradiation

Because of their high penetration, power gamma rays have been used to disinfect both water and wastewater. A high power-energy electron beam device, which generates the irradiation, disinfects the water while the stream of water is passing in a stream from through slim pathway.

Gamma irradiation as an alternative disinfectant is reported to be effective on three major waterborne microorganisms; *Escherichia coli*, coliphage MS-2, and *Cryptosporidium parvum*, chosen as representative bacterial, viral, and protozoan microorganisms, respectively (Thompson and Blatchley, 2000). A $^{60}$Co irradiator was used to expose test microorganisms to a controlled radiation dose. Experiments were performed for each of the test microorganisms to evaluate the effect of dissolved oxygen concentration and carbonate alkalinity on inactivation efficiency. For each microorganism, a strong effect of dissolved oxygen was observed, regardless of alkalinity. A subtle effect of alkalinity was observed for *E. coli* and coliphage MS-2, but only in air-saturated solutions. No significant alkalinity effect was observed for *Cryptosporidium parvum*. Inactivation kinetics was modeled for *E. coli* and coliphage MS-2 using single-target theory to calculate an inactivation rate constant. Multitarget theory was used to represent the inactivation response of *Cryptosporidium parvum*. The inactivation models based on target theory were found to provide suitable representations of experimental observations (Thompson and Blatchley, 2000).

4) Ultrasonic Irradiation

Recent studies with power ultrasound in aqueous systems have shown that such frequencies are capable of inactivating bacteria, viruses and fungi in water, but long contact or high intensities are required for accomplishing high rates of kill (Mason et al., 1990). It was further shown that bacterial survival under ultrasonic effects exhibits an exponential behavior, while the shear forces set up by cavitation bubbles are insufficient to rupture the cells (unless by prolonged contact), although they disengage the more delicate attachment sites of the DNA to the membrane (Singh et al., 1995). The results of a novel study on the effects of discrete frequencies and dissolved gases have shown that germicidal effectiveness of ultrasound depends strongly on the frequency (highest at 205 kHz), but moderately on the power intensity and gas properties, being highest in argon-oxygen mixtures (Hua and Thompson, 2000).

Ince and Belen investigated the use of ultrasonic irradiation in the presence of added solids as a viable alternative disinfection process at 20 kHz (Ince and Belen, 2001). The researchers sonicated synthetic solutions of *E.coli* in the presence of equivalent mass concentrations of ceramic, metallic zinc and activated carbon. It was found that the disinfection by ultrasound was accelerated in the order of activated carbon>ceramic > metallic zinc. The process kinetics assessed for each system was found to resemble a well-known expression describing the bacterial kill by chlorination. The authors also witnessed that the catalytic effects faded away with increased sonication time, and/ or reduced number of bacteria, indicating; (i) decreased probability of bacterial contact with the solid-liquid interface, (ii) erosion of solid surfaces by vibrational effects, and (iii) reduced cavity formation due to degassing effects of ultrasound.

2.1.1.3. Mechanical Means

1) Slow Sand Filtration

Being the oldest known water disinfection method, slow sand filtration is a simple and reliable process, where the untreated water percolates slowly through a bed of porous sand with the influent introduced over the surface of the filter and drained from the bottom (Sawyer and McCarty, 1978). Slow sand filters can remove suspended particles with effluent turbidities below 1.0 nephelometric turbidity units (NTU), achieving 90 to 99 + per cent reductions in bacteria and viruses, and providing virtually complete removal of

Giardia lamblia cysts and Cryptosporidium oocysts. However, slow sand filters do not remove all organic materials, dissolved organic substances or trihalomethane precursors.

2) Membrane Filtration

Microfiltration and ultrafiltration are low-pressure membrane filtration processes that have gained considerable acceptance in the drinking water treatment over the past ten years. These techniques are primarily used for particle removal as stand-alone treatment, retrofit existing conventional plants, or as pretreatment to advanced treatment processes such as nanofiltration or reverse osmosis. Micro and ultrafiltration have been demonstrated to be capable of removing protozoa cysts to below detection (USEPA, 2001). Removal of virus by these processes is more variable and depends on membrane properties, solution chemistry, and the formation of a dynamic cake over the membrane surface. However breaches in integrity can compromise the removal capability of membrane removal processes. Thus, even though intact membranes represent an absolute barrier, it is necessary to verify the integrity of the membrane system through routine testing. The advantages of using membrane technology are ease of operation, minimal staff requirements, ability to handle fluctuations in source water quality, and cost competitiveness with conventional processes.

## 2.1.2. Disinfection By-products

While pathogenic organisms provide the primary human health risk from drinking water, chemical disinfection by-products also provide an unintended health hazard. All the common chemical disinfectants such as chlorine, ozone, chlorine dioxide, and chloramines form their own suite of chemical disinfection by-products in finished drinking water.

As trihalomethanes were the first disinfection by-products identified and shown to be harmful to human health, they were also the first to be regulated by authorities. Studies have established the presence of haloacetonitriles, chloropicrin, chloral hydrate and other disinfection by-products in chlorinated drinking water as well as trihalomethanes and haloacetic acids (Williams et al., 1997). With stricter regulations for THMs and new regulations for haloacetic acids, many drinking water utilities are having to change from

chlorine to alternative disinfectants, including ozone, chlorine dioxide, and chloramines, to meet new regulations. However new issues and problems may result regarding the DBPs of these alternative disinfectants.
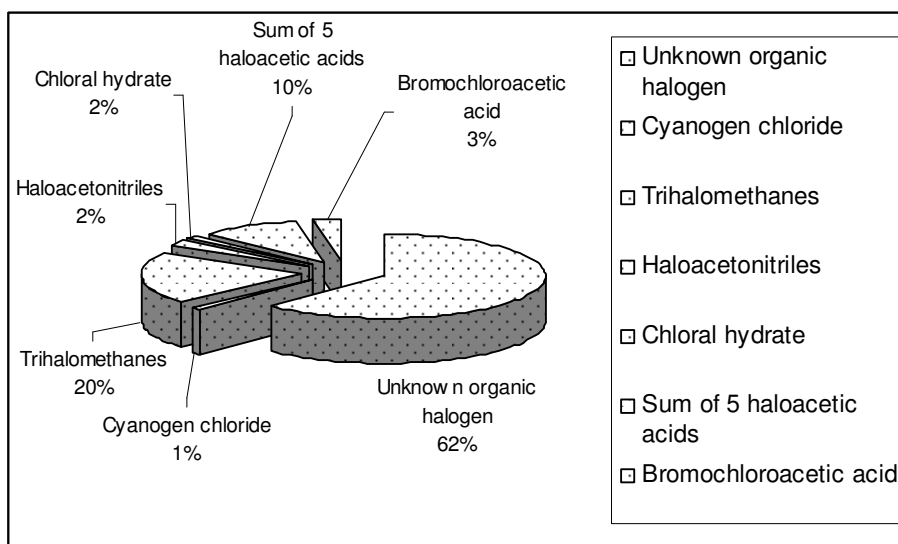


Figure 2.2. Relative amounts of halogenated DBPs as a proportion of total organic halogen (TOX) in a chlorinated drinking water (Richardson, 2003)

In more than 30 years since the THMs were first identified, DBPs have been the focus of active research. Significant research efforts have been directed toward increasing the understanding of DBP formation, occurrence and health effects. Although approximately 500 DBPs have been reported in the literature, only a small number have been addressed in either quantitative occurrence or health effect studies. The DBPs that have been quantified in drinking water are generally sub-µg/L (ppb) or low-to-mid µg/L levels. However, approximately 50 per cent of the total organic halide (TOX) formed during the chlorination of drinking water and more than 50 per cent of the assimilable organic carbon (AOC) formed during ozonation of drinking water are still not accounted for (see Figure 2.2 and Figure 2.3.), and nothing is known about the potential toxicity of many of the DBPs present in drinking water (Richardson, 2003).
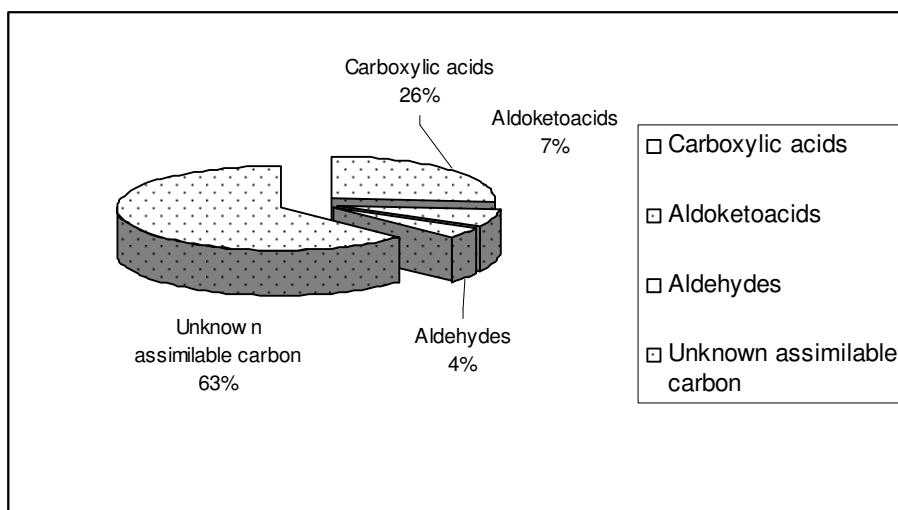
Figure 2.3. Relative amounts of ozone DBPs in drinking water as a proportion of the total assimilable carbon (AOC) (Richardson, 2003)

2.1.2.1. Formation. The formation of trihalomethanes during free chlorination of drinking water results from a complicated mechanism of attack by aqueous halogen species on natural aquatic humic substances, i.e. humic and fulvic acids, rather than organic compounds whose source is industrial water pollution. Thus, trihalomethanes result from the generalized reaction

$$\text{Free chlorine + Precursors} \rightarrow \text{Trihalomethanes + Other By-products} \quad (2.8)$$

Although the most common and important trihalomethanes are chloroform, bromodichloromethane, dibromochloromethane and bromoform, iodated trihalomethanes are also starting to draw attraction due to their highly toxic nature. Trihalomethanes are simple halogenated alkanes, some physical properties of which are given in Table 2.2.

Several studies have been carried out to evaluate the distribution and determinants of THMs. These studies showed that the most important factors influencing the formation of trihalomethanes were reaction time, temperature, bromide and iodide concentrations, pH, the characteristics and concentrations of precursors and chlorine dose and type.

Although, under some reaction conditions the formation of trihalomethanes may be completed in less than an hour, in other circumstances, several days may be required before the maximum yield of trihalomethanes occurs. Due to the complexity of reactions between aqueous free chlorine and the mixture of precursors of largely unknown structure, the precise effect of various parameters on the kinetics of trihalomethane formation, or the yield of formation at the completion of the reaction is difficult to predict. Thus, varying apparent yields of trihalomethanes reported throughout the literature under varying conditions may be influenced by the reaction rate. A lower reported yield may be the result of the reaction proceeding toward completion at a slower rate. El-Shafy and Grunwald reported that the THM concentrations reduced with increasing distance from the water treatment plant (El-Shafy and Grunwald, 2000), possibly as a result of incomplete formation reactions.

Increased temperature during chlorination has a positive effect on trihalomethane formation. In studies on the effect of temperature on THMs formation, an Arrhenius-type dependence has been found between the rate constant and temperature, with activation energies ranging from 10-20 kJ/mol (Peters et. al., 1980; Urano et. al., 1983), to below 10 kJ/mol (Kavanough et al., 1980; Stevens, et. al., 1976). Garcia-Villanova and co-workers found that increasing temperatures lead to a higher production of THMs, however, as from a given value (19 °C) upward, temperature drastically reduces THM levels (Garcia-Villanova et al., 1997). The authors explained this situation as a shift in the extent of two phenomena; temperature increasing the rate of formation up to a critical temperature, at which the rate of removal of THMs, most likely owing to their volatility, becomes higher than their formation rate.

Bromide and iodide ions are oxidized by aqueous chloride to species capable of participating in organic substitution reactions, resulting in the formation of pure and mixed-halogen trihalomethanes (Symons et al., 1981). The total molar yield of

trihalomethanes was observed to increase with increasing bromine substitution (Sorlini and Collivignarelli, 2004).

Numerous workers have shown that increasing the pH of the water being treated dramatically influences the rates of formation of trihalomethanes during water treatment. Given sufficient time, however, the yields for the two pH systems may be similar. The increase of trihalomethane formation rate is expected, because the limiting steps in the classic haloform reaction are base catalyzed (Snoeyink and Jenkins, 1980); however, this explanation is likely to be an oversimplification where rather complex humic acid structures are involved.

An alternative explanation for the effect of pH on rate and yield with humic acid precursor is that the macromolecule may simply be opening up by mutual repulsion of negative charges at high pH, thus increasing the availability of additional reactive sites on the molecule (Symons et al, 1981). The acidic functional groups of humic matter are not ionized, leading to the aggregation of molecules due to the Van der Waals forces. This phenomenon is also associated with folding of humic molecules, leaving fever sites available for chlorine attack (Adin et al., 1991).

Increasing the concentration of humic acid precursors in the presence of excess chlorine with otherwise constant reaction conditions cause trihalomethane yields to increase in direct proportion to the humic acid dose. Among the phenolic structures identified in humic substances, meta-dihydroxybenzene structures (resorcinol) have been considered as the main precursors of THMs. Natural organic matter reactions with halogens have been reported to react via oxidation (i.e., cleaving carbon-carbon double bonds) and/or substitution (i.e., replacement of functional groups by a halogen molecule). Reaction between chlorine and model organic compounds of natural organic matter have shown that aromatic compounds (e.g., phenols, aromatic amino acids) produce trihalomethanes (Westerhoff et al., 2004)

Norwood and co-workers chlorinated various compound known to exist among humic degradation products to identify the predominant THM precursors (Norwood et al., 1980).
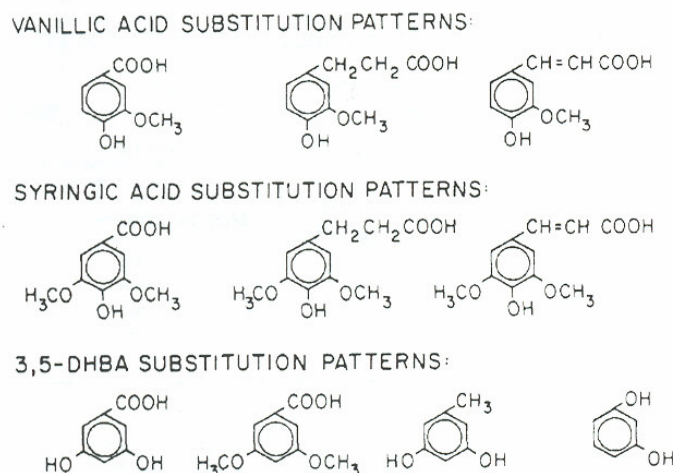


Figure 2.4. The series of compounds used as models of the monomeric components of aquatic humic material to investigate the trihalomethane formation reactions (Norwood et al., 1980)

The m-hydroxy substitution pattern of resorcinol was proved to produce chloroform very rapidly (Norwood et al., 1980). The chloroform yield was almost 93 per cent for the carbon between the two hydroxyl groups of these compounds. They also showed that the vanillic acid structure produces much less chloroform, which can be explained by the loss of a doubly activated carbon between two free hydroxyls. The number five carbon was still available for chloroform production, and because of the p-hydroxy configuration, the molecule would still undergo oxidative decarboxylation with substitution of chlorine in place of carboxyl. Continued chlorination and final cleavage could then occur at either of these chlorination sites.
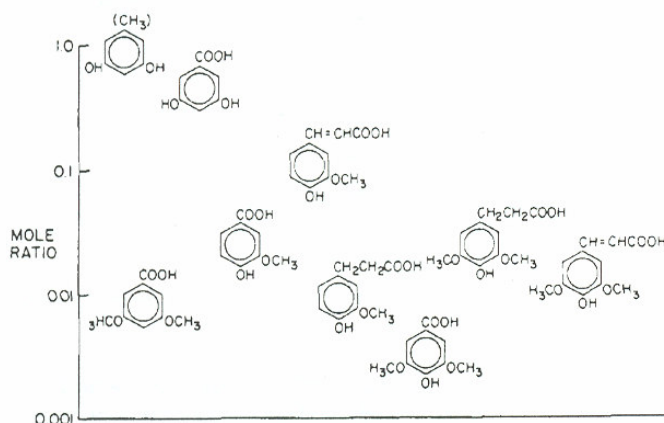
Figure 2.5. Relative chloroform yields of model precursor compounds after 40-min chlorination (Norwood et al., 1980).

The syringic acid substitution pattern was shown to produce approximately ten fold less chloroform than the vanillic structure. There was no longer an available position α to the hydroxyl group for chlorination, and Larson and Rockwell had previously shown that oxidative decarboxylation does not occur with syringic acid (Larson and Rockwell, 1979). The m-dimethoxybenzoic acid structure produced more chloroform than syringic acid, probably due to the fact that the carbon between the two methoxy groups was available for chloroform formation, although this production was markedly less than resorcinol due to the lack of keto-enol stabilization.

Substitution of the carboxyl group by unsaturated alkyl side chains resulted in a general increase in both chloroform production and chlorine demand. In the case of the 3-metoxy-4-hydroxycinnamic acid structure, Norwood and co-workers identified decarboxylation products with and without ring-substituted chlorine. When the side chain was saturated on the vanillic structure, chloroform production was reduced as was chlorine demand. With the syringic acid structure an apparent anomaly existed in that higher chloroform production and chlorine demand data were obtained for the saturated alkyl side chain.

The actual rates of chloroform production and chlorine consumption varied with each model compound studied, although the overall data exhibited two different patterns. The first pattern was typified by the orcinol data and reflected a generally rapid and

simultaneous exertion of both chlorine demand and chloroform production. Compounds exhibiting this pattern were orcinol, resorcinol, 3,5-dihydroxybenzoic acid, 3-methoxy-4-hydroxycinnamic acid, and 3,5-dimethoxybenzoic acid. These data suggested that chloroform was the primary reaction product for these model compounds. The second pattern was typified by the 3,5-dimethoxy-4-hydroxycinnamic acid., and reflected an initial chlorine demand in excess of chloroform production. Compounds exhibiting this pattern were 3-methoxy-4-hydroxyhydrocinnamic acid, syringic acid, vanillic acid and β-(3,5-dimethoxy-4-hydroxyphenil)propionic acid. These data suggested that chloroform was a minor reaction product for these model compounds (Norwood et al.,1980).

Other researchers investigated the reactions of chlorine with 1,3-dihydroxybenzenes. Zincke reported that chlorination of resorcinol in organic solvent produced 2,2,4,4,6-pentachlorcyclohex-4-ene-1,3-dione (pentachlororesorcinol), which was subsequently hydrolyzed to keto-carboxylic acid upon addition to water (Boyce and Hornig, 1983).
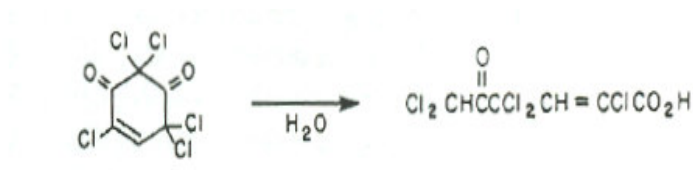


Figure 2.6. Hydrolyzation of pentachlororesorcinol to keto-carboxylic acid upon addition to water (Boyce and Hornig, 1983)

Boyce and Hornig investigated the mechanism of chloroform formation from the halogenation of dihydroxyaromatic compounds to propose a possible reaction scheme (Boyce and Hornig, 1983).
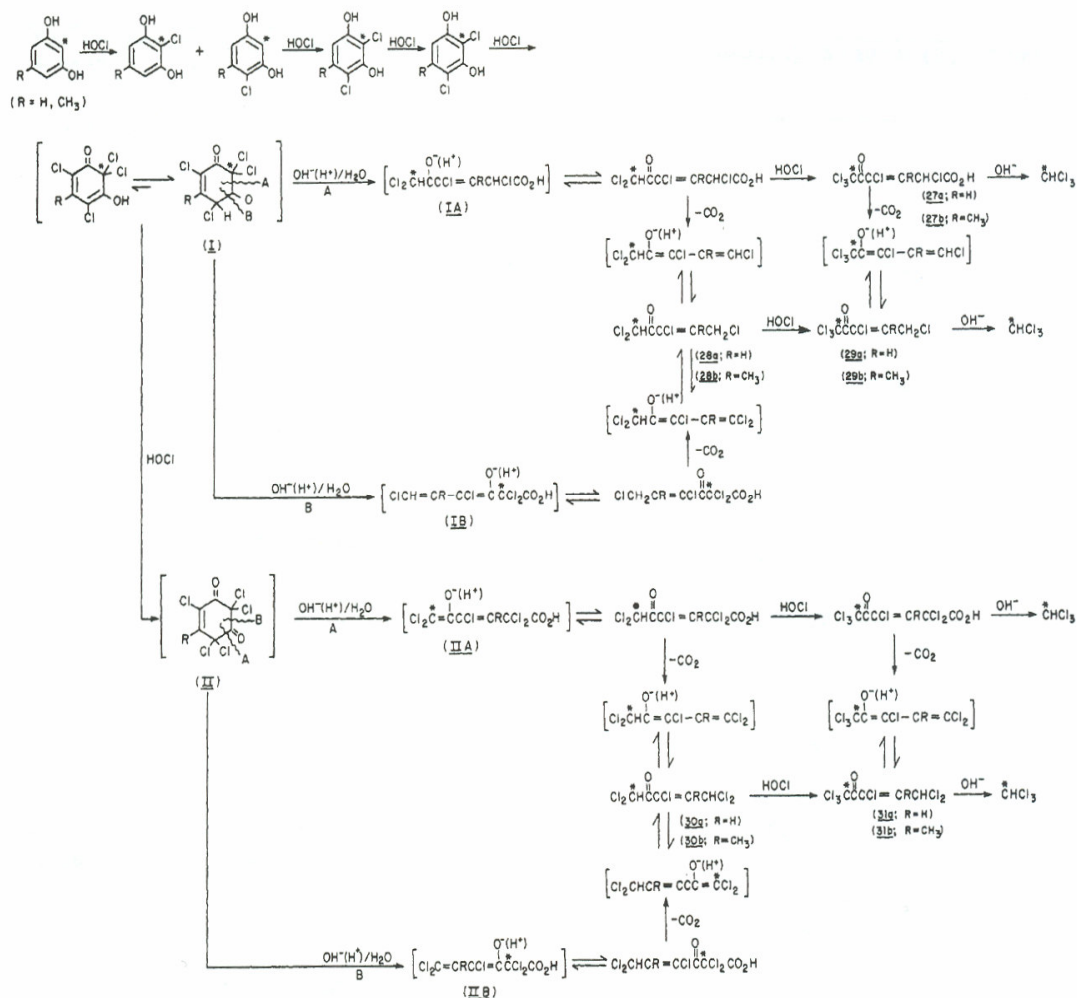
Figure 2.7. Reaction pathways proposed for the conversion of 1,3-dihydroxyaromatic substrates to chloroform. Structures outlines by brackets denote proposed intermediates that were not detected by GC/MS (Boyce and Hornig, 1983)

According to the proposed reaction scheme, initial electrophilic substitution yields trichloro-1,3-dihydroxybenzenes. Further addition of chlorine forms the cyclohexenedione intermediates I and II, and is followed by hydrolysis and oxidative bond cleavage (A or B) about the $C_2$ site of the ring structure via a complex series of steps to yield carboxyenolate species such as IA, IB, IIA and IIB. The corresponding carboxylic acids are expected to be fairly stable in acidic solution. In neutral and alkaline solution, decarboxylation is probably accompanied by direct incorporation of Cl to give, for example, chlorinated pentenones. These trichloromethyl ketones then undergo base catalyzed hydrolysis to chloroform.

Decarboxylation and chlorination of intermediates such as IA, IIA, IB and IIB may constitute the rate limiting processes in this mechanism (Boyce and Hornig, 1983).

Boyce and Hornig also synthesized an isotopocally enriched substrate, resorcinol-2-$^{13}$C, and followed the fate of the labeled carbon atom upon the reaction of the precursor with chlorine and bromine. At pH 4, 7, and 10, treatment of labeled resorcinol with a ten-fold excess of $Cl_2$ and $Br_2$ produced $^{13}CHCl_3$ and $^{13}CHBr_3$. The finding that the $^{13}C$ enrichment of the substrate and haloform reaction products were approximately equivalent, confirms that chloroform and bromoform were produced almost exclusively by reaction pathways involving carbon-carbon cleavage about the $C_2$ position of the ring structure of the aromatic precursor.

More recently, Gallard and von Unten combined the kinetics of chlorine consumption with kinetics of THM formation to elucidate the nature of THM precursors in NOM. They also concluded that resorcinol type structures may be responsible for the fast reacting THM precursors whereas other phenolic compounds may be responsible for the slowly reacting THM precursors. The authors also caution that other compounds such as β-diketones or β-keto acids might play an important role (Gallard and von Unten, 2002).

Where the precursor is kept constant only a slight influence on trihalomethane formation rate or yield occurs when the free chlorine dose is increased beyond the demand. On the other hand, the addition of combined chlorine (in the form of chloramines) does not cause the formation of trihalomethanes.

2.1.2.2. Health Effects of Disinfection By-products. The only compound belonging to the group of trihalomethanes about which the US Environmental Protection Agency has come to a conclusion that can be used in human risk assessment studies, is chloroform. USEPA concluded that chloroform is likely to be carcinogenic to humans in all routes of exposure under high-exposure conditions that lead to cytotoxicity and regenerative hyperplasia in susceptible tissues (USEPA, 2001). USEPA also concludes that chloroform is not likely to be carcinogenic to humans by any route of exposure under exposure conditions that do not cause cytotoxicity and cell regeneration.

Much of the health effects research directed toward understanding the effects of chronic exposure to DBPs have focused on cancer or mutagenicity. There are ongoing concerns that the types of cancer observed in animal studies (primarily liver cancer) for the DBPs that have been tested do not correlate with the types observed in human epidemiological studies (bladder, colon cancer). It is possible that new DBPs that have been identified but not yet tested for health effects (largely because of high costs of animal studies), may be linked to the effects observed in humans.

At the dose levels tested in laboratory experiments, a number of these DBPs were either carcinogenic or caused target-organ toxicity, including reproductive/developmental toxicity. These laboratory dose levels are high compared to the low level (ppb to ppt) found in drinking water. The vast majority of disinfection by products has not been investigated toxicologically, in fact fewer than 20 individual DBPs have been subjected to toxicity studies usable for risk assessment.

In addition, new concerns have been raised by epidemiological studies about potential adverse reproductive and developmental effects, such as low birth weight, intrauterine growth retardation, and spontaneous abortion. Also, because humans are exposed to mixtures of DBPs rather than individual DBPs, and because the currently available single-chemical studies in experimental animals cannot by themselves explain the adverse health effects observed in some human epidemiological studies, toxicological investigations of DBP mixtures in experimental animals are critically needed (Simmons et al., 2002).

In addition, routes of exposure other than ingestion for DBPs are now being recognized as significant. For example, recent work has revealed that a person can receive twice the exposure to THMs through showering (by inhalation), and equivalent exposure through dermal absorption (bathing, etc.) as compared to ingesting 2 liters of water (Richardson, 2003). For example, Landi and co-workers ranked trihalomethanes for their DNA damaging ability (genotoxicity) in primary human epithelial cells in the order of $CHBrCl_2 > CHBr_3 > CHCl_3 \approx CH_2Cl_2$; and found $CHBr_2Cl$ to be negative (Landi et al., 2003).

However, the multi-pathway risk assessment studies show that the combined lifetime cancer risks from chloroform, bromodichloromethane, and dibromochloromethane from tap water in 15 districts of Istanbul were higher than $10^{-6}$, the negligible cancer risk level defined by USEPA (Uyak, 2006).

2.1.2.3. Occurrence of Trihalomethanes. Following the initial reports on THM formation in chlorination facilities and upon the increased availability of analytical methods and equipment, researchers started to report the occurrence and concentrations of trihalomethanes in water supply systems from all over the world.

Abdullah and co-workers collected chlorinated drinking water samples from three districts in Selangor, Malaysia, for 12 months during the year 2001. The authors could detect only chloroform, bromodichloromethane and dibromochloromethane in all samples; whereas bromoform was not detected in all samples, and that the major component of total trihalomethanes was chloroform in the districts of interest. The mean value of chloroform in Tampin district ranged between 14.84 to 55.62 μg/L and the mean value of Total THM varied between 18.59 to 68.82 μg/L. The mean value of chloroform at Sabak Bernam district ranged between 42.92 and 81.00 μg/L, and total THM in the same district varied between 54.64 and 89.83 μg/L (Abdullah et al., 2003).

Duong and co-workers investigated the fate of trihalomethanes in the water supply system of Hanoi City, Vietnam from 1998 to 2001. Regarding THM formation the authors identified three types of water; (I) high bromide, (II) low bromide and (III) high bromide combined with high ammonia. The concentration ranges found in the finished water were reported as 0.3 μg/L $<CHCl_3<$ 11.1 μg/L., 0,5 μg/L $<CHBrCl_2<$ 7.3 μg/L, 0.3 μg/L $<$ $CHBr_2Cl<$ 22.3 μg/L, 1.2 μg/L $< CHBr_3<$ 18.5 μg/L for (1) type waters; 0.9 μg/L $<$ $CHCl_3<$7.7 μg/L, 0.2 μg/L $< CHBrCl_2 <$5.6 μg/L, 0.2 μg/L $< CHBr_2Cl<$3.8 μg/L, 0.2 μg/L $< CHBr_3<$3.7 μg/L for type (II) waters and 0.3 μg/L $< CHCl_3<$21.5 μg/L, 0.2 μg/L $<$ $CHBrCl_2 <$3.6 μg/L, 0,2 μg/L $< CHBr_2Cl<$3.7 μg/L and $CHBr_3<$0.2 μg/L for type (III) waters (Duong et al., 2003).

Malliarou and co-workers measured the concentrations of haloacetic acids and trihalomethanes in regions covered by three water companies in the UK. In two out of

three regions there was a high correlation between HAAs and THMs. But whereas the HAA and THM levels in one of these companies were approximately equal, in the second company the HAA levels 3-4 times higher than THM levels. In the third region, there was no correlation between the total THM and total HAA levels even though the average levels were approximately equal, indicating that total THM levels should not be considered a good indicator of HAA levels. In region A, they found the mean TTHM value to be 50.9 μg/L, in region B, 27.6 μg/L, and in region C 48.6 μg/L (Malliarou et al., 2005).

Williams and co-workers investigated the effects of applied disinfectants, seasonal variation and spatial variation of halogenated disinfection by-products in Canada (Williams et al., 1997). They found that chloroform, dichloroacetic acid and trichloroacetic acid were the major disinfection by-products found in all treated water samples and total haloacetic acids concentrations often equaled or exceeded total trihalomethane concentrations. Haloacetonitriles, halopropanones, chloral hydrate and chlorpicrin were usually detected in treated water samples but at lower concentrations. They measured total trihalomethanes as well as DCAA, TCAA, CH, levels in summer and winter and at treatment plants and at the distribution systems. Their findings in terms of TTHMs are summarized in Table 2.3.

Table 2.3. DBP concentrations (μg/L) in Canadian drinking water in summer and winter sampled at treatment plant and at the distribution system in 1993 (Williams et al., 1997).

| Treatment | Site | Winter | | Summer | |
|---|---|---|---|---|---|
| | | Mean | Range | Mean | Range |
| Chlorine/Chlorine | Plant | 16.8 | 2.0-67.9 | 33.5 | 1.6-120.8 |
| | System | 33.44 | 2.8-221.1 | 62.5 | 0.3-342.4 |
| Chlorine/Chloramine | Plant | 12.1 | 0.6-40.3 | 31.2 | 2.9-80.1 |
| | System | 13.7 | 1.5-42.1 | 32.8 | 4.3-85.1 |
| Ozone/Chloramine | Plant | 6.8 | 1.7-12.3 | 44.0 | 2.5-74.9 |
| | System | 9.9 | 2.4-15.4 | 66.7 | 4.9-107.8 |

El-Shafy and Grunwald measured total THM concentrations at the exit of treatment plant and at water reservoirs feeding the distribution network in South Bohemia, Czech Republic (Al-Shafy and Grunwald, 2000). The authors state that the main species of trihalomethanes found was chloroform, which represented about 82 per cent of the total

THMs. The average results of their measurements concerning THMs are summarized in table 2.4.

Table 2.4. Average $CHCl_3$ and total trihalomethanes concentrations measured in South Bohemia, Czech Republic, in 1997 (Al-Shafy and Grunwald, 2000).

| Place | | Distance from treatment plant (km) | Residence Time (days) | CHCl3 ($\mu g/L$) | TTHM ($\mu g/L$) |
|---|---|---|---|---|---|
| Plav Water Treatment Plant | Average | 0.0 | 0.0 | 4.61 | 5.2 |
| | Std. Dev. | | | 4.01 | 4.45 |
| | Range | | | 1.0-16.0 | 1.1-18.0 |
| Hosin Reservoir Outlet | Average | 15.5 | 1.35 | 5.89 | 7.1 |
| | Std. Dev. | | | 6.61 | 7.93 |
| | Range | | | 1.3-25.0 | 1.5-30.0 |
| Chotycany Reservoir Inlet | Average | 20.5 | 2.28 | 5.91 | 7.3 |
| | Std. Dev. | | | 6.26 | 8.2 |
| | Range | | | 1.4-24.0 | 1.5-31.0 |
| Chotycany Reservoir Outlet | Average | 20.5 | 2.61 | 7.01 | 8.6 |
| | Std. Dev. | | | 8.91 | 11.2 |
| | Range | | | 1.4-33.0 | 1.6-41.0 |
| Sach Veseli Reservoir | Average | 43.7 | 4.45 | 8.15 | 9.4 |
| | Std. Dev. | | | 8.43 | 10.6 |
| | Range | | | 1.6-31.0 | 1.7-39.0 |
| Sv.Anna Reservoir | Average | 80.9 | 6.83 | 8.50 | 10.3 |
| | Std. Dev. | | | 9.23 | 11.7 |
| | Range | | | 2.5-35.0 | 3.0-44.0 |

Seasonal distributions of trihalomethanes in water distribution network of Istanbul was investigated by Toroz and Uyak during spring, summer and the fall of year 2003 (Toroz and Uyak, 2005). The authors found that THM concentrations varied significantly between the treatment plant and the extremities of the distribution system. The authors also reported that the summer THM concentrations when water temperature exceeded 24°C,

were 1.2-1.8 times higher than finished water. The summary of average THM concentrations measured by Toroz and Uyak is given in Table 2.5.

Table 2.5. Summary of THM levels measured in tap water in 15 districts in Istanbul, (Toroz and Uyak, 2005)

| | Average THMs levels (µg/L) | | | | |
|---|---|---|---|---|---|
| District | $CHCl_3$ | $CHBrCl_2$ | $CHBr_2Cl$ | $CHBr_3$ | TTHM |
| B.Cekmece | 17 | 20 | 21 | 5.0 | 63 |
| Beylikduzu | 18 | 21 | 23 | 8.0 | 70 |
| Gurpinar | 22 | 23 | 27 | 9.7 | 82 |
| Avcilar | 25 | 28 | 31 | 9.1 | 94 |
| Esenyurt | 28 | 30 | 33 | 11 | 100 |
| Basaksehir | 12 | 11 | 8.0 | 2.0 | 33 |
| Gunesli | 15 | 14 | 12 | 2.0 | 43 |
| Yenibosna | 21 | 18 | 15 | 3.0 | 57 |
| Bahcelievler | 24 | 20 | 14 | 4.7 | 62 |
| Fatih | 28 | 19 | 14 | 4.7 | 66 |
| Kagithane | 24 | 15 | 6.7 | 1.3 | 47 |
| Sisli | 28 | 20 | 9.0 | 1.7 | 59 |
| Ayazaga | 27 | 24 | 9.0 | 1.3 | 61 |
| Bahcekoy | 38 | 23 | 9.7 | 4.7 | 76 |
| Sariyer | 42 | 27 | 12 | 1.0 | 82 |

## 2.2. Methods of Trihalomethanes Removal

There are three general approaches to the treatment of trihalomethanes:

1) The use of other disinfectants to avoid trihalomethane formation completely
2) Treatment to remove trihalomethane precursors
3) Treatment to remove trihalomethanes after formation

### 2.2.1. The Use of Other Disinfectants

Of the options above the use of alternative disinfectants seems to be the most effective and least costly. Chlorine dioxide, ozone and chloramines produce no significant concentrations of trihalomethanes when used as disinfectants. Theoretically, any water treatment utility with any trihalomethane precursor concentration could reduce its trihalomethane concentration almost to zero. Furthermore the cost of installing these alternative unit processes calculated with or without the contact chambers is very low (Symons et al., 1981).

The disadvantage of this approach is that it does not remove the THM precursors and merely replaces the THMs with another set of disinfection by-products depending on the alternative disinfectant used. Some of these alternative by-products are halogenated if chlorine dioxide and chloramines are used. Furthermore, each of the proposed alternatives has its own inherent disadvantages. For example ozone does not produce any residual for the distribution system, chloramines is a weaker bactericide than chlorine, chlorine dioxide produces chlorite and chlorate as inorganic by-products, the health effects of which are currently unknown.

### 2.2.2. Treatment to Remove Trihalomethane Precursors

Because trihalomethanes are formed when free chlorine is added to water that contains trihalomethane precursors, one approach to lowering TTHM concentrations would be to remove precursors. Thus, if the resulting trihalomethane concentrations are controlled by lowering the concentration of precursors, free chlorine can still be used as the disinfectant. The most important advantage of this approach is that free chlorine is used at most water treatment plants currently, and water utility managers and operators as well as consumers have confidence in its use and its ability to produce microbiologically safe water. Treating water to remove trihalomethane precursors before disinfection has the further advantage of the general reduction in the chlorine demand. Caused by the presence of less material with which chlorine can react. A lower disinfectant demand leads to the formation of fewer disinfection by-products of all types. When less disinfectant reacts with less precursor material, concentrations of the halogenated by-products as well as other

nonhalogenated oxidation by-products will be lowered. The most common methods of precursor removal are:

- clarification
- source control
- aeration
- adsorption
- ion exchange
- biologic degradation
- lowering of pH
- oxidation

The only disadvantage to precursor removal seems to be the reduction of the humic materials in water distribution systems which may have an importance in controlling corrosion in water distribution systems (Symons et al., 1981).

## 2.2.3. Treatment to Remove Trihalomethanes After Formation

As a treatment approach, the removal of trihalomethanes has some advantages. The more important are that the water utility would not need to change its disinfection practices and the treatment is targeted to the contaminant. Chlorination, a process in which many designers and operators have confidence, could continue to be practiced with the resulting trihalomethanes being removed by some unit process added to the treatment train. The flexibility to permit noncentral treatment of the finished water may also prove to be advantageous.

2.2.3.1 Aeration-Stripping. Among the several factors influencing the effectiveness of removing organic contaminants from water by aeration are contact time, ratio of air to water, temperature, vapor pressure, and solubility of the contaminants. Although contactor design is very critical to unit process efficiency and cost, vapor pressure and solubility are also very useful parameters for estimating the feasibility of aeration.

Theoretically, a counterflow aeration tower is the most efficient system with regard to air use to achieve a given treatment goal. In theory, when a counterflow aeration tower is operated ideally, the concentration in the water of the contaminant to be removed is in equilibrium with the concentration of the contaminant in the air at any point in the system. According to Henry's law constant;

$$H = \frac{C_a}{C_w} \qquad (2.9)$$

Where; $C_a$ = concentration of the compound in air (µg/L)

$C_w$ = concentration of the compound in water (µg/L)

The concentration in the water is equal to concentration in the air in divided by the Henry's law constant, at any point of the reactor. Because the concentration of the contaminant coming into the bottom of the reactor is zero, in a "perfect" tower the concentration of the contaminant must be zero, thus, the perfect system would remove all of the contaminant in question. The schematic representation of an ideal aeration column:
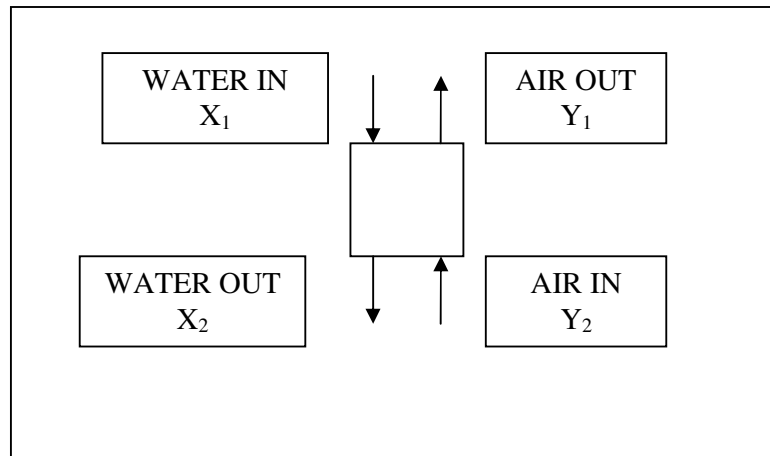


Figure 2.8. Schematic representation of ideal counterflow aeration system, where;

$X_1$ = initial concentration of the contaminant in the water

$X_2$ = final concentration of the contaminant in the water

$Y_1$ = initial concentration of the contaminant in the air

$Y_2$ = final concentration of the contaminant in the air

Calculating the mass balance based on figure , the loss of contaminants in water equals the gain of contaminants in the air :

$$(X_1\text{-}X_2)\, V_w = (Y_1\text{-}Y_2)\, V_a \qquad (2.10)$$

Where: $V_w$ = water volume

$V_a$ = air volume

In a perfect column, according to Henry's law, at any point,

$$\frac{c_a}{c_w} = \frac{Y_1}{X_1} = H \qquad (2.11)$$

Therefore at the top of the column $Y_1 = (H)(X_1)$

Substituting this in Equation (2.10) yields:

$$(X_1\text{-}X_2)V_w = [(H)(X_1)\text{-}Y_2]V_a \qquad (2.12)$$

Because both $X_2$ and $Y_2$ are zero in an ideal system, Equation (2.12) becomes;

$$(X_1)V_w = (H)\,(X_1)V_a \qquad (2.13)$$

Cancelling yields:

$$\frac{V_w}{V_a} = H \qquad (2.14)$$

This means that in the perfect system, the minimum air to water ratio that will achieve complete removal for the contaminant in the question is the reciprocal of the contaminants Henry's law constant. Henry's law constants for low concentrations of trihalomethanes in aqueous solutions are 0.152 for chloroform, 0.095 for bromodichloromethane, 0.035 for dibromochloromethane and 0.024 for bromoform (Symons et al., 1981). Experience has shown that compounds with Henry's law constant

greater than 0.05 could be removed relatively easily by aeration. Therefore trihalomethanes are considered to be contaminants easily removed by aeration. The theoretical minimum air to water ratios required to achieve complete removal in a perfect column, calculated from Equation 2.14., are 6.7:1, 10.2:1, 28:1, and 41:1 for chloroform, bromodichloromethane, dibromochloromethane, and bromoform, respectively.

However, no actual system is perfect, so less than 100 per cent removal always occurs, even with air-to-water ratios much higher than the theoretical minimum. This occurs because numerous design factors influence the rate of mass transfer from the liquid phase to gas phase. Departure from equilibrium condition provides the driving force that causes the contaminant to move across the air-water interface. This driving force becomes smaller as conditions approach equilibrium, as often is the case when THM concentrations get smaller.

In summary, aeration is a feasible approach to trihalomethane removal, with the difficulty of removal increasing with molecular weight from chloroform to bromoform. However from the environmental engineering point of view, this process merely transfers the pollutants from one phase to another instead of stabilizing/rendering it harmless, and rids of the problem only temporarily. On the other hand, it has been shown by several field studies that chlorination of humic material in soil through natural processes (chloroperoxidase activity possibly causing decarboxylation) produces chloroform, which is estimated to be the second largest source of chloroform in the environment by a flux of 220 Gg/yr (McCulloch, 2003). As total chloroform production in drinking water chlorination is estimated to be 2 Gg/yr for USA and 7 Gg/yr for the rest of the world, the total chloroform generated in drinking water chlorination in the world is 9 Gg/yr, which is about 1.5 per cent of the estimated global flow of 660 Gg/yr. Atmospheric oxidation seems to be the principal removal process, was calculated to be approximately in balance with the identified source fluxes. Definitive studies have shown that current environmental concentrations of chloroform do not present an ecotoxicological risk. By virtue of the very small amounts that actually become transported to the stratosphere, chloroform does not deplete ozone materially, nor is it photocemically active. It has a global warming potential that is less than that of the photochemically active VOCs and is not classified as a greenhouse gas. As a consequence, the release of chloroform to the atmosphere by aeration

does not seem to be an environmental issue of any significance. Although no data is available about the other trihalomethanes of interest, it may be plausible to envisage that their cycles in global scale are in similar standing.

To investigate the volatility of trihalomethanes under quiescent conditions, an open vessel containing tap water left standing at room temperature (25°C) was sampled periodically. A nearly complete loss of trihalomethanes occurred after three days, even though trihalomethanes were still forming during the experiment by the free chlorine residual (Symons et al., 1981).

2.2.3.2. Adsorption.  The adsorption isotherm is the relationship between the amount of substance adsorbed and its concentration in the surrounding solution at equilibrium. The adsorption isotherm consists of a curve plotted with residual concentration of the solute in solution on the "x" axis and the amount adsorbed per unit weight of adsorbent on the "y" axis. Thus any point on the line gives the adsorption capacity or loading at a particular concentration in solution. With activated carbon adsorption from dilute solutions, such as trihalomethanes in drinking water, a logarithmic plotting according to the empirical Freundlich equation:

$$x / M = k \, C^{1/n} \tag{2.15}$$

where;

x  =  amount of substance adsorbed, calculated from original and equilibrium concentrations, $C_0$ and $C_f$

M  = weight of activated carbon, and

k and n are constants; k is the intercept at $C_f = 1$ (log $C_f = 0$), and 1/n is the slope of the line

usually yields a straight line over the concentration ranges for trihalomethanes usually found in drinking water.

Applications of adsorption isotherms assume that the equilibrium is reached during the normal water treatment processes where activated carbon is applied. Even though the

rate of adsorption (approach to equilibrium) is typically rapid when powdered activated carbon is used, normally measured in minutes to hours, equilibrium may not always be reached at utilities using a short contact time. This kinetic effect would reduce the effectiveness of this treatment technique. Additionally, other solutes present in the water being treated may compete for the "active sites" on the adsorbent and disinfectant residuals may influence adsorbent qualities. Adsorption capacities for different activated carbons also vary. These effects complicate extrapolations from published isotherm data to actual water treatment practice.

The alternative method of adsorption to powder activated carbon adsorption is granular activated carbon. This method typically uses stationary beds full of granular activated carbon, with the liquid flowing downward through the adsorbent. The adsorbate accumulates at the top of the bed until the amount adsorbed at that point reaches a maximum. The maximum amount of contaminant that can be adsorbed on activated carbon occurs when the adsorbed material is in equilibrium with the concentration of the contaminant in solution surrounding the adsorbent. For any given concentration of the contaminant in solution this point may be determined from the appropriate adsorption isotherm. When the adsorbent is thus loaded to capacity, that portion of the bed is exhausted. In an ideal plug-flow operation, the exhausted zone moves downward with time in operation until the entire adsorbent bed is exhausted. The effluent concentration of the contaminant remains zero until the exhausted zone reaches the bottom then abruptly increases to the influent concentration. The capacity thus the service life of the column is calculated using data from adsorption isotherms.

Synthetic resins are also investigated by several researchers to adsorb trihalomethanes from drinking waters. Some were found to be more effective in THM removal than some powdered activated carbons. However these resins are still being developed and many are not available in commercial quantities.

Capar and Yetis investigated the effectiveness of granular activated carbon adsorption of THMs from Ivedik water treatment plant in Ankara (Capar and Yetis, 2002). Upon comparison of the column capacities and the capacities calculated from adsorption isotherms, the authors found the column capacities to be within 43-65 % of the isotherm

capacities at complete breakthrough, and only at 8-17 % of the isotherm capacities at 50% breakthrough.

2.2.3.3. Oxidation. Ozonation, chlorine dioxide, ozone coupled with ultra-violet irradiation and other oxidation methods have been applied to oxidate trihalomethanes. Recently advanced oxidation processes such as oxidation with Fenton's reagent and high energy electron beam irradiation are also being investigated (Tang and Tassos, 1997), but this approach is considered to be still in the research stage, and is not ready to be used in practical treatment applications.

The two major disadvantages of trihalomethane removal are the disregard of other disinfection byproducts, and the lack of precursor removal. Although the health significance of other disinfection by-products has not been fully evaluated, these compounds are often viewed with suspicion. The target specific methods for trihalomethane removal are not yet evaluated for their effects on the concentrations of these other by-products. The lack of precursor removal results in the formation of trihalomethanes through the reaction of residual chlorine with the remaining precursors, thus the chloroform concentration reaching the consumer would be higher than that measured at the treatment plant exit. However, the concentration reaching the consumer would be lower than that would be without treatment. Adsorption and some of the oxidation methods also incidentally reduce precursor concentrations.

## 2.3. Ultrasound and Its Uses in Water Remediation

### 2.3.1. Sonochemistry

Sound frequencies are recorded in units of Hertz (1 Hertz = 1 cycle per second). The range of human hearing for a young person is from about 20 Hz to 20 kHz (the upper limit reduces with age). Ultrasound itself is defined in terms of human hearing. It is the sound having a frequency higher than to which human ear can respond (i.e. 20 kHz). The upper limit of ultrasonic frequency is not so sharply defined but is usually taken as 5 MHz for gases and 500 MHz for liquids and solids. The uses of ultrasound within this range may be broadly divided into two areas.

The first area involves low amplitude (higher frequency) sound and is concerned with the physical effect of the medium on the wave and is commonly referred to as "low power" or "high frequency" ultrasound. Typically, these low amplitude waves are used for analytical and diagnostic purposes to measure the velocity and absorption coefficient of the wave in the medium in the 2 to 10 MHz range. Information from such measurements can be used in medical imaging, chemical analysis and relaxation phenomena.

The second area involving "high energy" (low frequency) waves, known as power ultrasound lies between 20 and 100 kHz. It is used for cleaning, dispersion, particle size reduction, filtration, plastic welding, degassing and more recently, for sonochemistry.

Table 2.6. Common applications of sound frequency ranges (Mason and Lorimer, 2002)

| Relevance | Frequency |
|---|---|
| Human hearing | 20 Hz to 20 kHz |
| Conventional Power Ultrasound | 20 kHz to 100 kHz |
| Extended range for sonochemistry | 20 kHz to 2 MHz |
| Diagnostic ultrasound | 5 MHz to 10 MHz |

Being a sound wave, ultrasound is transmitted through any substance, solid, liquid or gas, which possesses elastic properties. The movement of the vibrating body (i.e. the sound source) is communicated through the molecules of the medium, each of which transmits the motion to an adjoining molecule before returning to approximately its original position. For liquids and gases, particle oscillation takes place in the direction of the wave and produces longitudinal waves (Mason and Lorimer, 2002).

Power ultrasound influences chemical reactivity through an effect known as cavitation which was first characterized by Sir John Thornycroft and Sidney Barby at the beginning of 21st century. They discovered that the rapid erosion of the propellers of a new high speed destroyer was due to cavitation phenomena. The source of ultrasonic waves (the transducer) can be pictured as a piston dipping into the fluid and operating with very small but extremely rapid strokes. In this analogy, the pressure wave is clearly understood as the

forward stroke into the medium which is transmitted by a series of molecular interactions through the fluid. It is the pull stroke which produces the rarefaction portion of the wave. When the piston is operating at a rate of 20 000 strokes per second, ultrasound at the frequency of 20 kHz is generated in the medium. If the rarefaction wave is sufficiently powerful it can develop a negative pressure large enough to overcome the intermolecular forces binding the fluid. In this situation the molecules will be torn apart from each other to form tiny microbubbles throughout the medium, called cavities. The compression cycle that follows the rarefaction cycle can cause the microbubbles to collapse almost instantaneously with the release of large amounts of energy. It has been estimated that temperatures of 5000 K and pressures of the order of 1000 atmospheres are generated by the collapse of cavitation bubbles generated by ultrasound in water at 25 °C (Mason, 1990).

Whenever an acoustic field is applied to a liquid, the pressure waves of the sonic vibrations create an acoustic pressure which travels through the medium. As the soundwave propagates through the liquid, it induces oscillation of the molecules about their mean rest position and increases their translational energy momentarily. Some of this energy is lost owing to viscous and thermal effects. When the net negative pressure developed in the rarefaction cycle of the sound wave is applied to the liquid such that the distance between the molecules exceeds the critical molecular distance necessary to hold the liquid intact, the liquid will break down and voids, i.e. cavitation bubbles, are created (Mason, 1990).

Acoustic cavitation can be considered to involve at least three discrete stages: nucleation, bubble growth, and, under proper conditions, implosive collapse. The dynamics of cavity growth and collapse are strikingly dependent on the local environment. Cavity collapse in a homogenous liquid is very different from the collapse near a liquid-solid interface. Formation of cavities in liquids is a nucleated process. The theoretical tensile strength of a pure liquid is so high as to preclude cavity formation simply from the negative pressure of an acoustic expansion wave under typical laboratory conditions. Instead, nucleation of bubbles occurs at weak points in the liquid, such as gas filled crevices in suspended matter or from transient microbubbles from prior cavitation events (Suslick, 1990).
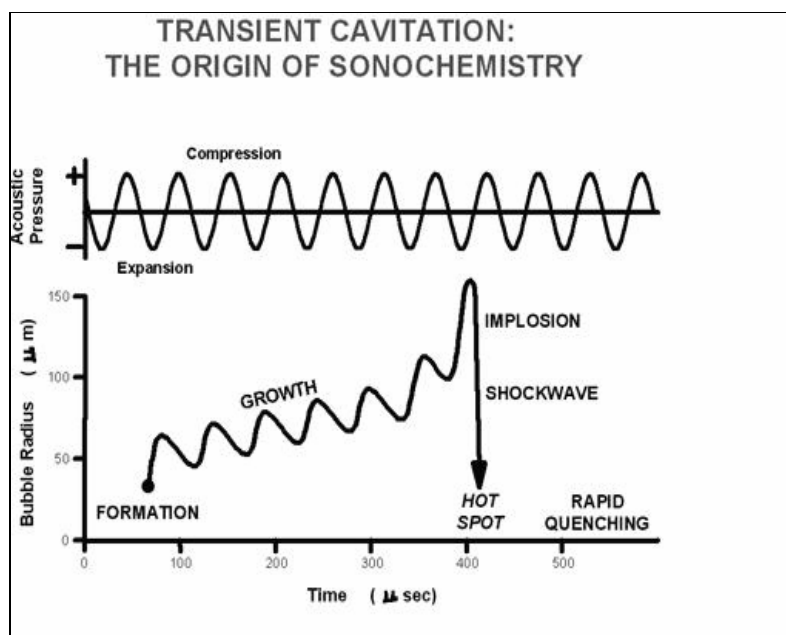
Figure 2.9. Formation, growth and implosion of a cavitation bubble (Suslick, 1994).

When the acoustic pressure of the propagating wave is large enough to give explosive growth to the local inhomogeneities in the liquid, the cavity that is formed is inherently unstable, and its subsequent collapse can result in an enormous concentration of energy (Suslick, 1997). This violent cavitation event is termed transient cavitation. A normal consequence of this unstable growth and subsequent collapse is that the cavitation bubble is destroyed. Gas filled remnants however, may give rise to reinitiation of the process.

There are two basic groups of theories advanced to explain energy-consuming chemical and physicochemical effects caused by cavitation, namely thermal and electrical. These effects include primarily sonochemical reactions and sonoluminescence whose inception requires the formation of excited particles, radicals, and under definite conditions, ions also. The thermal theories relate the presence of sonochemical effects to the appearance of a high temperature in a cavitation bubble during its adiabatic compression at a continuously growing velocity, while the electrical theories relate them to a discharge in a cavitation bubble because of the formation of electric charges on its walls (Margulis, 1995).

Noltingk and Neppiras advanced the thermal theory; the "hot spot" theory, by which a temperature of about $10^4$ K develops in a cavitation bubble during its adiabatic collapse. The sonoluminescence that appears is explained as black body emission at thermal equilibrium (Noltingk and Neppiras, 1950).

The second most accepted theory is "electrical theory" by Margulis (Margulis, 1995). This theory suggests that during bubble formation and collapse, enormous electrical field gradients are generated and these are sufficiently high to cause bond breakage and chemical activity.

The supercritical theory recently proposed by Hoffmann and co-workers (Hua et al., 1995), suggests the existence of a layer in the bubble-solution interface where temperature and pressure may be beyond the critical conditions of water (647 K, 22.1 MPa) and showed that supercritical water is obtained during the collapse of cavitation bubbles generated sonolytically.

The plasma theory by Lepoint and Mullie (Lepoint and Mullie, 1994), also suggests extreme conditions associated with the fragmentative collapse is due to intense electrical fields and seems not to involve true implosion. They compared the origin of cavitation chemistry to corona-like discharge caused by a fragmentation process and supported and indicated the formation of microplasmas inside the bubble.

The most generally accepted explanation of the origin of sonochemistry is the "hot spot" theory, in which the potential energy given the bubble as it expands to maximum size is concentrated into a heated gas core as the bubble implodes.

The principal cause of the sonochemical reactions in aqueous media is considered to be the pyrolysis of water vapor due to the extreme conditions experienced during the implosive collapse of a cavity. The pyrolysis of water molecules cases the formation of hydroxyl and hydrogen radicals;

$$H_2O \rightarrow \bullet OH + \bullet H \qquad (2.16)$$

These radicals may recombine to form water molecules;

$$\bullet OH + \bullet H \rightarrow H_2O \qquad (2.17)$$

or, form hydrogen peroxide;

$$\bullet OH + \bullet OH \rightarrow H_2O_2 \qquad (2.18)$$

or, start radical chain reactions with various radical side products and end products;

$$H\bullet + O_2 \rightarrow HO_2\bullet \qquad (2.19)$$

$$H_2O\bullet + H\bullet \rightarrow H_2\, O_2 \qquad (2.20)$$

$$H_2O\bullet + H_2O\bullet \rightarrow H_2\, O_2 + O_2 \qquad (2.21)$$

$$\bullet OH + H_2O \rightarrow H_2\, O_2 + O\bullet \qquad (2.22)$$

$$H\bullet + H\bullet \rightarrow H_2 \qquad (2.23)$$

$$H\bullet + \bullet OH \rightarrow H_2O \qquad (2.24)$$
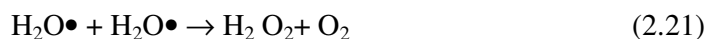
Some of the hydroxyl radicals and other reactive species formed through the chain reactions. may react with impurities present in water at different locations in association with the imploded cavity, depending on the properties of the impurities.

## 2.3.2. Sonochemical Reaction Sites

Experience in homogenous sonochemistry has shown that there are three potential sites for chemical reactions in ultrasonically irradiated liquids; (i) the cavitation bubble itself, (ii) the interfacial sheath between the gaseous bubble and the surrounding liquid, and (iii) the bulk solution (Weavers et al, 1998; Suslick et al, 1986).

In water or effluent treatment practices, organic pollutants may be destroyed either at the first two sites upon combined effects of pyrolytic decomposition and hydroxylation, or in the bulk solution via oxidative degradation by hydroxyl radicals and hydrogen peroxide (Ince et al., 2000). The intensity of oxidation in the bulk solution is exclusively related to the quantity of available uncombined hydroxyl radicals, as they migrate into the aqueous phase during the collapse of cavity bubbles. The rate of free radical transfer from the bubble interior (and its interfacial sheath) into the solution bulk depends on the lifetime and collapse duration of cavities, and therefore, the intensity of the pressure, the geometry of the reactor and frequency of the applied ultrasonic waves.
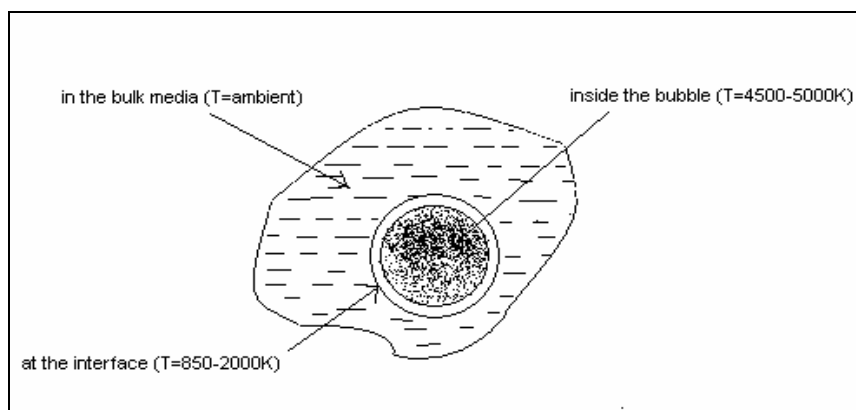


Figure 2.10. Possible sites of chemical reactions in homogeneous reaction media (Ince et al., 2001).

### 2.3.3. Parameters Affecting Sonochemical Reaction Systems

Assuming that the critical distance for water is $10^{-5}$ cm, then the tensile stress necessary to rupture water can be calculated to be of the order of 10 000 atmospheres (Mason, 1990). This calculation assumes that water is completely pure. In practice the required pressure to cause water to cavitate occurs at much lower applied acoustic pressures than such calculations would suggest. This is due to the presence of weak spots which lower the tensile strength of the liquids.

Many parameters affect the sonochemistry of liquids, and it would seem that for almost all the variable parameters which influence cavitation, there is an optimum value (Berlan and Mason, 1992).

2.3.3.1. Frequency.    To completely rupture a liquid and hence provide a void, which may subsequently become filled with gas or vapour, requires a finite time. For sound waves with high frequencies, the time required to create the bubble may be longer than that available during the rarefaction cycle. At 20 kHz for example, the rarefaction cycle lasts 25 μs, attaining its maximum negative pressure in 12.5 μs, whereas at 20 MHz the rarefaction cycle lasts only 0.025 μs. Thus it might be anticipated that as the frequency increases the production of cavitation bubbles becomes more difficult to achieve in the available time and that the greater sound intensities (i.e. greater amplitudes) will need to be employed, over these shorter periods, to ensure that the cohesive forces of the liquid are overcome.

Thus the treshold for aerated water is lower than that for gas free water and the treshold intensity increases with increase in frequency. In fact ten times more power is required to make water cavitate at 400 kHz than at 10 kHz (Mason and Lorimer, 2002).

2.3.3.2. Properties of Solute. The sonolysis of organic compounds depends on the caharacteristics of the solute as well as the sonication conditions. Hydrophobic and volatile organic compounds are expected to degrade mainly by thermal decomposition inside the cavitataion bubble, while hydrophillic and less volatile compounds degrade mainly by hydroxyl radicals oxidation (Shemer and Narkis, 2004; .Hoffmann et al, 1996).

2.3.3.3. Properties of Solvent. The formation of voids or vapour filled microbubbles in a liquid requires that the negative pressure in the rarefaction region must overcome the natural cohesive forces acting within the liquid. It follows that cavitation should be more difficult to produce in viscous liquids, or liquids with higher surface tensions, where the forces are stronger and waves with greater amplitude and hence greater intensity will be necessary. Once a liquid produces cavitation bubbles however, the temperature and the pressure effects resulting from the bubbles collapse will be greater, since the pressure at the start of the collapse will be larger.

Another solvent factor effecting cavitation bubbles is that of vapour pressure. Since vapour pressure and temperature are directly related, the issues discussed for the solvent temperature apply for vapour pressure as well (Mason and Lorimer, 2002).

2.3.3.4. Power Intensity. In general an increase in the intensity will provide for an increase in the sonochemical effects. Cavitation bubbles, initially difficult to create at higher frequencies (due to the shorter time periods involved in the rarefaction cycle) will now be possible, and since both collapse time and the temperature and the pressure on the collapse are dependent on the pressure in the liquid at the time of collapse, bubble collapse will be more violent. However, it must be realised that intensity can not be increased indefinitely, since the maximum bubble size is also dependent upon the pressure amplitude.

2.3.3.5. Properties of Saturating Gas. Employing gases with large polytropic ratio values ($\gamma$) will enhance the adiabatic conditions in the collapsing bubble and improve sonochemical effects. For this reason monatomic gases (He, Ar, Ne) are used in preference to diatomic gases ($N_2$, air, $O_2$). However it must be remembered that this dependence on $\gamma$ is a simplistic view, since the sonochemical effects also depend on the thermal conductivity of the gas, even if a strict relationship between the properties of gases and the sonochemical effect has not been observed.

Increasing the gas content of a liquid leads to the lowering of both cavitation treshold and the intensity of the shockwave released on the collapse of the bubble. The treshold is lowered as a consequence of increased number of gas nuclei (or weak spots) present in the liquid, whils the cavitational collapse intensity is decreased as a result of the greater cushioning effect in the microbubble (Mason and Lorimer, 2002).

2.3.3.6. Solids as Catalysts.  The addition of solid catalysts, such as glass beads, ceramic disks, $SiO_2$, $Al_2O_3$ and talc into the reaction medium is a common method for enhancing the cavitation effects (Ince et al., 2000). The presence of solids at a given particle size causes higher attenuation with higher frequencies and particle concentrations. On the other hand, sonolysis of water in the presence of quartz particles leads to higher sonochemical yields of e.g. hydrogen peroxide due to the particles acting as permanent nuclei for cavitation bubbles (Keck et al., 2002).

2.3.3.7. Temperature. In general the threshold limit has been found to increase with decrease in temperature. This may in part due to increases either in the surface tension or

viscosity of the liquid as the temperature decreases, or it may be due to decreases in the liquid vapor pressure (Mason and Lorimer, 2002).

## 2.4. Use of Advanced Oxidation Methods for Trihalomethane Removal

It has been demonstrated in many studies that the free-radical mediated degradation of halogenated organic compounds may eventually lead to complete mineralization, i.e., $CO_2$ and the respective hydrogen halide acids. Several molecular organic intermediates such as halogenated alcohols, aldehydes, ketones and organic acids have been identified en route to these inorganic substrates.

The chemistry leading to mineralization is based on three essential cleavage processes; the scission of

    i)       carbon-carbon bonds

    ii)      carbon-hydrogen bonds

    iii)    the elimination of the halide atoms

A higher amount of energy is usually required for the rupture of carbon-carbon bonds (C-C, C=C, C≡C). Free radical attack and, for unsaturated compounds, ozonation, are probably the most efficient chemical methods for this. Mechanistically, they include displacements, addition (to multiple bonds), and insertion (ozonation) reactions. The energy necessary for the release of the halogen, either as halogen atom, or halide ion is usually lower. In aqueous systems any halide formation benefits significantly from the solvation energy. Owing to the differences in electronegativity between the atoms involved, redox-active initiators are particularly efficient.

Although the modern methods applied for the degradation of pollutants are commonly referred to as "Advanced Oxidation Techniques" (AOTs), the corresponding processes including halogenated organic compounds comprise both oxidations and reductions.

$$\bullet \, OH + HCCl_3 \rightarrow H_2O + \bullet \, CCl_3 \tag{2.25}$$

Oxidations, in fact practically never involve the carbon-halogen bond directly. Such a process is thermodynamically not feasible. An oxidative initiation is rather typically limited to an attack at the C-H bond

An example is the $\bullet$ OH reaction with chloroform (equation 2.25). Such a process requires the presence of at least one C-H bond. Accordingly $CCl_4$ can not be attacked oxidatively. Reactions of $\bullet$ OH with double bonds and aromatic systems typically proceed via an addition (Equation 2.26), irrespective of the presence or absence of halogen substituents.

$$\bullet\, OH + > C = C < \rightarrow > C \bullet - C(<) - OH \tag{2.26}$$

A different approach for the degradation of halogenated compounds is an initial reductive step by radicals capable of acting as electron donors. This includes also solvated electrons, conduction band electrons and electrochemically generated electrons. It is however, necessary that the electron donor or free electron has a sufficiently negative redox potential. Thus, chloroform is readily reduced by hydrated electrons ($E° = -2.7$ V), while conduction band electrons available in, for example, UV irradiated $TiO_2$ ($E° = -0.3$ V) do not possess sufficient reductive power. This renders radiation chemically (electron-beam) generated electrons an extraordinarily efficient reductive initiator.

Mechanistically, reduction leads to the cleavage of a halide anion via a transitory state in which the incoming electron is temporarily accommodated in an antibonding, i.e., bond-weakening $\sigma^*$ orbital within an overall three electron (2 $\sigma$/1 $\sigma^*$) bond.

$$e_{aq}^- + CCl_4 \rightarrow (Cl_3 \therefore Cl)\text{-} \rightarrow \bullet CCl_3 + Cl^- \tag{2.27}$$

Although a direct cleavage of a halogen atom can practically only be achieved via a reductive process all subsequent degradation steps typically involve participation of oxygen. This provides the justification to include the reductively initiated degradation of halogenated organics into the AOTs. Taking the above chloroform / carbon tetrachloride example the trichloromethyl peroxyl radical is the starting point for the eventual complete

mineralization (Equation 2.28), formulated only with respect to essential products and intermediates).

$$\bullet CCl_3 \rightarrow \rightarrow \bullet OOCCl_3 \rightarrow \rightarrow COCl_2 \rightarrow \rightarrow CO_2 + 3\ Cl^- \tag{2.28}$$
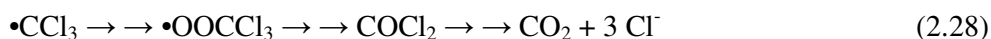
While the reductive and oxidative initiation of halogenated aliphatics, from the mechanistic point of view, is a more or less straightforward and simple process, this is not the case for halogenated aromatics (Asmus and Flyunt, 2003).

## 2.5. Application of Ultrasonic Methods for Trihalomethanes Removal

Henglein and Fischer investigated the complete products of sonolysis of pure chloroform at 300 kHz, with a GC / MS (Henglein and Fisher, 1984). The main products they found to be formed at sonolysis of chloroform are listed in Table 2. The authors found that the highest HCl yield was obtained with oxygen saturation of the solution followed by helium, argon, and hydrogen; nitrous oxide and carbon dioxide yielded no HCl. In the case of oxygen the yields of all the organic products were smaller than under helium by a factor of 8, and mainly $CO_2$ formed. The total rate of conversion was $4.5 \times 10^{-3}$ M/h of consumed chloroform, under the same conditions $H_2O_2$ was formed in aerated water at a rate of $3.3 \times 10^{-3}$ $Mh^{-1}$, showing that sonolytical reactions occur with comparable yields in chloroform and water. The authors have repeated the experiments with carbon tetrachloride and have found a rate of decomposition smaller by more than a factor of ten than for chloroform. The authors conclude that the large number of products observed in Table 2.7, the sonolysis of chloroform is not specific. Henglein and Fisher (1984) suggested that one mode of decomposition of chloroform must consist of breaking of single bonds

$$CHCl_3 \rightarrow \bullet CHCl_2 + \bullet Cl \tag{2.29}$$

or

$$CHCl_3 \rightarrow \bullet CCl_3 + \bullet H \tag{2.30}$$
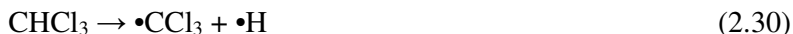
However all the products also appear which could be formed from combinations of the carbenes CHCl and $CCl_2$. A second mode of decomposition by molecular elimination was therefore postulated

$$CHCl_3 \rightarrow CCl_2 + HCl \tag{2.31}$$

$$CHCl_3 \rightarrow CHCl + Cl_2 \tag{2.32}$$

From the abundances of $CHCl_2$, $CCl_3$ $CCl_2$ and CHCl groups in the products one derives that reaction 2.31 is roughly three times more frequent than reaction 2.32, and that the molecular processes 2.31 and 2.32 occur about as twice as frequently as the radical processes 2.29 and 2.30.

Table 2.7. Product yield and material balance in the sonication of chloroform irradiated under helium for 1.5 hours at 300 kHz (Henglein and Fisher, 1984).

| Product | | Concentration $(10^{-1}$ M$)$ | Sum |
|---|---|---|---|
| Inorganic | $H_2$ | 0 | 46 |
| | HCl | 46 | |
| Saturated organic | $CH_2Cl_2$ | 5 | 28 |
| | $CCl_4$ | 10 | |
| | $C_2H_2Cl_4$ | 2 | |
| | $C_2HCl_5$ | 7 | |
| | $C_2Cl_6$ | 4 | |
| Unsaturated organic | Trans-$C_2H_2Cl_2$ | <1 | 13 |
| | $C_2HCl_3$ | 4 | |
| | $C_2Cl_4$ | 8 | |

Their experiments could not, however, distinguish between the formation of carbenes via true first order elimination as it was expressed by equations 2.31 and 2.32, and second order processes in which two radicals are involved, such as the disproportionation reactions

$$2 \bullet CHCl_2 \rightarrow CH_2Cl_2 + CCl_2 \qquad\qquad (2.33)$$

and

$$\bullet CCl_3 + \bullet CHCl_2 \rightarrow CCl_4 + CHCl \qquad\qquad (2.34)$$
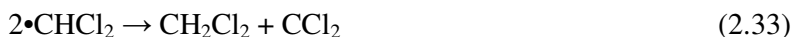
In order to understand why carbenes are formed more frequently in the sonolysis of chloroform, the authors guessed that, one must either assume an additive carbene formation via true molecular elimination or a different type of behavior of the radicals. Such a different kind of behavior could indeed be expected, as reactions 2.33 and 2.34 probably do not occur in the liquid but in the gas bubbles. It is known from free radical chemistry that the ratio of disproportionation to combination of free radicals is strongly dependent on the phase. Furthermore, the high temperatures of several thousand K known to exist in the cavitation bubbles may considerably change the ratio of disproportionation to combination. The thermal decomposition of chloroform has been studied by Shilov and Sabirova (Shilov and Sabirova, 1960), who came to the conclusion that carbenes occur as the most important intermediates of thermal decomposition. Henglein and Fischer also came to the conclusion that carbenes occur as the most important intermediates of decomposition. The authors also found that the decomposition of chloroform was enhanced in the presence of c-hexene, which was explained by the scavenging of chlorine atoms, which in the absence of c-hexene undergo back reactions to re-form chloroform. The authors also suggest that volatile solutes that reduce the polytropic ratio of the mixture inside the cavitation bubble quench the sonolysis of water.

Shemer and Narkis employed ultrasonic irradiation at 20 kHz at a power density of 0,184 W/mL to degrade the trihalomethanes $CHCl_3$, $CHBrCl_2$, $CHBr_2Cl$, $CHBr_3$, and $CHI_3$ (Shemer and Narkis, 2005a). The authors studied the reaction kinetics of the target compounds in single component aqueous solutions with 10 mg/L initial concentration. They found that the sonodegradation rates of the studied THMs increased as their vapor pressure increased. The authors observed a linear relationship between the half lives of the target compounds and their log $K_{ow}$ values. They also report that the main sonodegradation mechanism of $CHCl_3$, $CHBrCl_2$, $CHBr_2Cl$ and $CHBr_3$ was pyrolysis. They conclude that the vapor pressure of the THMs is the most important parameter affecting the

sonodegradation kinetics and efficiency. The bond dissociation energy and hydrophilic/hydrophobic characteristics of the target compounds were found to be of secondary importance.

Shemer and Narkis (2005b) investigated the relative efficiencies of the advanced oxidation processes of ultrasonic irradiation, hydrogen peroxide, Fenton's oxidation and the combinations of these processes on the destruction and removal of $CHCl_3$, $CHBrCl_2$, $CHBr_2Cl$, $CHBr_3$ and $CHI_3$ in another study. They found that the $H_2O_2$ process had no effect on the THMs sonodegradation. The coupled ultrasound and Fenton's process enhanced the degradation of $CHBr_3$ but did not effect the degradation of $CHCl_3$, $CHBrCl_2$ and $CHBr_2Cl$. $CHI_3$ was degraded by the Fenton's process alone, during sonication Fenton's treatment. The combination of sonication with $H_2O_2$ or Fenton's reagent did not affect the mineralization of the THMs aqueous mixture. The authors used a 20 kHz temperature controlled cell operated at the power density of 0.184 W/mL with no sparging.

The authors also added tert-butanol, which is a known radical scavenger, to determine the sonodegradation mechanism of the THMs. They found that tert-butanol had no significant influence on the sonochemical degradation of $CHCl_3$, $CHBrCl_2$ and $CHBr_2Cl$ when all radical oxidation reactions were inhibited. They thus concluded that, the main degradation mechanism of $CHCl_3$, $CHBrCl_2$ and $CHBr_2Cl$ was pyrolysis, whereas the main sonodegradation mechanism for $CHBr_3$ was free radicals oxidation.

Shemer and Narkis applied ultrasonic irradiation at 20 kHz to synthetic aqueous THM mixtures of $CHCl_3$ + $CHBrCl_2$ + $CHBr_2Cl$ + $CHBr_3$ + $CHI_3$, containing 10 mg/L of each constituent (Shemer and Narkis, 2005c). Their findings showed that the removal of all the compounds fitted first order reaction kinetics. They found that the fastest removed THM was chloroform with a rate constant of $24.2 \pm 0.2 \times 10^{-3}$ $min^{-1}$, followed by $CHBrCl_2$ with k = $19.9 \pm 1.2 \times 10^{-3}$ $min^{-1}$ , $CHBr_2Cl$ with k= $13.5 \pm 0.6 \times 10^{-3}$ $min^{-1}$ , and $CHBr_3$ with k= $8.5 \pm 0.5 \times 10^{-3}$ $min^{-1}$ .

Shemer and Narkis also studied the effect of different parameters on the aqueous sonolysis of five trihalomethanes (Shemer and Narkis, 2005 b). They found that initial pH of solution did not affect the reaction rate, whereas, increased solution temperature

increased the reaction rate. They found that the sonodegradation rate was not affected by the initial solute concentration in the range from 0.1 mg/L to 10 mg/L, but was inhibited when the initial concentration of each solute was increased to 100 mg/L. The authors conclude that this effect might suggest that the mass transfer of the pollutants into the bubble and the interfacial region depends on the organics and by-product concentration. An increase in the organic compounds concentration leads to a decrease in cavitation bubble collapse temperatures, since more organic molecules enter the cavitation bubbles as their initial concentration was increased. A decrease in the bubble collapse temperature leads to decreasing degradation rates.

Bhatnagar and Cheung investigated the ultrasonic destruction of chlorinated volatile organic compounds in water with a 20 kHz ultrasonic generator (Bhatnagar and Cheung, 1994). They irradiated aqueous solutions of methylene chloride, chloroform, carbon tetrachloride, 1,2-dichloroethane, 1,1,1-trichloroethane, trichloroethylene, perchloroethylene in concentrations ranging from 50 to 350 mg/L at a power density of 0.1 kW/L. They observed that the concentration of solutes decreased rapidly accompanied with rapid decrease of pH in all cases, indicating that a significant fraction of chlorine was converted to HCl or other acid species. The authors reported that the GC/MS analysis indicated that no other chlorinated products were formed. They also found that the initial pH of the solution and the presence of other chlorinated VOC's had little effect upon the destruction of the compounds. Experimental data of removal of all C1 compounds indicated first order reaction kinetics. The authors presume that the primary reaction pathway for these compounds to be thermal dissolution in the cavities based on literature. They also observed that as the vapor pressure of the C1 compounds increased, the first order rate constant seemed to go down. The authors also reported that headspace analysis showed that relatively little VOCs were volatilized in the absence of gas sparging, and that nearly all of the removed VOCs were destroyed rather than volatilized.

## 3. MATERIALS AND METHODS

### 3.1.    Materials

#### 3.1.1.  Chemical Materials and Glassware

Deionized water used for synthetic samples was produced from distilled water daily, using a Labconco deionized water purification apparatus. The apparatus produces deionized water with a conductivity of approximately 1.0 μS/cm.

Chloroform of 99.8 per cent purity was obtained from Riedel de Haen. Bromoform, Bromodichloromethane, Dibromochloromethane, and Humic Acid were obtained from Fluka.

Pentane for trace analysis of highly volatile halogenated hydrocarbons was obtained from Fluka and used as the solvent for liquid-liquid extraction of trihalomethanes with micro-ECD detection.

Pure argon that was used for sparging the sonochemical cells was of 99.995 % (v/v) purity and oxygen was of 99.5 % (v/v) purity. Compressed air was used as was without any further purification.

Mixed gravimetric trihalomethanes standards of 100 μg/mL and 200 μg/mL obtained from Supelco were used for GC calibration.

Both nitrogen and helium used for gas chromatography were of high purity of over 99.999 % by volume. The same nitrogen was also used as sparging gas in sonication reactors in appropriate experiments. Helium was also used as purging gas in Purge and Trap analyses.

High purity synthetic air produced through mixing of nitrogen and oxygen was used as the carrier gas of the TOC analyzer.

All the glassware were cleaned through repeated washing with deionized water and baked in the oven at 100°C for 12 hours before reuse to ensure removal of volatile contaminants.

### 3.1.2. Experimental Equipment

3.1.2.1. 20 kHz Reactor.



Figure 3.1. Photographic view of 20 kHz system

The system consists of a Bandelin Sonopuls HD2200 probe type transducer inserted into a 100 mL glass cylindrical cell equipped with a cooling jacket for temperature control. Area of the titanium tip used was 2.5 cm$^2$. A 180 W generator was used to emit ultrasonic waves at 20 kHz. The horn was submerged approximately 2 cm into the test solution. Allowing for freeboard, the maximum reaction volume is 80 mL. Reaction volumes smaller than 80 mL were not feasible due to overheating. The generator/reactor system was placed in a glass cubicle with polyurethane isolation material to reduce excessive audible sound leakage. Sparging gas was introduced  through a glass pasteur pipette to the bottom

of the reactor. Due to the placing of the horn and reactor shape restrictions the reaction volume is open to the atmosphere and could not be sealed. The small and rather rigid reaction volume also reduces the flexibility of the reaction system.

3.1.2.2. 300 kHz Reactor. The system is made up from a generator (Undatim Ultrasonics-Belgium) coupled with a 150 mL glass cylindrical reactor with a plate-type transducer placed at the bottom of the reaction vessel. The minimum reaction volume is 100 mL. The piezoelectric transducer has a vibrational area of 22 cm$^2$. The generator produces sound waves at 300 kHz at a maximum power output of 25 W. Sparging gas is introduced through a glass pasteur pipette to the bottom of the reactor. Although the reactor is normally open to the atmosphere, its shape allows it to be sealed in a gastight manner and enables controlled stripping experiments.
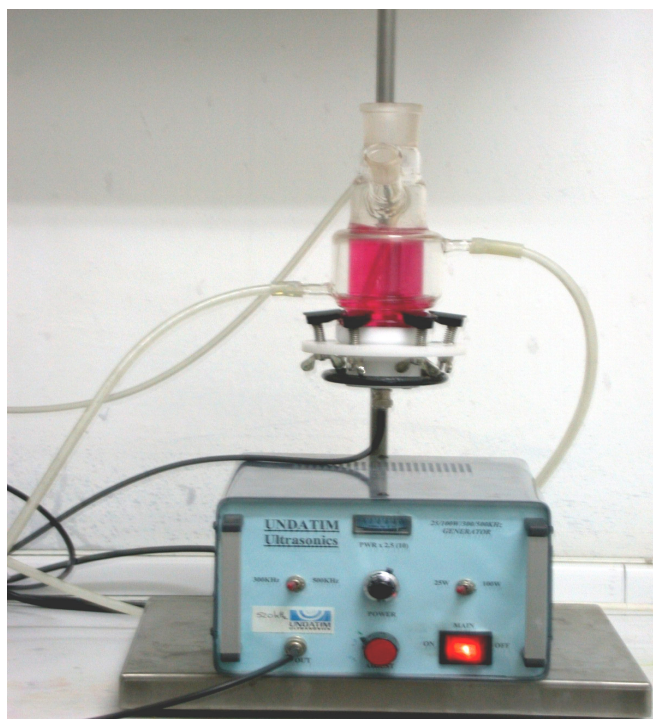


Figure 3.2.  Photographic view of 300 kHz system

3.1.2.3. 520 kHz Reactor. The Undatim Ultrasonics-Belgium generator can alternatively be used to produce sound waves at 520 kHz at 100 W.  The reactor has a plate-type piezoelectric transducer with a vibrational area of 22 $cm^2$, placed at the bottom of a 1200 mL cylindrical glass vessel, emitting sound waves at 520 kHz. The minimum reaction volume is 300 mL. The sparging gas is introduced to the bottom of the reactor with a glass pasteur pipette. Due to the large volume of the vessel and relatively low power output, the reactor contents do not mix as rigorously as in 20 kHz and 300 kHz systems. In order to achieve better mixing, a peristaltic pump was used to pump the ingredients of the reactor at a rate of 600 mL/min, withdrawing from the bottom of the reactor and discharging just below the surface, thus avoiding further contact with the atmosphere. The reactor surface is open to the atmosphere.
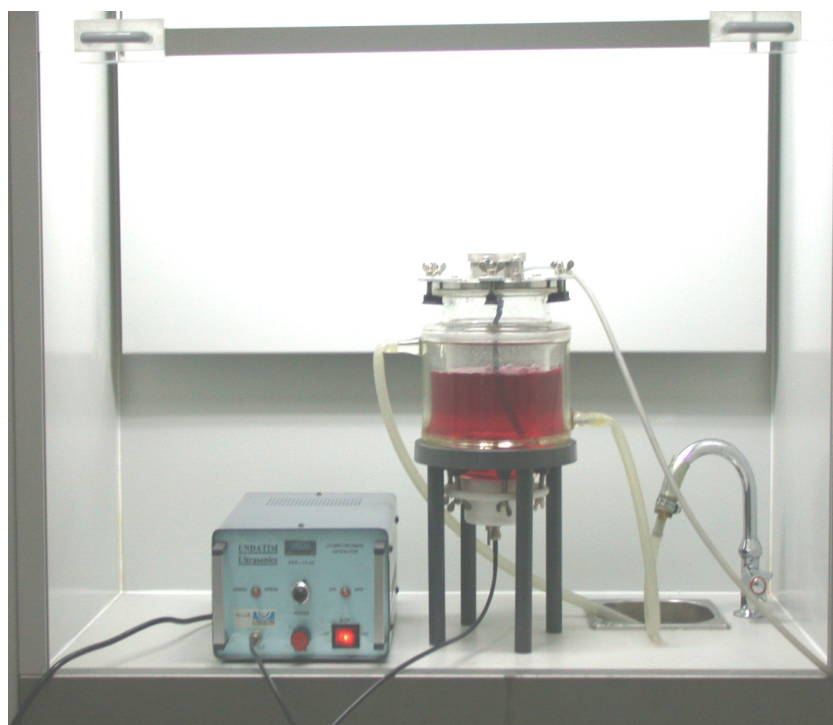


Figure 3.3. Photographic view of 520 kHz system

## 3.2. Methods

### 3.2.1. Experimental Methods

Synthetic samples were prepared by dilution of a stock solution prepared by mixing target compound with deionized water daily. The stock solution was kept in a refrigerator at 4°C for a maximum of three days, and re-prepared after the third day. The sample solutions were prepared daily and their initial concentrations were measured along with the data obtained from that experiment within the same day.

The removal studies were conducted at 20 kHz, 300 kHz and 520 kHz systems. Argon was used as sparging gas to improve ultrasonic cavitation efficiency unless otherwise stated. The experimental volumes used were 80 mL for the 20 kHz system, 150 mL for the 300 kHz system, and 300 mL for the 520 kHz system unless otherwise stated. Gas sparging of the reactors were not started before the initiation of ultrasonic irradiation to prevent excessive loss of solutes. The temperatures of the reactors were kept constant at $20 \pm 0.5$°C throughout the experiment with the use of the cooling jackets.

The kinetic studies were conducted through half-hour long experiments. Samples were analyzed at the beginning of the experiment to avoid the effect of depletion and at least seven time dependent samples were taken to ensure good representation.

### 3.2.2. Analytical Methods

3.2.2.1. Calorimetric Measurements. An ultrasonic irradiation system transforms electrical energy to vibrational energy, which is then transmitted into the sonicated reaction medium. Part of it is lost to produce heat, and another part produces cavitation, but not all of the cavitation energy produces chemical and physical effects. Some energy is reflected and some is consumed in sound re-emission. Hence, there can be significant differences between the power supplied from the generator and that delivered into the reactor. In a pure liquid, one might assume that almost all of the mechanical energy is transformed to heat by absorption. Of the methods available to measure the amount of ultrasonic power entering a sonochemical medium, the most common and easiest is calorimetry, which

involves a measurement of the initial rate of heating produced when a system is irradiated by ultrasound (Mason, 1999). The method involves the measurement of the temperature rise T against time for about 30 seconds, using a thermocouple placed in the reaction vessel. From T versus t data, the temperature rise dT/dt can be estimated either by curve fitting the data to a polynomial in t, followed by constructing a tangent to the curve at time zero. The ultrasonic power ($P_d$) actually entering the system can then be calculated by substituting the value of dT/dt into Equation 3.1 (Mason, 1999; Mason and Cordemans, 1998):

$$P_d = (dT/dt).Cp.M \tag{3.1}$$

where $P_d$ = Power dissipated in the system ,W

Cp= specific heat of water, 4.184 J/g.°C

dT/dt = the change in temperature at a certain time interval, °C/sec

M= mass of water in the reaction vessel, g

The power which is calculated by calorimetric method is used to determine the ultrasonic intensity in the reactor. Ultrasonic intensity may have the unit W/cm$^2$ (power per unit emitting area), or W/mL (power per unit volume of water in the reactor).

3.2.2.2. THM Analysis. THM concentrations were determined by gas chromatographic methods. An Agilent 6890N gas chromatograph equipped with a split/splitless injection port, HP-1 capillary column and μ-ECD detector were used for the analyses. Aqueous samples were introduced through an Agilent 7683 automatic injector after liquid-liquid extraction with pentane. The GC parameters were set to be in compliance with USEPA 551.1 method with minor modifications for faster analysis.

THM concentrations in the aqueous phase were determined by a modification of USEPA 551.1 method. In the USEPA method the initial oven temperature is 35 °C and the initial temperature is maintained for 1 minute before the temperature ramp begins. In the modified version used for analyses initial temperature was 50 and the 1 minute initial lag was omitted to achieve faster analysis upon observation of good chromatographic separation. The analytical conditions of the method are given in Table.3.2.

Table 3.1. Gas Chromatography system used in trihalomethanes analyses

| Gas Chromatograph | Agilent 6890N |
|---|---|
| Injection Port | Split/Splitless |
| Injector | Agilent 7683 Automatic Injector, fitted with a 10μL injector |
| Column | HP-1 19095Z-123 (100% methyl siloxane) 30 m × 0.53mm (Inner Diameter)× 2.65 μm (film thickness) |
| Detector | μ-ECD |
| Data Handling | HP Chemstation |

Table 3.2. Analytical conditions of the chromatography system for trihalomethanes analyses

| Inlet | Splitless mode, 250°C |
|---|---|
| Injection Volume | 1 μL |
| Carrier Gas | Helium |
| Column Flow | Constant at 5.5 mL/min |
| Oven | Initial Temperature 50°C Temperature Ramp 10°C/min to 125°C |
| Detector Temperature | 340°C |
| Detector Make-Up gas | Nitrogen, constant at 60 mL/min |

The samples were prepared for GC injection by liquid-liquid extraction. 1 mL aqueous sample was vigorously mixed with 0.5 mL solvent in 2 mL automatic injector bottles for 45 seconds and injected within the same day from the unopened bottles to avoid dilution and contamination. Pentane was used as the extraction solvent. The automatic injector bottles used for liquid-liquid extraction were 2 mL glass bottles with plastic screw type caps and teflon covered rubber septa. Glass bottles and plastic screw type caps were reused after repetitious washing with deionized water and drying in the oven at 100°C for at least 12 hours, whereas the septa were discarded after single use. In order to avoid cross contamination and bubble formation in the syringe, the injector syringe was washed twice with pentane and twice with the sample and pumped twice with the sample before, and washed twice again with pentane after each injection.

Pentane and deionized water to be used in experiments was screened daily for the analytes and the necessary corrections were performed on the analytical results accordingly.

An external standard GC calibration curve was generated using certified gravimetric standards obtained from Supelco and Agilent. The calibration was repeated upon observation of changes in baseline or in expected peak height. The extraction solvent contained an unknown peak with an approximate height of 5000 Hz that eluded 0.2 minutes after chloroform. This peak was used as an internal standard to check on the accuracy of injection volume.
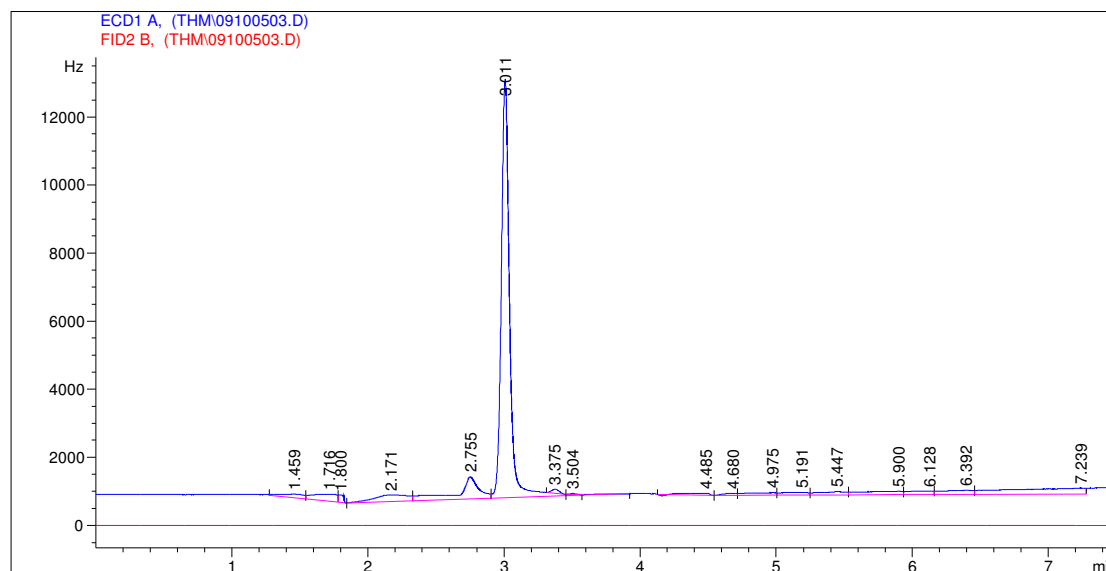


Figure 3.4. Chromatogram output of Pentane showing unknown peak with retention time of 3.011 minutes, used as ISTD

3.2.2.3. TOC Analysis. A Shimadzu TOC-V CSH instrument equipped with a high sensitivity catalyst was used for Total Organic Carbon analyses. Oxidative combustion followed by infrared analysis of carbon dioxide is the detection mechanism of the instrument that measures the amount of total carbon (TC) in water. The instrument also measures the amount of inorganic carbon (IC) in water through acidification with HCl and sparging and subsequent measurement of sparged carbon dioxide. As the sparged carbon dioxide is carried directly to infrared detector, without going through the combustion tube, the carbon content of volatile compounds that also volatilize during sparging do not

interfere with the IC measurement results. The total organic carbon is calculated by subtraction of IC value from the TC value of the same sample.

3.2.2.4. pH, ORP and Conductivity Measurements. pH measurements were done using a WTW-pH 330 pHmeter with a SenTix 41 pH electrode. The probe was inserted into the reaction volume and the first reading was taken when it stabilized which usually took approximately 5-10 minutes. Upon the initiation of the experiment the pH readings were taken at every 30th second during the initial 5 minutes of the experiment and then at every 60th second till the end of 30 minutes.

Conductivity measurements were conducted using a WTW LF 320 conductivity meter with a WTW tetracon 325 probe. The probe was inserted into the reaction volume and the first reading was taken just before the beginning of the experiment along with pH and ORP measurement. Although the conductimeter readout stabilized much faster than pHmeter and ORP meter, all three were readings were recorded simultaneously for the sake of compatibility. During the first five minutes of the experiments a conductivity measurement was taken at each 30th second, and from the sixth minute onwards at each sixtieth second till 30 minutes.

Oxidation-reduction potential was measured using a Cole-Parmer Oakton ionmeter. The response of the probe was checked using a Fe solution before each experiment. The initial reading was taken when the readout stabilized which took 5-10 minutes approximately. During the first five minutes of the experiments an ORP reading was recorded at each 30 second and from the sixth minute onwards a reading was recorded at each sixtieth second.

3.2.2.5. Toxicity Measurements. Toxicity measurements were conducted using a Microtox Model 500 Toxicity Analyzer. The Microtox test utilizes living bioluminescent bacteria (*V.fisheri*) for the measurement of toxic effect of samples. The test measures the light output of the luminescent bacteria after they have been exposed to a sample of unknown toxicity and compares it to the light output of a control (bacteria-reagent blank) that contains no sample. A difference in the light output is attributed to the effect of the sample on the organisms (Microtox Manual, 1992). The degree of light loss (an indication of

metabolic inhibition in the test organisms) indicates the degree of toxicity of the sample. Microtox 100 % protocol was employed for the determination of a dose-response curve, on which the desired effective concentration is found that causes a particular percent of light loss.

Due to the very low levels of toxicity of the samples, 100 % test protocol was preferred as test protocol over the basic test protocol. This protocol enables the testing of higher sample concentrations (up to 90 % sample) but the samples are only compared to the reagent control and can not be normalized for pipetting errors. These errors were minimized by running the samples in triplicates. All the operations including sample preparation, osmotic adjustment, serial dilutions and data processing were carried out by reference to the 100 % Test Protocol of Microtox Assay. According to the 100% test, a $\Gamma$ % value was calculated for each dilution with the formula:

$$\Gamma \% = I_{tc} / I_t \quad - 1 \tag{3.2}$$

where $I_{tc}$ is the light level (I) at incubation time (t) of the blank control (c)

$I_t$ is the light level (I) at incubation time (t) for various sample concentrations.

The calculated $\Gamma$ % values were plotted versus the sample concentrations on a log-log scale. The EC50 value, which is the concentration where the light emission of the test bacteria is inhibited by 50%, is the concentration where the straight line that passes through the data points intersects with the log gamma value of 1.

3.2.2.6. Hydrogen Peroxide Analysis. Hydrogen peroxide ($H_2O_2$) determination was carried out following the procedure described by Klassen et.al. (1994). The triiodide method is based on the reaction of ($I^-$) with hydrogen peroxide to form triiodide ion ($I_3^-$), which has a strong absorbance at 351 nm. The analysis of $H_2O_2$ at concentrations as low as 1 mM is conveniently proceeded by determining the yield of $I_3^-$ formed when hydrogen peroxide reacts with KI in a potassium hydrogen phthalate buffered solution containing ammonium molybdate tetrahydrate as catalyst. Two reactant solutions, A and B, were prepared as described below and 2.5 mL of each was mixed with oneanother and 1 mL of sample to record the absorbance at 351 nm. A calibration curve was prepared using reagent

grade $H_2O_2$ in the concentration range of 0.11 mg/L-1.1 mg/L to allow the conversion of absorbance values to concentration units.

Solution A: 33 g of KI, 1g of NaOH and 0.1 g of ammonium molybdate tetrahydrate diluted to 500 mL with deionized water. The solution was stirred for 1 h to dissolve the molybdate. It must be kept in dark in order not to cause $I^-$ to oxidize.

Solution B: 10 g of potassium hydrogen phthalate was dissolved in 500 mL to act as the buffer solution

# 4. RESULTS AND DISCUSSIONS

## 4.1. Determination of Sonochemical Characteristics of the Reaction Systems Used

It is a matter of necessity to characterize the behaviour of sonoreactors in order to identify the active processes and to provide an accurate picture of the reactive environment in the sonoreactor, as different behaviour can be observed even when using the same generator with different reactors (Faid et al., 1998).

The chemical and physical effects of ultrasonic irradiation are closely dependent on the electrical power applied, the resulting cavitation events and the hydroxyl radical formation characteristics of the generator/reactor systems in use. In order to achieve comparability between the results of studies conducted by different researchers with various equipments and experimental conditions, these conditions and responses of the used equipment under standard conditions need to be reported (Henglein and Fischer, 1984).

The definition of power supplied to the sonochemical reaction systems is often significantly different from that supplied from the mains. A great variety of techniques for the measurement of ultrasonic or cavitation intensity have been listed in the literature: chemical reactions, elastic sphere radiometry, aluminium foil erosion, calorimetry, optical methods and thermoprobes have been used for characterization of ultrasonic intensity (Faid et al., 1998). The easiest and probably most commonly applied way of measuring the acoustic power is calorimetry (Mason and Cordemans, 1998). The power density values for each generator/reactor system were calculated by the calorimetric method as described in section 3.2.2.1. of this dissertation.

The power density in a sonochemical system is dependent on the power input and the reaction volume. The power density outputs of the reaction systems used were investigated with respect to each of these parameters.

An alternative approach to the power density measurements for the characterization of sonochemical properties of a reaction system is the measurement of radical production rate. The radical concentrations can be accurately measured by electron spin resonance (ESR) spectrometry (Mason and Cordemans, 1998; Yanagida et al., 1999), or indirectly through the measurement of hydrogen peroxide (Mason and Lorimer, 2002).

## 4.1.1. Characterization of 20 kHz System

4.1.1.1. Determination of Ultrasonic Power in 20 kHz System. The generator was operated at the set fractions of power switch on the instrument operation panel that indicated the power fraction applied. 10, 20, 30, 40 and 50 per cent settings were used for the experiments, corresponding to 18 W, 36 W, 54 W, 72 W and 90 W respectively. Higher power settings and lower volumes were not used for fear of inflicting thermal damage on the probe as a consequence of heat build-up in the absence of cooling. The power input was calculated as the product of the applied fraction and the total instrument power which was 180 W. Tap water was used as the test sample. The power density values were calculated by fitting the data obtained from calorimetric measurements into Equation 3.1. The change of calculated power density values with instrumental power input is given in Figure 4.1.
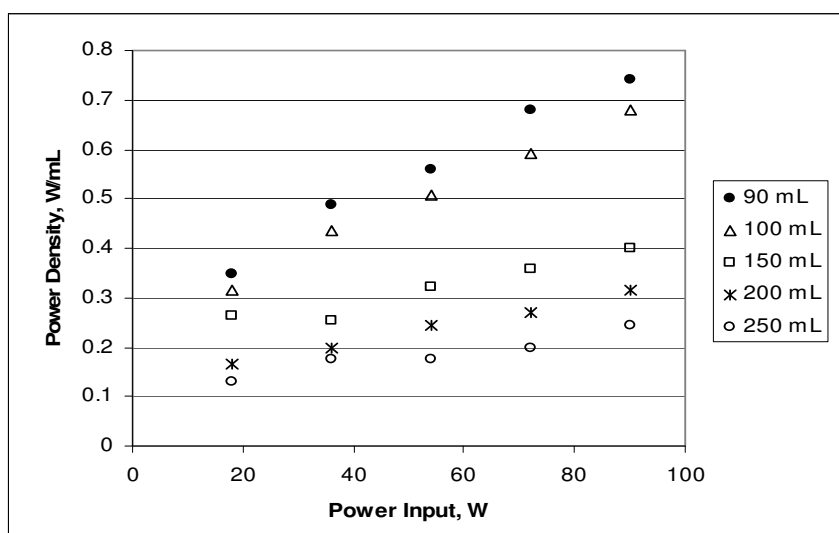


Figure 4.1. The change of power density with power input in the 20 kHz generator/reactor system as a function of reaction volume

At constant volume, the relation between power density and power input is linear and the slope of which decreases as the volume is increased. The power density achieved at each value of power input is inversely proportional with the reaction volume as indicated in Equation 3.1.

Plotting the power density calculated for each power input value against reaction volume provides an interesting graph that suggests that the optimum operational volume for the 20 kHz reactor is 80 mL as can be seen in Figure 4.2. The graph shows that for each power setting a maximum power density value is reached at around 80 mL, confirming that the optimum operation volume for this generator is 80 mL. This phenomenon points to the effect of reaction vessel geometry on soundwave attenuation that directly affects the cavitation events which are among the important determining factors in attaining the desired power density.
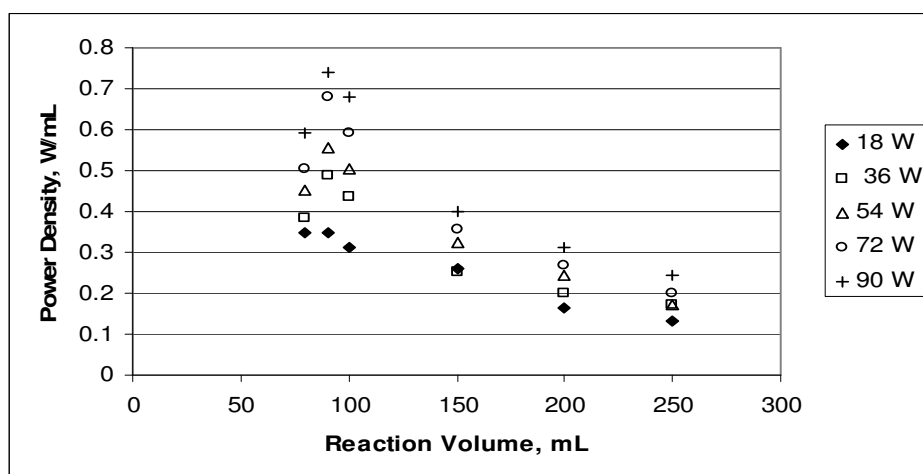


Figure 4.2. Change of power density versus the reaction volume in the 20 kHz generator/reactor system.

4.1.1.2. Determination of Hydrogen Peroxide Production Capacity of 20 kHz System. An alternative approach to the power density measurements for the characterization of sonochemical properties of a reaction system is the measurement of radical production rate. The radical concentrations can be accurately measured by electron spin resonance (ESR) spectrometry, but this method requires expensive equipment that is not available in

many laboratories (Mason and Cordemans, 1998; Yanagida et al., 1999). An indirect way of measuring radical production is the measurement of hydrogen peroxide. During sonolysis of water hydrogen peroxide formation takes place due to the recombination reactions of hydroxyl radicals (•OH) and hydroperoxyl radicals (•OOH), and so, hydrogen peroxide production gives an indication of the radical formation capacity of the system (Mason and Lorimer, 2002).

$$H_2O \rightarrow •H + •OH \qquad\qquad (4.1)$$

$$O_2 \rightarrow 2O• \qquad\qquad (4.2)$$

$$H• + H_2O \rightarrow HO•+ H_2 \qquad\qquad (4.3)$$

$$O• + H_2O \rightarrow 2HO• \qquad\qquad (4.4)$$

$$H• + O_2 \rightarrow HOO• \qquad\qquad (4.5)$$

$$2HO• \rightarrow H_2O_2 \qquad\qquad (4.6)$$

$$2\ HOO• \rightarrow H_2O_2 + O_2 \qquad\qquad (4.7)$$

The hydrogen peroxide production of the 20 kHz reaction system was measured with the triiodide method descibed by Klassen et al (Klassen et al., 1994). The system was operated at 80 mL reaction volume and at two power densities of 0.48 W/mL and 0.58 W/mL to investigate the effect of power density on hydroxyl radical formation rate.

The data plotted in Figure 4.3 gives the hydrogen peroxide concentration data for 80 mL deionized water irradiated with 20 kHz at 0.48 W/mL for 30 minutes. This is the minimum hydrogen peroxide formation in the system due to the high cavitation threshold of deionized water, in the absence of impurities that act as seeds of cavitation (Mason, 1990). The same experiment was repeated by increasing the power density to 0.58 W/mL. A linear trendline fitted to the data gives a slope of 0.0039 1/min for 0.48 W/mL, and 0.0043 1/min for 0.58 W/mL, corresponding to theorethical minimum hydrogen peroxide

production rates of 0.25 mM/h, and 0.27 mM/h respectively. Having been produced in a reactor of 80 mL, the total hydrogen peroxide formation rate of the reactor can be calculated as 0.020 mM/h and 0.021 mM/h. These values are in the range of one half per cent of the total hydrogen peroxide production rate reported as 3.3 mM/h by Henglein and Fischer used during their chloroform sonolysis studies (Henglein and Fischer, 1984).
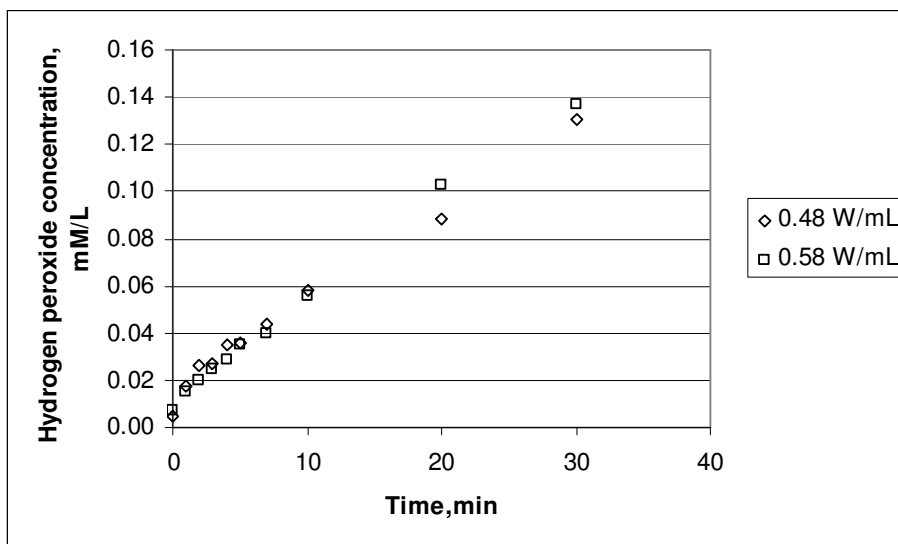


Figure 4.3. Hydrogen peroxide production rate in 80 mL deionized water at 20 kHz system at 0.48 and 0.58 W/mL power densities

The proximity of the two plots obtained at 0.48 W/mL and 0.58 W/mL, indicates that the minimum rate of hydrogen peroxide formation is not significantly enhanced by an increase in power density at the 20 kHz system. Although it is known that at low frequencies hydroxyl radicals are formed in the bubble, the cushioning effect of the liquid vapors and gases due to the long lifecycle of the bubble reduce the temperatures and pressures that may be achieved inside the bubble (Mason and Lorimer, 2002). Therefore, it can be deduced that power density is not a crucial factor in radical formation of this system.

**4.1.2. Characterization of 300 kHz System**

4.1.2.1. Determination of Ultrasonic Power in 300 kHz System. The 300 kHz generator was operated at various power settings attained by adjusting the instrument power control

dial at the fixed values of 10 W, 15 W, 20 W and 25 W with the reaction volumes of 100 mL, 115 mL, 125 mL, 135 mL, and 150 mL. Figure 4.3. shows the effect of power input changes on calculated power density values at various reaction volumes.
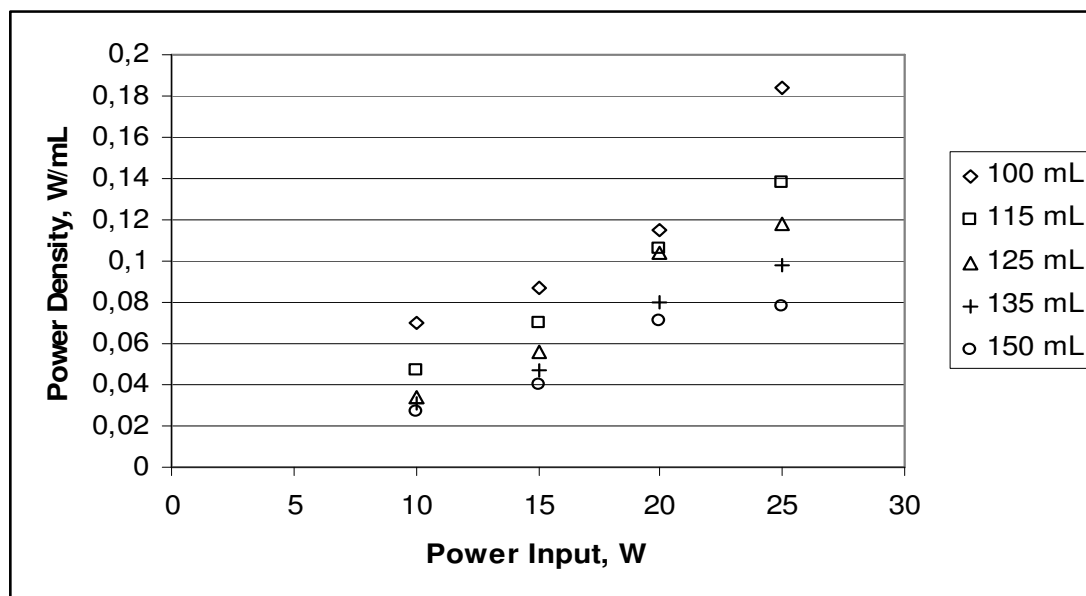


Figure 4.4. The change of power density with power input for reaction volumes of 100 mL, 115 mL, 125 mL, 135 mL, and 150 mL in the 300 kHz generator/reactor system.

The data plotted in Figure 4.4 reveals a linear relationship between the power input values and power density amounts measured for each reaction volume at 300 kHz reaction system. As indicated in Equation 3.1, an inverse relationship can be distinguished between the reaction volume and the power density obtained at each level of power input. The highest power density value of 0.184 W/mL was obtained at the maximum power input i.e. 25 W, and lowest reaction volume that was 100 mL. Whereas, the lowest power density value where the system can be operated was obtained with the lowest power input value of 10 W at the largest applicable reaction volume of 150 mL, as expected.

The shape of the curves of power density versus reaction volume for each power setting indicate that the optimum operation point for this system, i.e., the reaction volume and power setting that gives the highest power density values may be higher than 0.184 W/mL, i.e. well below 100 mL and above 25 W. But, cooling requirements associated with the geometric shape of the reactor and the sampling requirements for analytical purposes

do not allow operation in smaller volumes than 100 mL, and the maximum power input capacity of this reactor is 25 W.
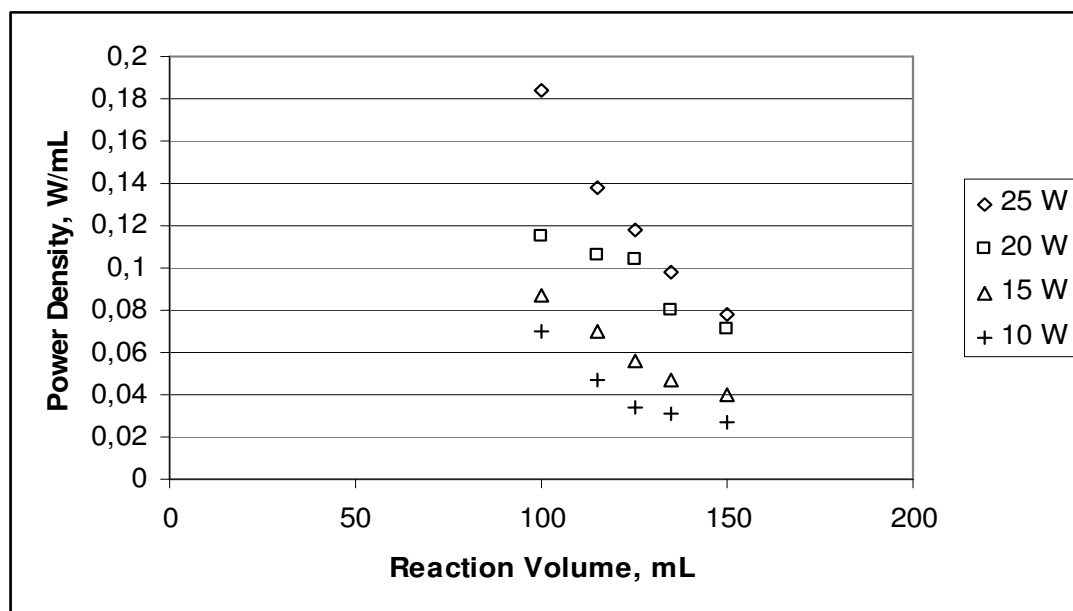


Figure 4.5. Change of power density versus the reaction volume in the 300 kHz generator/reactor system.

4.1.2.2. Determination of Hydrogen Peroxide Production Capacity of 300 kHz System. As can be seen in Figure 4.6, application of increased power density results in increased hydrogen peroxide formation in the 300 kHz system, unlike the 20 kHz system. Implying that increasing the power input causes more cavitation events and consequenly produces more hydroxyl radicals, resulting in an environment richer in radical species in this system. A linear trendline fitted to the data gives a slope of 0.0056 min$^{-1}$ for 0.078 W/mL, and 0.0106 min$^{-1}$ for 0.184 W/mL, corresponding to theorethical minimum hydrogen peroxide production rates of 0.34 mM/L.h, and 0.64 mM/L.h respectively. Having been produced in reaction volumes of 150 mL and 100 mL, the total hydrogen peroxide formation rate of the reactor can be calculated as 0.051 mM/h and 0.064 mM/h for these power densities. These values are in the range of one per cent of the total hydrogen peroxide production rate reported as 3.3 mM/h by Henglein and Fischer used during their studies (Henglein and Fischer, 1984).
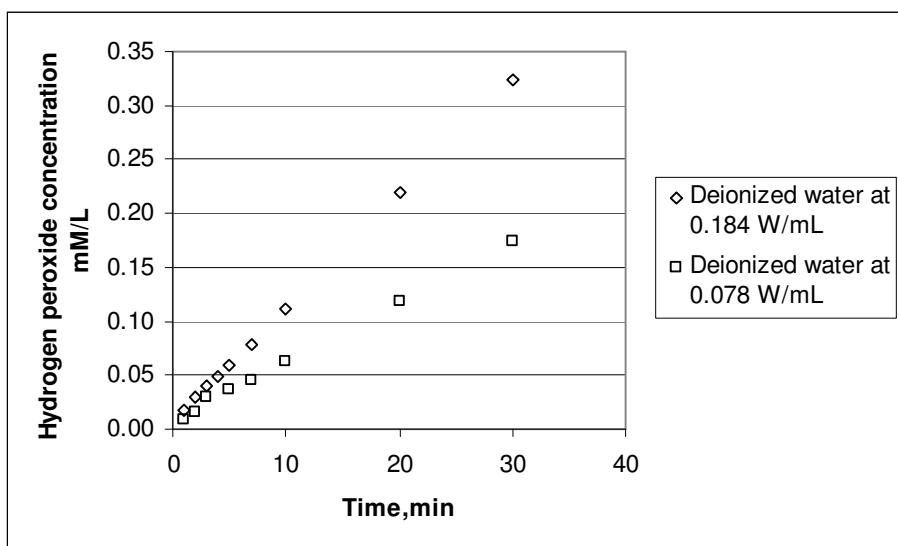
Figure 4.6. Effect of power density on hydrogen peroxide formation rate in deionized water at 0.078 W/mL and 0.184 W/mL in 300 kHz

Comparison of the Figures 4.3 and 4.6 reveals that the 20 kHz system produces only 0.14 mM/L of hydrogen peroxide at 0.5 W/mL at 30 minutes, whereas the 300 kHz system produces 0.3 mM/L hydrogen peroxide at less than 0.2 W/mL at the same time interval: This evidence supports the work of other authors stating that ultrasonic waves at 20 kHz produce less radicals compared to higher frequencies (Mason, 1990; Mason, 1999; Mason and Lorimer, 2002; Petrier and Francony, 1997).

### 4.1.3. Characterization of 520 kHz System

4.1.3.1. Determination of Ultrasonic Power in 520 kHz System. The generator was operated at different settings of the power switch providing 40 W, 60 W and 100 W of the 100 W maximum power the generator supplied, for irradiating 300 mL, 600 mL, 900 mL and 1200 mL tap water as sample. The power density values calculated from the experimental data using Equation 3.1 that were plotted against the power input values for each experimental volume are presented in Figure 4.7.
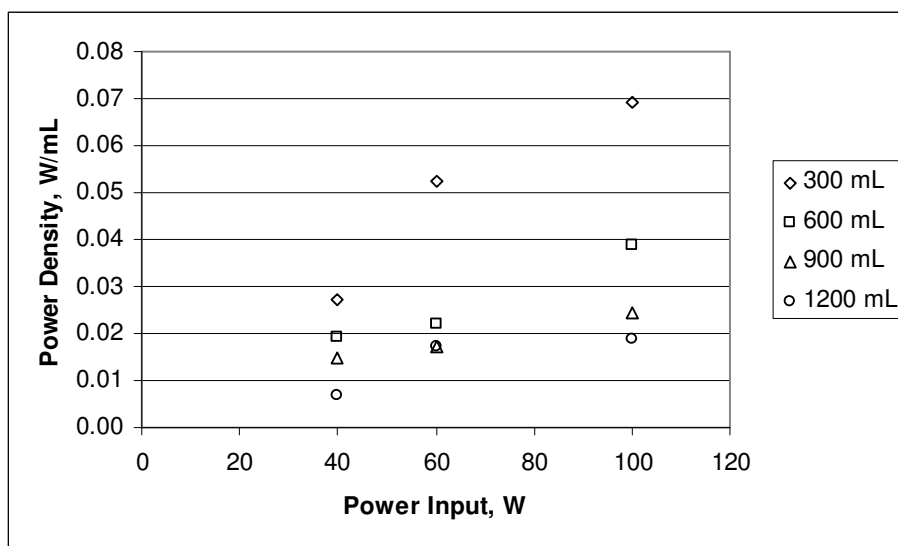
Figure 4.7. The change of power density with power input in the 520 kHz generator/reactor system.

The power density values plotted versus power input values in Figure 4.7, exhibit a logarithmic relationship for each reaction volume tried. The levelling of the curve, i.e. the reduction of the increase in power density while increasing the power input suggests the presence of a plateau where further increase in the power input can not increase the power density any further. Such a plateau is reached probably where the increased power input is lost in the form of heat through the reactor surroundings, and is a property of the reactor design. The plateau can also be an indication of decoupling effect, which is observed when the excessive energy applied to the liquid causes the formation of a great number of cavities, which absorb acoustic energy and lower the effective yield of the reaction desired (Luche et al., 1998).

The inverse correlation indicated in Equation 3.1 between the power density and the reaction volume can be witnessed at the 520 kHz reactor as well as the 20 kHz and the 300 kHz reactors. As can be seen in Figure 4.7 the smallest reaction volume of 300 mL coupled with the highest power input of 100 W present the highest power density value, whereas, the highest reaction volume of 1200 mL coupled with the lowest power input at 40 W generate the lowest power density value.
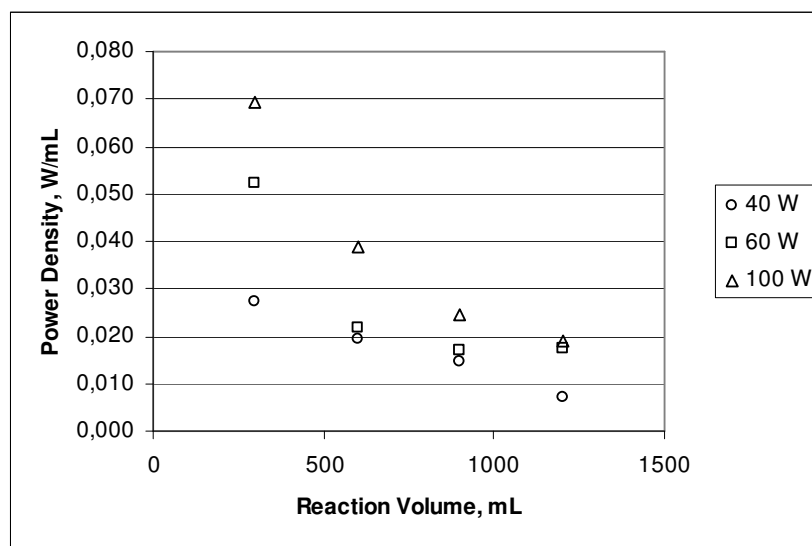
Figure 4.8. Change of power density versus the reaction volume in the 520 kHz generator/reactor system

The shape of the curves of power density versus reaction volume that can be seen in Figure 4.8, for each level of power input, indicate that the optimum point of operation for this system, where the maximum power density may be obtained, may be well below the 300 mL minimum volume limit and the 100 W maximum power input limit.

4.1.3.2. Determination of Hydrogen Peroxide Production Capacity of 520 kHz System. Effect of increased power density on the hydrogen peroxide production of the 520 kHz reactor was measured at two power densities with the triiodide method (Klassen et al., 1994), and the findings are presented in Figure 4.9.

As can be seen in Figure 4.9, application of increased power density results in increased hydrogen peroxide formation at the 520 kHz system, like the 300 kHz system. Suggesting that increased power input causes more cavitation events and consequenly produces more hydroxyl radicals, resulting in an environment richer in radical species in the system. A linear trendline fitted to the data gives a slope of 0.0032 min$^{-1}$ for 0.069 W/mL, and 0.0019 min$^{-1}$ for 0.0039 W/mL, corresponding to theorethical minimum hydrogen peroxide production rates of 0.192 mM/L.h, and 0.114 mM/L.h respectively. Having been produced in reaction volumes of 300 mL and 600 mL, the total hydrogen peroxide formation rate of the reactor can be calculated as 0.058 mM/h and 0.068 mM/h

for these power densities. These values are in the range of one per cent of the total hydrogen peroxide production rate reported as 3.3 mM/h by Henglein and Fischer used during their studies (Henglein and Fischer, 1984).
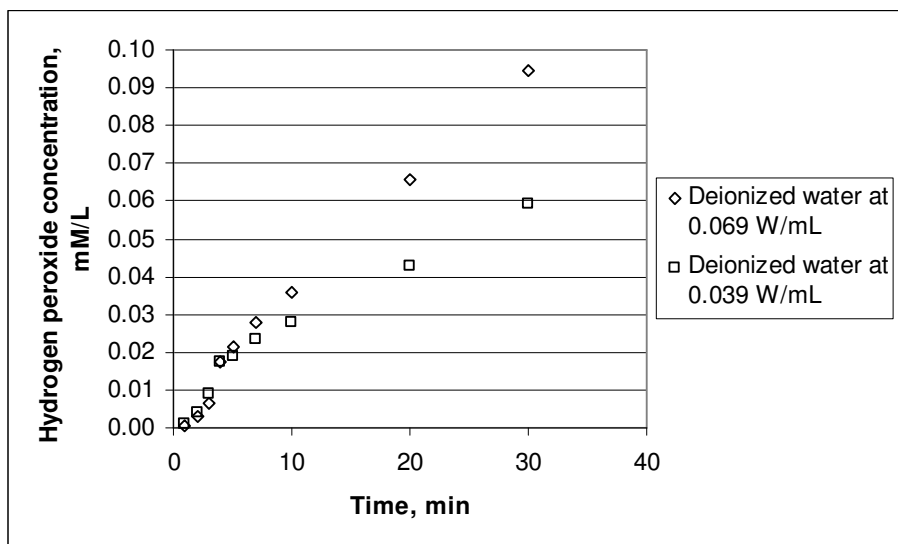


Figure 4.9. Effect of power density on the hydrogen peroxide production of 520 kHz reactor at 0.069 W/mL and 0.039 W/mL

### 4.1.4. Comparison of the Sonochemical Characteristics of the Systems Used

A comparison of the hydrogen peroxide formation capacities of 20 kHz. 300 kHz and 520 kHz systems is presented in Figure 4.10. by summarizing the data given in Figures 4.3 and 4.6 and 4.9 . The Figure 4.10 reveals that 20 kHz system produces only 0.14 mM/L of hydrogen peroxide at 0.5 W/mL, whereas the 300 kHz system produces 0.3 mM/L hydrogen peroxide at less than 0.2 W/mL, and 520 kHz system produces 0.09 mM/L, using nearly 0.04 W/mL: The linear curves fitted to the data give slopes of 0.1 mM $H_2O_2$/W for 20 kHz, 1 mM $H_2O_2$/W for 520 kHz and 1.5 mM $H_2O_2$/W for 300 kHz, showing that the 300 kHz system has the highest capacity for producing hydroxyl radicals per W/mL power density applied, and the 20 kHz system has the lowest. These data support the work of other authors stating that ultrasonic waves at 20 kHz produce less radicals compared to higher frequencies (Mason, 1990; Mason, 1999; Mason and Lorimer, 2002; Petrier and Francony, 1997).
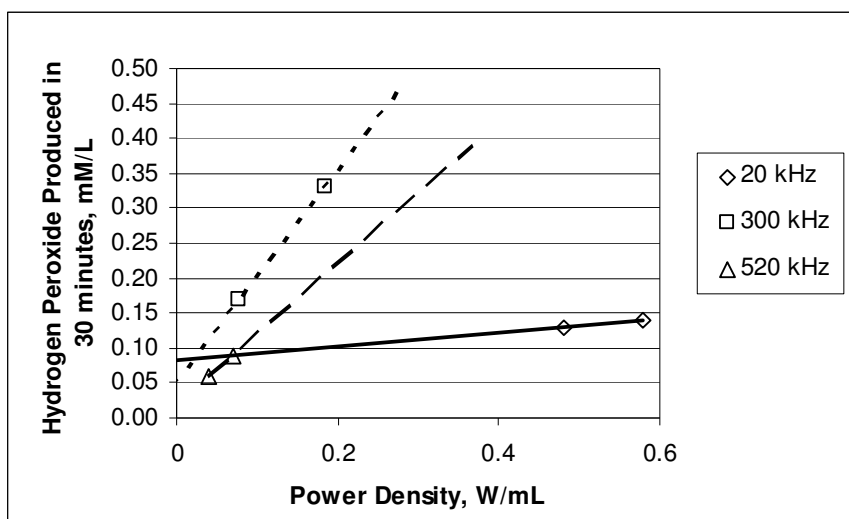
Figure 4.10. Comparison of hydrogen peroxide production capacities of 20 kHz. 300 kHz and 520 kHz systems

## 4.2. Sonolysis of Chloroform as a Model Compound Representing THMs

Chloroform was selected as a model compound for the investigation of sonolytical treatment of trihalomethanes largely due to its cheapness and availability, as well as its being the most prominent of trihalomethane species found in chlorinated drinking waters (Duong et al., 2003; Abdullah et al., 2003). Other researchers also used chloroform as a model compound for representing trihalomethanes (Shemer and Narkis, 2005a; 2005b; 2005c; Bhatnagar and Cheung, 1994; Peters, 2001; Tang and Tassos, 1997). The effect of major parameters that influence sonolytical processes were examined in detail on the example of chloroform to shed light on the processes involved.

## 4.2.1. Effect of Initial Solute Concentration on the Reaction Rate at 300 kHz and 20 kHz Sytems

The sonolyical removal of chloroform from aqueous solutions was studied at 300 kHz system with a power density of 0.078 W/mL. Synthetic samples of 2200 μg/L chloroform in deionized water were exposed to ultrasonic irradiation while being sparged with argon to improve cavitational yield. The range of initial concentration was chosen for its relative proximity to the THM concentrations found in tap water (<100 μg/L), as well as

to allow for accurate measurement of reduced concentrations as treatment progressed, in contrast to other researchers who preferred to work with higher concentrations (Shemer and Narkis, 2005c). Being a highly volatile and aquaphobic compound, chloroform can be removed from the aqueous solutions through the stripping effect of purge gas alone (Linek et al., 1998). However, sonication has been shown to be a particularly effective treatment system for volatile and aquaphobic compounds since they can partition to the bubble or interfacial sheath rapidly (Weaver et al., 1998). In order to determine the effect of sonication on chloroform removal, the sample was exposed to ultrasonic irradiation with sparging, ultrasonic irradiation without sparging, and sparging without ultrasonic irradiation. As can be seen in Figure 4.11 the most efficient treatment of the three was ultrasonic treatment enhanced with argon sparging.
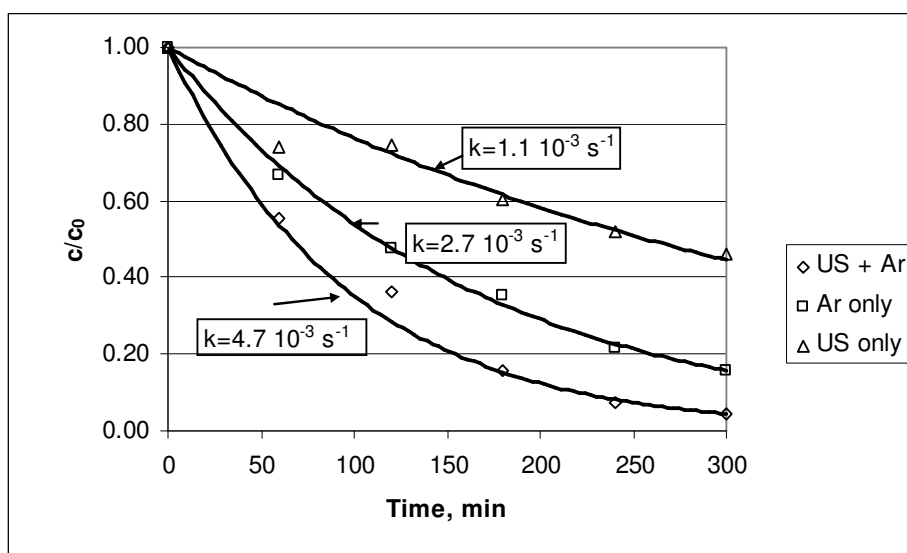
Figure 4.11. The effect of ultrasonic irradiation on chloroform percentage remaining in aqueous solution with and without argon sparging at 300 kHz at 0.078 W/mL power density

Data from all three modes of treatment revealed that the overall removal process in treatment, with and without argon as the cavitation enhancer, followed first order reaction kinetics, in agreement with the reports of other researchers (Shemer and Narkis, 2005a; 2005b and 2005c). The observed reaction kinetics could be fitted successfully to first order rate kinetics, and the rate constants were calculated accordingly using the integrated form of the rate equation;

$$\frac{C}{C_0} = e^{-kt} \tag{4.8}$$

where C is the chloroform concentration at time =t

$C_0$ is the chloroform concentration at time =0

And k is the first order removal rate coefficient.

The rate constants were calculated as $4.7 \times 10^{-3}$ $s^{-1}$ for ultrasound with argon sparging, $2.7 \times 10^{-3}$ $s^{-1}$ for argon sparging with no ultrasound, and $1.1 \times 10^{-3}$ $s^{-1}$ for ultrasonic irradiation with no sparging. However, these data are not comparable to data given of other researchers, as the treatment conditions (i.e. power density) are not reported in literature. The first order removal rate constant for ultrasound coupled with argon sparging is larger than the sum of the rate constants of ultrasound and argon only treatments, meaning that the combined treatment involves more than the combination of two removal mechanisms.

Henglein and Fischer (1984) were the only researchers who conducted a detailed study on the identification of major sonolytical degradation by-products of pure chloroform and reported these to be HCl and carbenes which suggests that the degradation mechanism of chloroform at 500 kHz is pyrolysis at the bubble interior. This report is supported by indirect findings of other researchers (Bhatnagar and Cheung, 1994; Shemer and Narkis, 2004). However, as the study of Henglein and Fischer was conducted in nonaqueous medium, it does not investigate the possibility of the reaction of chloroform molecules with the hydroxyl radicals known to form during the sonolysis of aqueous medium. Chloroform reacts with •OH as follows (Asmus and Flyunt, 2003):

$$\bullet \, OH + HCCl_3 \rightarrow H_2O + \bullet \, CCl_3 \tag{4.9}$$
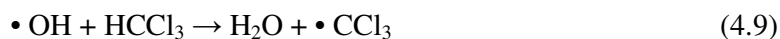
Research has shown that sonochemical reactions occur in three zones in the irradiated liquids; in the cavitation bubble itself, in the interfacial sheath between the gaseous bubble and the surrounding liquid, and the bulk solution (Ince et al., 2000). The observed removal rate is an overall $CHCl_3$ removal rate that can be calculated as the total

sum of the rates of removal by stripping-degassing, by pyrolysis in the bubble, and by hydroxyl radical and other radical reactions in the bulk solution and the bubble-solution interface. This relation rate can be formulized as follows

$$r_{obs} = r_r + r_s + r_p \tag{4.10}$$

where, $r_r$ is the chloroform removal rate by radical reactions,

$r_s$ is the rate of chloroform removal through stripping,

$r_p$ is the rate of chloroform removal by pyrolysis,

Assuming that the only radical reactions responsible for $CHCl_3$ removal are those with •OH, Equation 4.10 can be written in an open form as follows:

$$r_{obs} = k'[CHCl_3] = k''\ [CHCl_3][•OH] + k_s\ [CHCl_3] + k_p\ [CHCl_3] \tag{4.11}$$

where dC/dt is the change in chloroform concentration with respect to time

k' is the observed pseudo-first order rate constant, $min^{-1}$

$[CHCl_3]$ is the molar concentration of chloroform, M

k'' is the 2$^{nd}$ order rate constant of $CHCl_3$ removal by •OH, $M^{-1}min^{-1}$

[•OH] is the hydroxyl radical concentration, M

$r_{obs}$ is the observed first order rate, M/min

dividing both sides with $[CHCl_3]$ gives:

$$k' = k''[OH] + k_s + k_p \tag{4.12}$$

In Equation 4.12, k' is a constant that can be obtained experimentally, k''[OH] can also be considered constant at steady state. The constant $k_r$ is only partially known, thanks to Haag and Yao, who reported that the oxidation rate constants of chloroform and bromoform with hydroxyl radical are 5.4 ± 3.0 x 10$^7$ $M^{-1}s^{-1}$ and 1.3 ± 0.6 x 10$^7$ $M^{-1}s^{-1}$, respectively (Haag and Yao, 1992). Eventhough the rate of stripping is affected by ultrasonic irradiation, the $k_s$ value can be assumed to be similar in magnitude to that

obtained from the stripping experiments. Thus, the rate constant for pyrolysis can be written as:

$$k_p = k' - k''[OH] - k_s \qquad (4.13)$$

inserting the known values of $k'$ and $k_s$

$$k_p = 2.0 \times 10^{-3} - 5.4 \times 10^{7}[OH] \qquad (4.14)$$

as $[OH] > 0$.

$$k_p < 2.0 \times 10^{-3} \qquad (4.15)$$

However, it must be remembered that this value is highly speculative and is subject to experimental conditions, thus, it souldn't be used out of context.
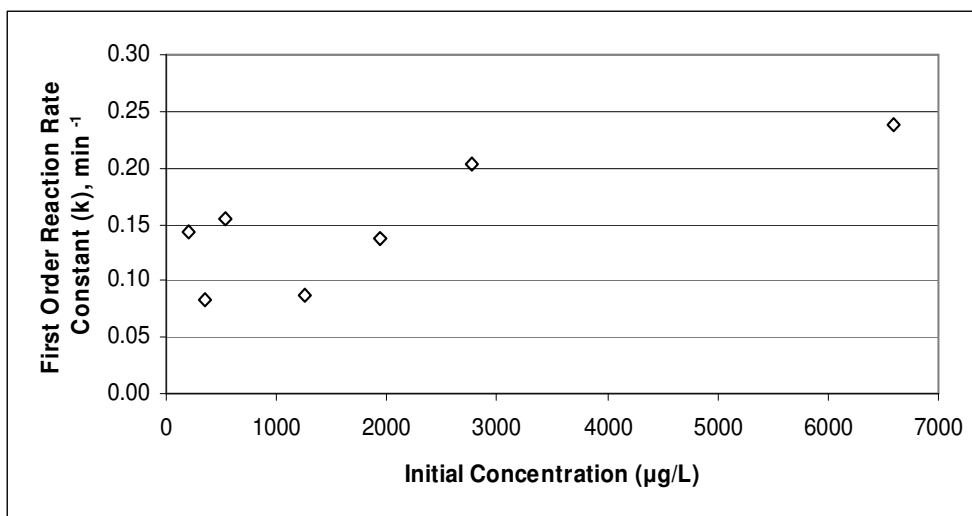


Figure 4.12. The change of observed first order removal rate constant with initial chloroform concentration at 300 kHz, 0.078 W/mL, with argon sparging

The effect of initial concentration on chloroform removal was studied by treating solutions with varying initial concentrations under the same experimental conditions. In Figure 4.12 the change of observed first order removal rate constants with initial chloroform concentration can be seen.

Increasing concentrations above 1000 ug/L were observed to increase the first order removal rate constant. The data plotted in Figure 4.13 presents the change in hydrogen peroxide production rate in the 300 kHz reactor with varying initial chloroform concentrations.
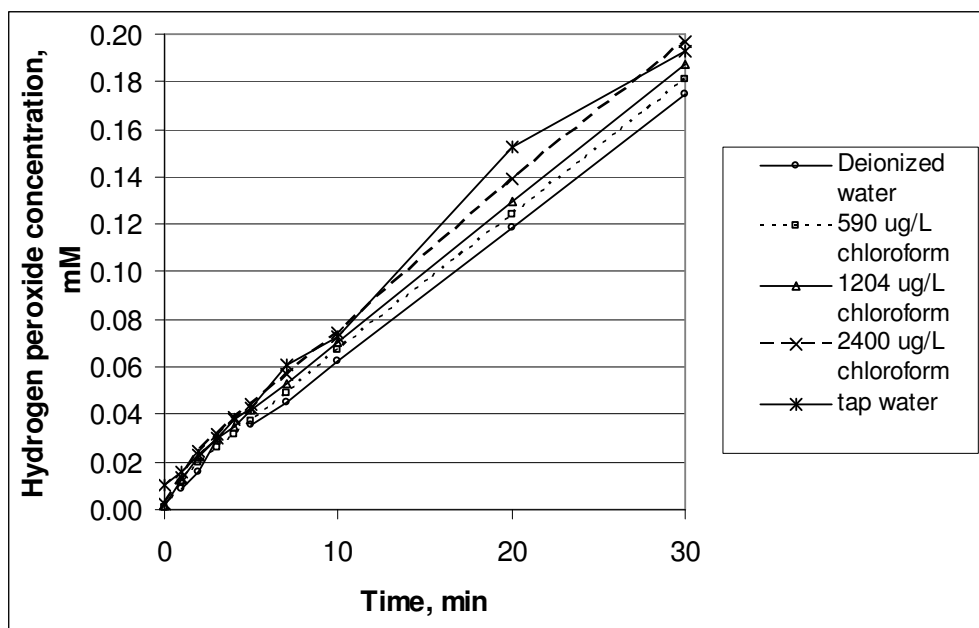


Figure 4.13. The effect of initial chloroform concentration on hydrogen peroxide production in 300 kHz reactor at 0.078 W/ml power density

Hydrogen peroxide concentrations at the 300 kHz reactor operated at a power density of 0.078 W/mL were measured with triiodide method (Klassen et al., 1994). As can be seen in Figure 4.13, the hydrogen peroxide concentration has a positive correlation with initial solute concentration. The minimum hydrogen peroxide production rate is naturally obtained with deionized water (Margulis, 1995), due to the absence of cavitation nuclei , and the maximum production rate is obtained with tap water. Introduction of 590 μg/L of chloroform to deionized water reduces the cavitation threshold, resulting in slightly higher •OH radical formation rate which is indirectly measured as $H_2O_2$. Increasing the initial solute concentration to 1204 μg/L and to 2400 μg/L increases the $H_2O_2$ production further. An interesting finding was that tap water containing 65 mg/L alkalinity as $CaCO_3$, as well as other impurities, actually increases the hydrogen peroxide production rate even further.

Although carbonates are known to scavenge the hydroxyl radicals through reactions 4.15 and 4.16 (Buxton et al., 1988);

$$CO_3^{-2} + \bullet OH \rightarrow HO^- + \bullet CO_3^- \qquad k=3.8 \times 10^8 \text{ M s}^{-1} \qquad (4.16)$$

$$HCO_3^{2-} + \bullet OH \rightarrow H_2O + \bullet CO_3^- \qquad k= 8.5 \times 10^6 \text{ M s}^{-1} \qquad (4.17)$$
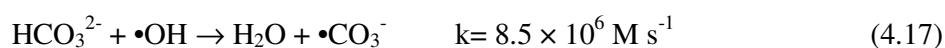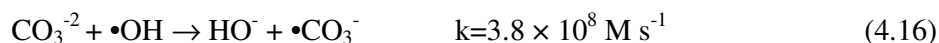
The effect of decreased cavitation threshold enhances the net •OH formation more rather than hindering it.

The positive correlation between the initial solute concentration and the hydrogen peroxide formation rate, and the removal rate constants observed in Figures 4.12 and 4.13 suggests that thermal pyrolysis may not be the only degradation mechanism for sonolytical chloroform removal at 300 kHz at the studied concentration range, but that, radical reactions may have more significance than supposed previously (Shemer and Narkis, 2004; Bhatnagar and Cheung, 1994).

In Figure 4.12, chloroform solutions with initial concentrations below 1000 μg/L show a much higher observed removal rate constant than expected. Data points below the initial chloroform concentration of 1000 μg/L are scattered and point to much higher removal rate constants than data at higher concentrations indicate. Although an obvious explanation is the reduction in the accuracy of analytical method, repeated experiments at this range never actually gave smaller rate constants than expected, which they should if the only explanation of their presence was reduction in analytical accuracy.

The phenomenon of surpisingly high degradation rate at micromolar concentrations was observed by other researchers during the sonolysis of chlorobenzene and trichloroethylene at 520 kHz (Dewulf et al., 2001), and was modelled as occurence of gas phase hydroxyl radical induced degradation alongside pyrolysis. Dewulf and co-workers found that the removal reaction kinetics increased with decreasing initial substrate concentrations of chlorobenzene and trichloroethylene at the micromolar concentrations, which could no longer be explained by pyrolysis even taking into account the positive effect of the reduced concentration of the solutes on the reaction temperature. The model

they developed incorporating gas phase OH radical induced degradation next to pyrolysis demonstrated that concentrations of chlorobenzene larger than 1000 μM the degradation was due to pyrolysis for over 99.97 per cent, but at concentrations between 1 and 5 μM, the OH radical mechanism contributed 48.5 per cent of the total degradation. As 1000 μg/L chloroform corresponds to 8 μM, the data presented in Figure 4.12 may be suggesting that a similar mechanism to that proposed by Dewulf and colleagues may be in action during the sonolysis of chloroform as well.
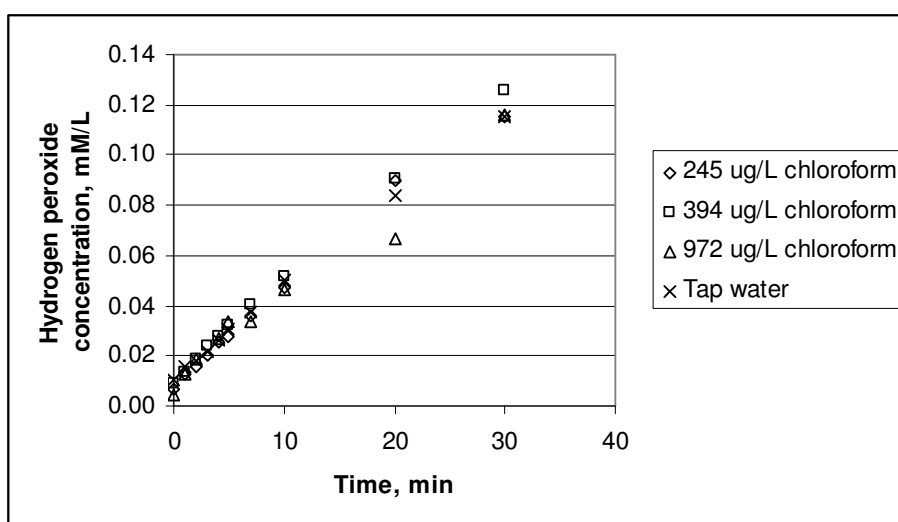


Figure 4.14. Effect of initial chloroform concentration on the hydrogen peroxide formation in the 20 kHz system.

Figure 4.14 demonstrates that a stepwise increase in the initial solute concentration does not increase the hydrogen peroxide formation rate significantly at the 20 kHz system. As hydrogen peroxide formation is an indirect measure of hydroxyl radical formation in a sonochemical system, these findings point to the conclusion that even if OH radical reactions were somehow operative in the chloroform removal at 20 kHz, the increase in initial solute concentration does not enhance radical formation as measured by hydrogen peroxide accumulation in the bulk liquid. Thus, any change at the removal rate constants observed with the change of initial concentration can not be justified through a change of hydroxyl radical initiated reactions in the bulk liquid. Such a change needs to be explained by reactions , pyrolytical or otherwise, that take place in the cavitation bubble.
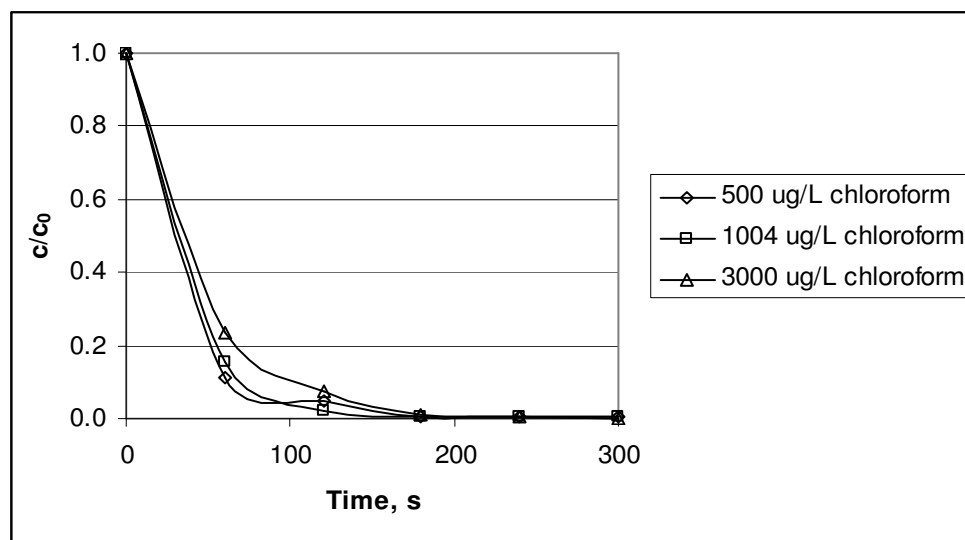
Figure 4.15. The change of chloroform removal rate with initial chloroform concentration at 20 kHz at a power density of 0.48 W/mL

The change of observed removal rate with initial chloroform concentration at 20 kHz is given in Figure 4.15. The observed first order removal rate constants were calculated as 0.012 mM/s for 500 ug/L, 0.013 mM/s for 1004 ug/L and 0.010 mM/s for 3000 ug/L initial chloroform concentration. The difference between the removal rate constants is so small as can be ignored. It can be assumed that the increase in initial chloroform concentration does not change the chloroform removal rate at 20 kHz. Shemer and Narkis also reported that initial concentration did not change the removal rate constant at 20 kHz, even if their removal rate constant was at $24 \times 10^{-3}$ min$^{-1}$ (Shemer and Narkis, 2004), corresponding to $4 \times 10^{-4}$ s$^{-1}$. The large difference may be partially explained by the authors not using Ar for sparging, and the resulting reduced cavitational activity as well as their low power density value (0.184 W/mL compared to 0.48 W/mL in our experiments) and other unknown differences in reactor characteristics.

The formation of HCl as a major end product of sonolysis of pure chloroform was first reported by Henglein and Fischer (Henglein and Fischer, 1984). With the use of an ion chromatograph, Shemer and Narkis detected and quantified hydrogen peroxide, nitrate, chloride, bromide, iodide and iodate as the inorganic products of THMs sonication (Shemer and Narkis, 2004). Cheung and co-workers reported reduced pH of the reactor contents during the sonochemical destruction of chlorinated hydrocarbons including

methylene chloride and carbon tetrachloride in dilute aqueous solutions (Cheung et al., 1991). The authors concluded that the reduction in the solution pH and a corresponding decrease in the concentration of the chlorinated reactants measured by GC/MS indicated the formation of HCl in the solutions. Cheung and colleagues also concluded that the reduction of pH in solutions of carbon tetrachloride further indicated that the hydrogen necessary for HCl formation was obtained from water as the target compound contained no hydrogen.
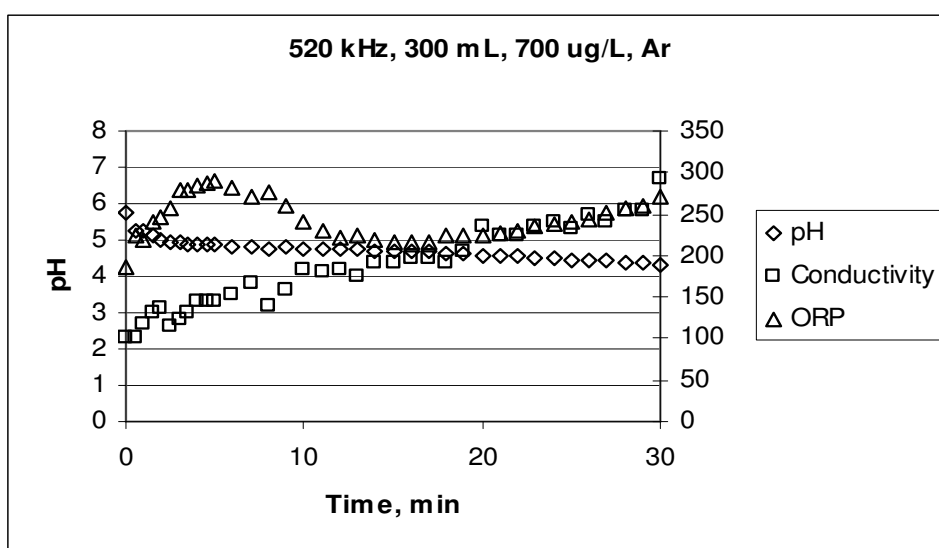


Figure 4.16. Change of solution pH, ORP and conductivity during sonolysis of 700 ug/L chloroform at 520 kHz

During chloroform removal experiments a pH, an ORP and a conductivity probe were inserted into the reactor, and readings were taken at every 30 seconds for the first five minutes, and after the fifth minute at every minute from each of the three probes. The pH values were observed to drop rapidly at the beginning of the experiment; within the first two minutes a drop of one digit was measured. The conductivity values of the solution were observed to increase steadily throughout the experiment, indicating the formation of conductive ionic species, i.e. HCl. The Cl$^-$ levels in the treated solutions were below the detection limit of 1,.5 mg/L Cl$^-$ of the argentometric method used (APHA/AWWA/WPCP, 1992), and could not be measured analytically. Figure 4.15 presents the time dependent data of pH, conductivity and ORP readings during the sonolysis of 700 μg/L chloroform at 520 kHz.

The oxidation-reduction potential probe gave an interesting response to sonication of chloroform solutions. At low initial solution concentrations, this curve presented an increase followed by a valley, which was followed by a steady increase. The peak of the initial rise was lower and the following valley shallower in more concentrated chloroform solutions but a direct correlation could not be established. However, the ORP probe obviously responded to the oxidative environment produced in the reactor during sonolysis of aqueous solutions.
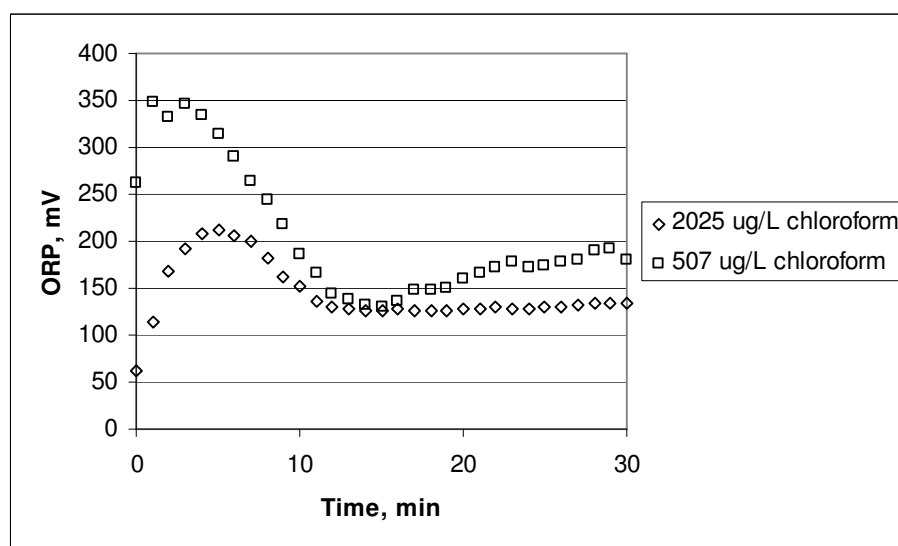


Figure 4.17. Change of oxidation-reduction potential during sonolysis of chloroform with initial concentrations of 2000 ug/L and 500 ug/L at 300 kHz, 0,078 W/mL under argon

Figure 4.17 shows the change of oxidation-reduction potential of solutions with initial chloroform concentrations of 2000 and 500 ug/L with 300 kHz at 0.078 W/mL. The shape of the curves is consistent with those that were observed at 520 kHz.

**4.2.3. Effect of Power Density on Removal**

Because of differences in the geometric properties, power densities and instrumental efficiencies it is not possible to compare experimental runs under similar conditions in different reactors. The optimum power density values are known to change from equipment to equipment for the same reaction (Sivakumar and Pandit, 2001).

Comparison of efficiencies of different reaction systems is only possible by comparing power densities, which give a direct idea about the amount of energy dissipated inside the given volume of solution. In Figure 4.18 one can see the effect of increased power density at 20 kHz on the first order rate constants of chloroform removal.
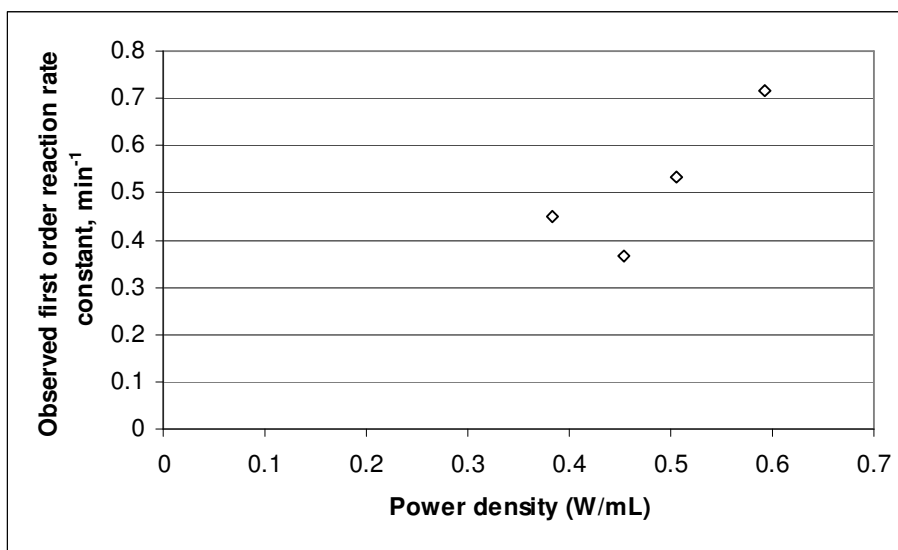


Figure 4.18. The effect of power density on the first order removal rate constant at 20 kHz for 1400 ug/L chloroform

In section 4.1.1 of this dissertation, it was reported that the increased power density did not increase the hydroxyl radical formation rate in the 20 kHz system. Thus, the observed increase in the first order removal rate through the escalation of power density can not be attributed to increased radical reactions in this system, but to increased cavitation events that supply enhanced cavitation bubble-bulk liquid interface, boosting escape of chloroform into the bubbles for pyrolytic destruction.

The effect of power density on the removal of 1400 ug/L chloroform at 300 kHz can be seen in Figure 4.19
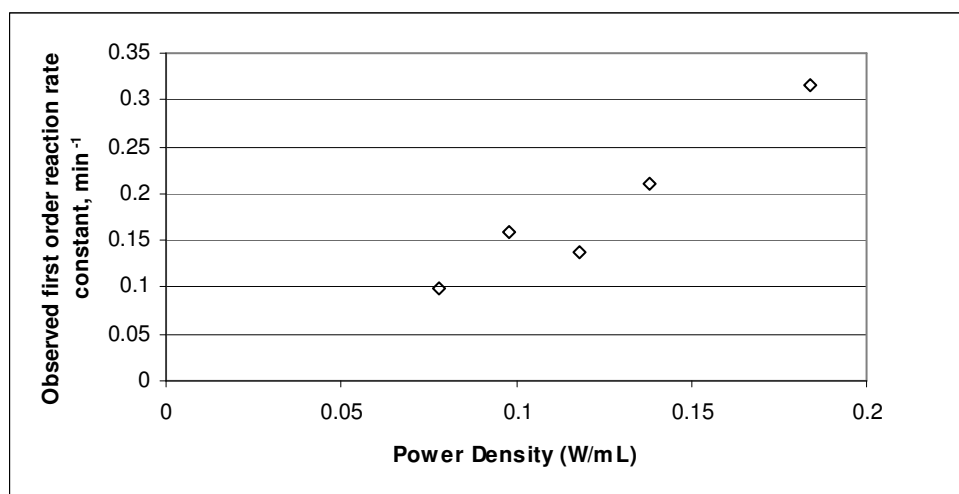
Figure 4.19. Effect of power density on first order removal rate constant of 1400 ug/L chloroform at 300 kHz

Increased power density increases the observed first order removal rate constant of chloroform with initial concentration of 1400 μg/L. It has been reported that a logarithmic relationship exists between the power density and degradation fraction of Rhodamine B dye (Sivakumar and Pandit, 2001).
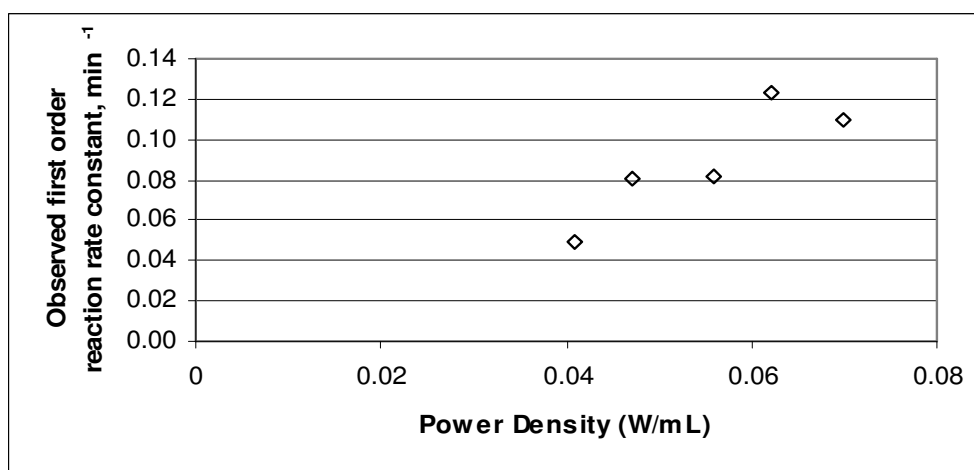


Figure 4.20. Effect of power density on the pseudo-first order reaction rate constant of chloroform at 520 kHz ($c_0 = 1400$ μg/L)

Power density increase is expected to increase cavitation events to an extent which in turns accelerates rates of chemical reactions. However, the rates can not increase

indefinitely with an increase in power parameters, but rather should reach a plateau, or decline with further increases in the power density. When the optimum point is exceeded, there may be heat build-up in the reactor, as well as absorption and or scattering of the acoustic energy by the excessive bubbles, lowering the effective yield of the reaction (Mason and Cordemans, 1998).

Figures 4.18, 4.19 and 4.20 show that in all three systems used in this study, the optimum power density for chloroform removal is not reached, implying that higher power densities could result in higher removal rates, had the generators been able to supply it.

Increased power density was also shown to increase the hydrogen peroxide formation which is an indirect measure of the hydroxyl radical formation in Figure 4.6 for the 300 kHz system and in Figure 4.9 for the 520 kHz system, indicating the presence of a correlation between the hydroxyl radical formation of the systems and the chloroform removal rate. But, for the 20 kHz system, the increase in power density was shown to have no impact on the hydrogen peroxide formation in Figure 4.3, even if it did increase the chloroform removal rate as can be seen in Figure 4.18. It must be remembered that the correlations observed between the chloroform removal rates and the hydrogen peroxide formation rates may not point at cause-and-effect relationships, but the two parameters may have the same cause, i.e. increased cavitation events resulting in increased pyrolytical activity inside the bubbles (measured as increased chlororform removal) and at the same time increase the amount of hydroxyl radical that escapes into the bulk solution (measured as hydrogen peroxide formation).

### 4.2.4. Effect of Frequency on Removal

In most of the experimental work found in the literature, reports of efficiencies and removal rates at different power intensities and frequencies make it difficult to compare data. Application of ranges of power densities for each reactor enables us to draw tentative power density versus observed reaction rate constant curves for the same initial chloroform concentration, thus allowing us to isolate the effects of frequency alone.
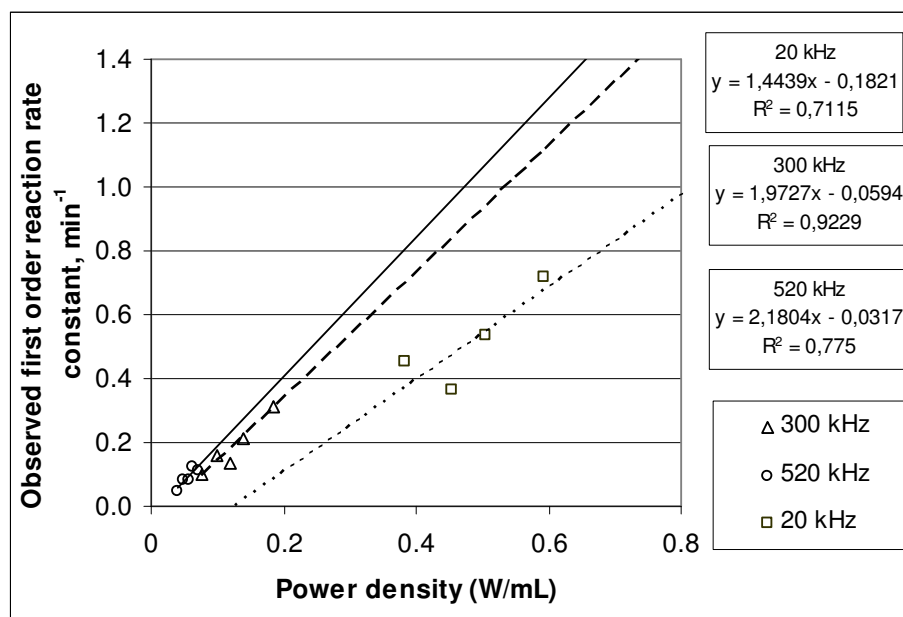
Figure 4.21. Effect of ultrasonic frequency on chloroform removal rate constant with the power density ($c_0$ = 1400 μg/L)

In the limited literature available on sonochemical removal of trihalomethanes, authors often measure THM removal at a single frequency, which is often 20 kHz based on the work of Henglein (Henglein and Fisher, 1984). The presumption in the reported studies is that the removal mechanism is pyrolysis, although they (except for Henglein and Fischer) have not reported the end products (Shemer and Narkis, 2005a; Bhatnagar and Cheung, 1994).

Our study of the removal rate of chloroform from aqueous solutions of equal concentrations at three different frequencies indicate that 20 kHz is not a particularly energy efficient frequency for chloroform removal. Although we did not attempt to identify any end-products either, we assumed that pyrolysis is the major removal mechanism other pathways may exist as well. However, we found that at 20 kHz, although pyrolytical destruction seems to be predominant, the frequency is not the optimum in terms of energy efficiency. The data obtained at 300 kHz and 520 kHz proved both of these systems to be more efficient than 20 kHz.

### 4.2.4. Effect of Gas Type on Removal

Assuming adiabatic bubble collapse, the maximum temperatures ($T_{max}$) and pressures ($P_{max}$) within the collapsed cavitation bubbles are predicted by Noltingk and Neppiras from approximate solutions of Rayleigh-Plesset equations as follows (Noltingk and Neppiras, 1950; Neppiras,1980):

$$T_{max} = T_o \left\{ \frac{P_a(\gamma - 1)}{P} \right\} \tag{4.17}$$

$$P_{max} = P \left\{ \frac{P_a(\gamma - 1)}{P} \right\}^{\left[ \frac{\gamma}{\gamma - 1} \right]} \tag{4.18}$$

where  $T_o$ = ambient temperature in the solution bulk

$P_a$ = pressure in the bubble at the moment of collapse (acoustic  pressure)

$P$ = pressure in the bubble at its maximum size or the vapor pressure of the

solution

$\gamma$ = polytrophic ratio.

Polytropic ratio is the ratio of the heat capacity at constant pressure to that at constant volume

$$\gamma = \frac{c_p}{c_v} \tag{4.19}$$

where $\gamma$ is the polytropic ratio of the gas

$c_p$ is the heat capacity at constant pressure

$c_v$ is the heat capacity at constant volume

As the maximum temperature achieved in the bubble is dependent on the properties of gas species, it is considered that the degradation of volatile organic compounds is strongly affected by the gaseous components in the cavitation bubble (Kojima et al., 1997). The specific nature of the saturating gas, i.e. its tendency to form radicals, influences the relative proportion of pyrolytic or free-radical reaction steps (Hoffmann et al., 1996).

Wayment and Casadonte reported that the sonochemical degradation rate or alachlor in argon atmosphere was higher than that in air and oxygen atmospheres, independent of frequency (Wayment and Casadonte, 2002).

Kojima and co-workers studied the effects of dissolved gas species on the ultrasonic degradation of 4-chloro-2-methylphenoxy acetic acid in aqueous solutions (Kojima et al., 2005). They found that lowest first-order rate constant was in pure nitrogen atmosphere, the highest rate constant was obtained with oxygen atmosphere and air gave the second highest rate constant, and argon provided the third best rate constant for the sonolytical removal of 4-chloro-2-methylphenoxy acetic acid at 500 kHz.

Kıdak on the other hand, found that sonochemical degradation rate of phenol under air atmosphere was higher than that obtained under argon atmosphere (Kıdak, 2005). Whereas Tezcanli-Güyer reported sonochemical decolorization rates of textile dyestuff Acid Orange 7 to decrease in the sequence: Ar>$O_2$>Air (Tezcanli Güyer, 2003).

4.2.4.1. Stripping Effect of Argon on Chloroform Removal in the Absence of Ultrasound. Being a highly volatile and aquaphobic compound, chloroform can be removed from the aqueous solutions through the stripping effect of a purge gas alone (Linek et al., 1998). The effect of gas stripping in different volumes of chloroform solution was investigated to estimate the rate of removal without ultrasonic irradiation. The ultrasonic reactors of 20 kHz, 300 kHz and 520 kHz systems were used for 80 mL, 150 mL, and 300 mL reaction volumes for the stripping experiments, and the data obtained are presented in Figure 4.22.
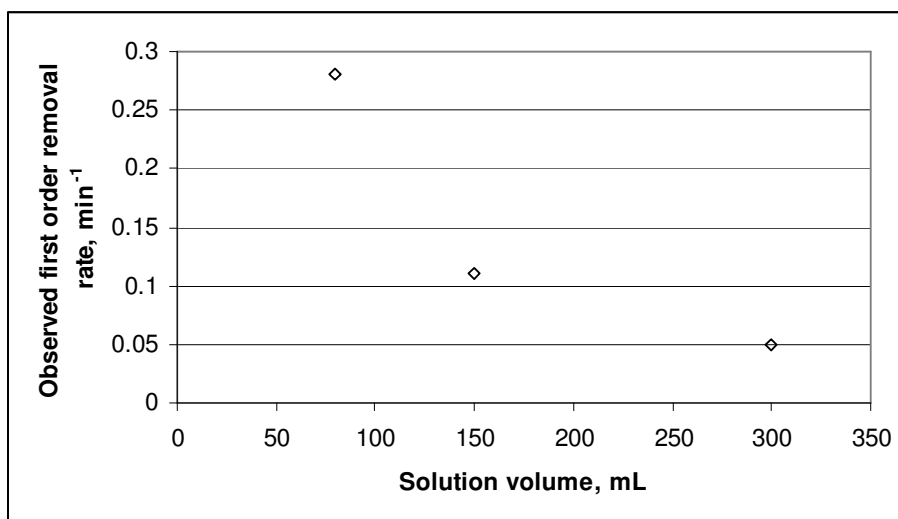
Figure 4.22. The variation of chloroform ($c_0$ = 1400 µg/L) removal rates of with Argon purging only, with no ultrasonic irradiation.

The data in Figure 4.22 points to the dependency of removal rate of stripping to the liquid/gas volume ratio. As the Argon flowrate was kept constant, the highest removal rate of chloroform is observed at 20 kHz reactor which has a liquid volume of 80 mL, followed by 300 kHz reactor that operates at 150 mL and the lowest removal rate is observed at the 520 kHz reactor which can only operate at a minimum liquid volume of 300 mL.

The effect of initial chloroform concentration on the argon stripping rate was studied at the 300 kHz reactor with the initial chloroform concentrations of 894 µg/L, 2104 µg/L and 4295 µg/L and the obtained first order removal rates are plotted in Figure 4.23.

The first order removal rate constant of chloroform can be seen to decline with increasing initial chloroform concentration. Even though these findings may seem to be contrary to the fact asserted in section 2.2.3.2 of this dissertation, which states that in order to achieve complete removal of chloroform through aeration, a theoretical minimum air to water volume ration of 6.7:1 is required regardless of initial contaminant concentration, this rule is proposed for a perfect aeration column where mixing is complete. However, in the experiments conducted, the gas sparging is performed only to enhance sonochemical cavitation, so a flowrate of 1 L/min is maintained throughout the experiments, which is the minimum flowrate measurable and controllable with the Aalborg GFC 371S mass

flowmeter / controller used. Thus, the liquid/gas contact was severely hindered by the low gas flowrate and the poor mixing conditions, and the contact was largely diffusion controlled.
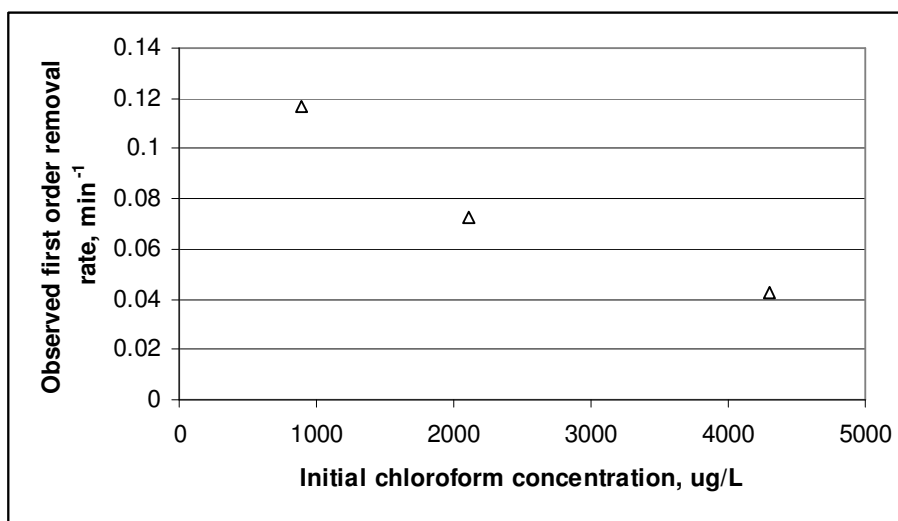


Figure 4.23. The effect of initial chloroform concentration on chloroform removal rate of argon purging using the 300 kHz reactor with no ultrasonic irradiation

The observation that increased initial chloroform concentration does not increase the removal rate by stripping, reveals that the increased chloroform removal rate observed during sonication experiments at increased chloroform concentrations, can not be attributed to the stripping effect of the purged gas, but needs to be explained as a result of ultrasonic activity.

4.2.4.2. Ultrasonic Irradiation Without Gas Sparging. The effect of ultrasonic irradiation on chloroform solutions without gas sparging to enhance cavitation events was studied at 520 kHz with three different initial concentrations of chloroform, and the data are presented in Figure 4.24.
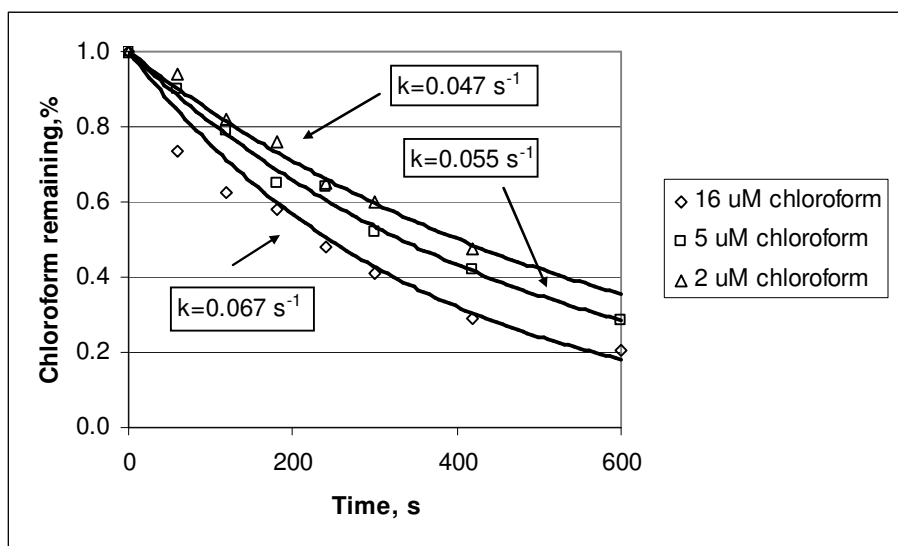
Figure 4.24. Effect of ultrasonic irradiation on chloroform solutions with initial concentrations of 16 µM, 5 µM and 2 µM chloroform with 520 kHz at the power density of 0.069 W/mL

The data plotted in Figure 4.24 shows that the observed first order removal rate of chloroform increases with increased initial chloroform concentration. This trend is in accordance with the findings summarized in Figure 4.12, which showed that the increased initial chloroform concentration increases the observed first order removal rate constant. However, the unexpected increase below 5 µM, in Figure 4.12 was not observed in the absence of gas sparging. According to the hot spot theory, higher initial concentrations of volatile organic solutes result in a lower polytropic ratio ($\gamma$) in the cavitation bubbles, reducing the maximum temperature of collapse (Dewulf et al., 2001). As chloroform is held to be removed through pyrolysis inside the bubbles (Henglein and Fischer, 1984, Shemer and Narkis, 2004), the reduction of bubble temperature through increased initial chloroform concentration can be expected to reduce the chloroform removal rate. However as the chloroform concentration is reduced from millimolar to micromolar range, the ratio of OH radicals to chloroform molecules inside the bubble will be increased (Dewulf et al., 2001). Whereas pyrolysis is not affected by this increase, the reaction of chloroform with radical species will become more likely at these lower concentrations, resulting in an increase of the contribution of OH radicals on the degradation. During irradiation without gas sparging however, the cavitation events are restrained through the lack of nuclei that would be otherwise provided by argon bubbles. The only difference in the amount of

available nuclei between chloroform solutions of different concentrations prepared in deionized water, are those provided by the target compound itself. Thus the solution with the higher initial chloroform concentration will produce more cavitation events and more hydroxyl radicals, but this increase in the radical concentration will be balanced by the chloroform molecules near those cavities. Also the reduced initial chloroform concentration will cause reduced cavitation events which naturally will reduce the pyrolytic removal rate, causing a reduction in the overall removal rate.

4.2.4.3. Effect of Gas Type on Removal. For the investigation of the effect of gas type on chloroform removal, experiments were conducted with argon, air, oxygen and nitrogen at different initial chloroform concentrations, at 300 kHz and a power density of 0.078 W/mL. Gas flowrates were kept at the minimum constantly attainable rate of 1 L/min with an Aalborg GFC 371S model gas mass flowmeter/controller. The polytropic ratios of the gases used are given in Table 4.2.

Table 4.1. Polytropic ratios and thermal conductivities of saturating gases used for the sonolysis of chloroform solutions (Mason and Lorimer, 2002)

| Gas | Argon | Air | Oxygen | Nitrogen |
|---|---|---|---|---|
| $\gamma$ (cp/cv) | 1.66 | 1.40 | 1.39 | 1.40 |

Among the gases that were investigated, argon was the one with the highest polytropic ratio of 1.66, followed by nitrogen with 1.40 and oxygen with 1.39. The polytropic ratio of air was calculated as a mixture consisting of 79 per cent nitrogen and 21 per cent oxygen, resulting in a ratio of 1.40. Gases with large polytropic ratio values ($\gamma$) enhance the adiabatic conditions in the collapsing bubble thus improving sonochemical effects. For this reason, monatomic gases (He, Ar, Ne) are often used in preference to diatomic gases ($N_2$, air, $O_2$). However it must be remembered that this dependence on $\gamma$ is a simplistic view, since sonochemical effects also depend on the thermal conductivity of the gas, even if a strict relationship between properties of gases and sonochemical effect has not been established.

The observed first order removal rate coefficients obtained by sparging with different gases and varying initial chloroform concentrations at 300 kHz are plotted in Figure 4.25.
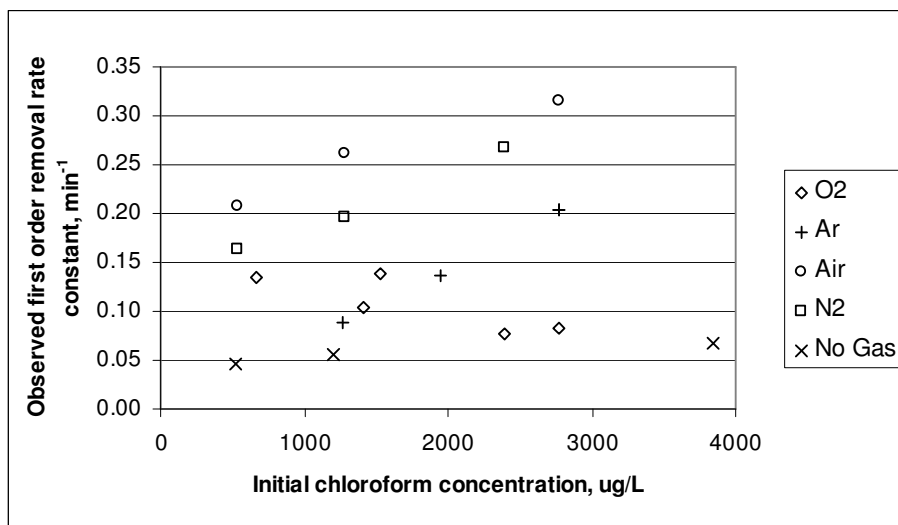


Figure 4.25. Effect of gas type on first order chloroform removal rate constants for 300 kHz system (0.078 W/mL)

The data presented in Figure 4.25 show that air provides maximum chloroform removal rate constants. Irradiation of increased initial chloroform concentrations under air atmosphere gave rise to increased removal rate constants. Nitrogen gave a similar profile of increased removal rate constants with increased initial concentrations, but the rates constants obtained were slightly smaller than those obtained with air. Argon was observed to be the poorest gas in that context. An increase similar to that observed with air and nitrogen was also in evidence with argon with increased initial chloroform concentration. Application of ultrasonic irradiation in the absence of gas sparging was also observed to give increased removal rate constants with increased initial concentration. The only gas that diverged from this behavior was oxygen; increased initial chloroform concentrations resulted in slightly reduced first order removal rate constants.

The reaction sequence of water pyrolysis during the irradiation of an aqueous solution in the presence of argon is as follows (Ince et al., 2000):

$$H_2O + ))) \rightarrow \bullet OH + \bullet H \qquad \text{(thermolysis)} \qquad (4.20)$$

$$\bullet OH + \bullet H \rightarrow H_2O \qquad (4.21)$$

$$\bullet OH + \bullet OH \rightarrow H_2O_2 \qquad (4.22)$$

$$2 \bullet OH \rightarrow H_2O + O \qquad (4.23)$$

The presence of argon increases the maximum achievable temperature inside the bubble during implosion. Thus, it promotes the pyrolytic reactions inside the bubble. However, despite the well-accepted knowledge that monatomic gases in sonicated liquids are more favorable than diatomic gases for output temperatures of collapse, as a consequence of their higher polytrophic gas ratios, (Suslick, 1990), we found that argon does not always provide better sonochemical yields than diatomic gases.

If the solution is saturated with oxygen, peroxyl and additional hydroxyl radicals are formed in the gas phase (Beckett and Hua, 2000) as:

$$O_2 + ))) \rightarrow 2 \bullet O \qquad (4.24)$$

$$O_2 + O \rightarrow O_3 \qquad (4.25)$$

$$O_2 + \bullet H \rightarrow \bullet O_2H \ (\text{or} \ \bullet OH + O) \qquad (4.26)$$

$$O + \bullet O_2H \rightarrow \bullet OH + O_2 \qquad (4.27)$$

$$\bullet O_2H + \bullet O_2H \rightarrow H_2O_2 + O_2 \qquad (4.28)$$

$$\bullet O + H_2O \rightarrow 2 \bullet OH \qquad (4.29)$$
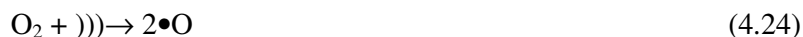
Larger yields in the presence of air despite its lower polytrophic gas ratio may also be obtained due to the reactions of nitrogen with molecular oxygen to yield nitric acid and radical species such as $\bullet OH$, $\bullet NO_2$, and $\bullet NO_3$ that accelerate the oxidation process.

Chemical reactions that take place during air injection into a sonoreactor in addition to the reactions 4.20-4.29, are as follows (Ullerstam et al., 2000):

$$2N_2 + O_2 \rightarrow 2N_2O \qquad (4.30)$$

$$2N_2O + H_2O \rightarrow 2HNO_2 + 2N_2 \qquad (4.31)$$

$$\bullet H + N_2O \rightarrow N_2 + \bullet OH \qquad (4.32)$$

$$\bullet OH + N_2O \rightarrow 2NO + \bullet H \qquad (4.33)$$

$$HNO_2 + H_2O_2 \rightarrow HNO_3 + H_2O \qquad (4.34)$$

$$HNO_3 + ))) \rightarrow \bullet OH + \bullet NO_2 \qquad (4.35)$$

$$HNO_3 + ))) \rightarrow \bullet H + \bullet NO_3 \qquad (4.36)$$

The formation of nitrous and nitric acids (reactions 4.31, 4.34) enhance the generation of excess •OH and introduce the radicals of nitrite and nitrate, which are comparably strong oxidants of organic compounds that may support the oxidation process ($k_{\bullet NOx} = 10^7$ L/ mol.sec) (Gogate et al., 2003).

The relative slowness of the reactions in the presence of argon to those with air and nitrogen suggests that pyrolysis is not the only destruction mechanism for chloroform inside the bubbles. The presence of nitrite and nitrate radicals can be deduced to increase the removal rate, despite the reduction of maximum implosion temperature. The very low first order rate constants obtained with oxygen indicate that the primary accelarating factor in the air atmosphere is the presence of nitrogen.

The reports of best results for different gas types for sonochemical degradation of different compounds support the hypothesis that different types of radicals formed and their abundance as well as their selectivity towards the target compounds, combined with

the thermal conditions obtained in the imploding bubble determine the removal efficiency of target compounds through highly complex mechanisms (Kojima et al., 2005; Kidak, 2005; Tezcanli-Guyer, 2003; Hoffmann et al., 1996).

### 4.2.5. Effect of Scavenger Compounds on Removal

Sonochemical reactions can take place in three different parts of the irradiated solution; in the bulk solution, inside the bubble and at the bubble-solution interface (Ince et al., 2001). The reaction that takes place inside the bubble is pyrolytic and is affected by the maximum temperature and pressure achieved during implosion. The reactions at the bubble-solution interface and inside the bulk solution are largely induced by the radicals that are produced during thermolysis and ejected into the surrounding medium, e.g. hydroxyl radicals, or the side-products of the reactions of these radicals with other species present in the solution. Thus, through the addition of appropriate compounds that can scavenge these radicals, light can be shed onto the reaction mechanism of ultrasonic chloroform removal.

Tert-butanol (t-buOH) is a known •OH radical scavenger that inhibits the hydroxyl radical reactions at the bulk solution during sonochemical treatment (Nagata et al., 1996). Shemer and Narkis used t-buOH to suppress hydroxyl radical reactions in THM sonolysis studies (Shemer and Narkis, 2004). They used initial THM concentrations of 10 mg/L of chloroform, bromodichloromethane, dibromochloromethane and bromoform. Addition of t-buOH as the scavenger compound did not affect the removal rate of chloroform, bromodichloromethane and dibromochloromethane, but had a negative impact on the bromoform removal rate, leading to the conclusion that reactions with hydroxyl radicals were not effective in the sonolysis of the three THMs, but that, pyrolysis was the active mechanism in their removal. The reduction in the removal rate of bromoform was explained by the scavenging of the hydroxyl radicals that would otherwise be utilized for bromoform removal, thus the observed reduction in removal rate.

Humic acid is known to degrade under sonochemical treatment at the bulk solution exclusively through hydroxyl radical reactions (Nagata et al., 1996; Naffrechoux et al., 2003). Humic acid solutions prepared in three concentrations of 0.68 mg/L TOC, 1.22

mg/L of TOC and 1.92 mg/L of TOC and spiked with 1400 μg/L of chloroform were sonicated at 300 kHz to investigate the effect of the presence of humic materials in solution. The concentrations of humic acid were selected to represent the TOC content of tap water in Istanbul which was measured as 3 mg/L NPOC. Figure 4.26 shows the change of chloroform removal rate with varying concentrations of humic acid.
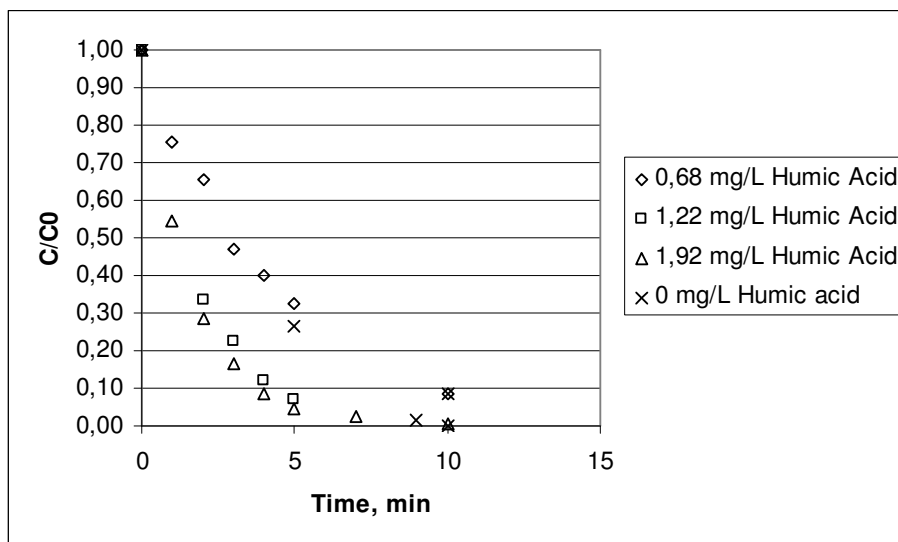


Figure 4.26. Change in chloroform removal rate with various humic acid concentrations at 300 kHz, 0.078 W/mL

Increasing the concentration of humic acid was observed to increase chloroform removal rate very slightly. If the removal mechanism of chloroform was through radical reactions in the bulk solution, the scavenging of hydroxyl radicals by humic acid molecules would be expected to reduce the chloroform removal rate. The slight increase in the removal rate however, can be explained as the scavenging of •Cl radicals in the solution by humic compounds, thus reducing the rate of recombination reactions of chloroform as follows (Henglein and Fischer, 1984):

$$CHCl_2 + •Cl \rightarrow CHCl_3 \qquad (4.37)$$

The scavenging of •Cl radicals may also explain the inability of detecting $CCl_4$ as an end-product of sonolysis of chloroform. The enhancement of chloroform removal rate

through introduction of humic acid molecules in the solution may also be the consequence of enhanced cavitation events upon increased nuclei.

The absorbances of humic acid solutions at 254 nm were measured during sonication to observe the possible changes in humic acid structure. As can be seen in Figure 4.27, the absorbances showed a slight reduction during the 30 minutes of irradiation at 300 kHz, 0.078 W/mL, indicating the cleavage of aromatic rings of humic acid molecules as was reported by others (Chemat et al., 2001).
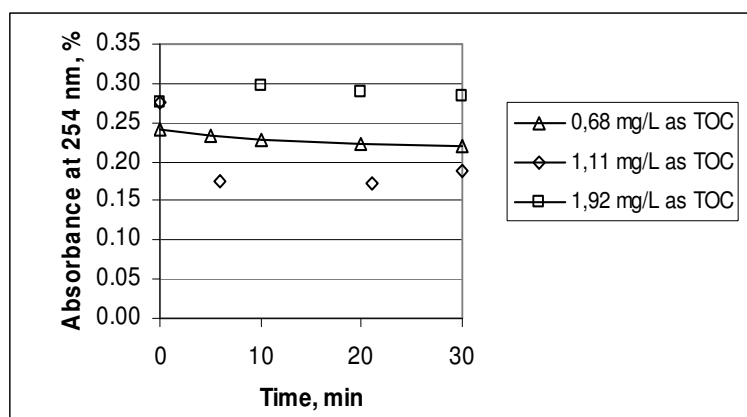


Figure 4.27. The change of absorbance at 254 nm with varying humic acid concentrations as TOC during ultrasonic irradiation at 300 kHz, for 30 min.
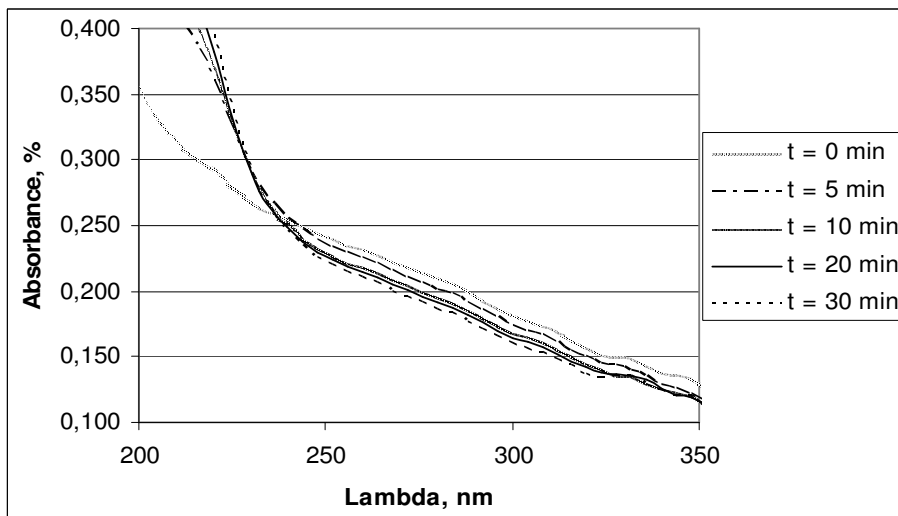


Figure 4.28. The change in absorption spectra of humic acid as 0.68 mg/L NPOC during irradiation at 300 kHz with a power density of 0.078 W/mL for 30 min.

Figure 4.28 shows the change in the UV absorption spectra of humic acid as 0.68 mg/L NPOC during irradiation at 300 kHz with a power density of 0.078 W/mL. The absorption around 240 and 280 nm both assigned to aromatic rings (Silverstein et al., 1991, Nagata et al., 1996) decreased slowly during the sonolytical treatment, supporting other research reporting the cleavage of aromatic rings by ultrasonic irradiation (Ince and Tezcanli, 2004; Goskonda et al., 2002)

The effect of ultrasonic irradiation on the TOC content of the humic acid solutions was also measured during the experiments. Figure 4.29 presents the data obtained from irradiation of humic acid solutions of 0.68 mg/L as TOC, 1.11 mg/L as TOC and 1.92 mg/L as TOC in the presence of 1400 µg/L of chloroform.
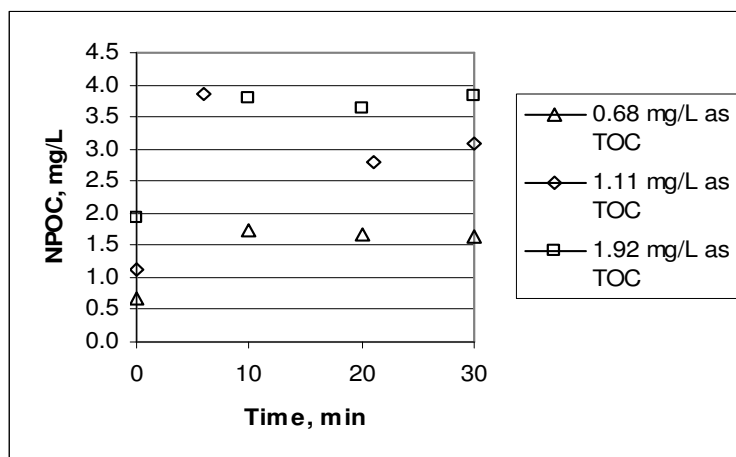


Figure 4.29. Change of TOC values of humic acid solutions during ultrasonic irradiation at 0.078 W/mL at 300 kHz

As can be seen in Figure 4.29, TOC values increase during the first 5 minutes followed by a slight but steady decrease afterwards. The initial increase can be explained by the effect of ultrasound increasing the solubility of humic acid, it must be noted that TOC analyses were conducted as TC measurements therefore, TOC values include the carbon content of chloroform in the solution as well.

The effect of carbonates on the removal rate of chloroform was investigated through the addition of three different concentration levels of sodium bicarbonate to

chloroform solutions of 1500 µg/L initial concentration. The solutions were irradiated at 300 kHz at a power density of 0.039 W/mL. Figure 4.30 shows that the rate of chloroform removal was not affected by the carbonate concentration in the solution. However, the observed first order removal rate constants were seen to increase slightly with increasing carbonate concentration, supporting the results of the experiments conducted with humic acids. The observed first order removal rate constants were calculated as $1.8 \times 10^{-3}$ $s^{-1}$ for 0.25 M $CO_3$, $1.9 \times 10^{-3}$ $s^{-1}$ for 0.5 M $CO_3$ and $2.0 \times 10^{-3}$ $s^{-1}$ for 1.0 M $CO_3$.
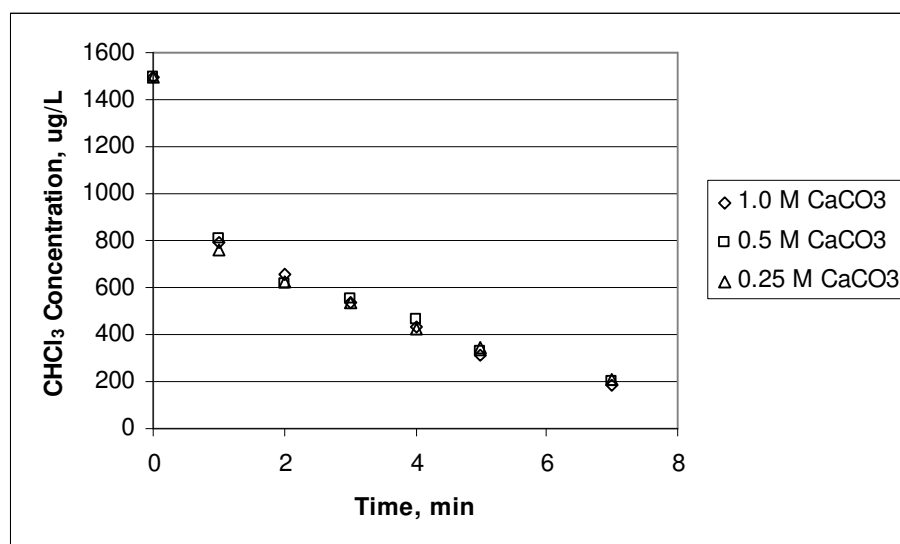


Figure 4.30 The effect of sodium bicarbonate in solution to the observed removal rate of chloroform

### 4.2.6. Effect of Solute Mixture on Removal

In order to investigate the effect of solute mixtures on chloroform removal, mixtures of chloroform, bromodichloromethane, dibromochloromethane and bromoform were sonicated at 300 kHz, 0.078 W/mL for 30 minutes. Mixtures were prepared with 15.8 µM chloroform, 11.4 µM bromodichloromethane, 5.4 µM dibromochloromethane, and 16.7 µM bromoform.

In Figure 4.31 the relative removal rates of chloroform, bromodichloromethane, dibromochloromethane and bromoform in the same solution are presented.

Figure 4.31. Relative observed removal rates of four trihalomethanes in synthetic aqueous solution at 0.078 W/mL

As can be seen in Figure 4.30, of the four trihalomethanes experimented with, the fastest removed compound was chloroform, followed by bromodichloromethane, dibromochloromethane and finally bromoform. The observed first order removal rate constants a reported in Table 4.2. 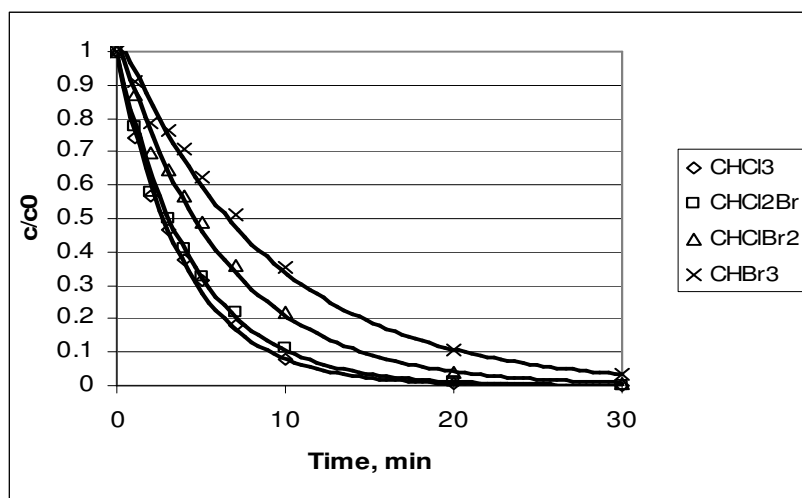The data could not be compared with the only data reported in the literature, because sonolysis was carried out at a frequency of 20 kHz, and the applied power density was not reported (Shemer and Narkis, 2004).

Table 4.2. The observed first order removal rate constants (as estimated by regression analysis) for a mixture of trihalomethanes sonicated at 300 kHz for 30 min. with a power density of 0.078 W/mL.

| Compound | Initial Concentration | Observed first order removal rate constant |
|---|---|---|
| Chloroform | 15.8 μM | $1.8 \times 10^{-3} \, M^{-1} s^{-1}$ |
| Bromodichloromethane | 11.4 μM | $1.6 \times 10^{-3} \, M^{-1} s^{-1}$ |
| Dibromochloromethane | 5.4 μM | $1.2 \times 10^{-3} \, M^{-1} s^{-1}$ |
| Bromoform | 16.7 μM | $0.8 \times 10^{-3} \, M^{-1} s^{-1}$ |

It was found that the removal rate of chloroform was not affected by the presence of other trihalomethanes in solution, implying that the cavity production in the system is in excess of the demand of the target compounds. The data are presented in Figure 4.32.

Figure 4.32. Effect of other trihalomethanes in solution on the rate of chloroform removal



Figure 4.33. Effect of other trihalomethanes in solution on the rate of bromoform removal

It was found that the removal rate of bromoform was not affected by the presence of other trihalomethanes in solution, indicating that the cavity production in the system is in excess of the demand of the target compounds as can be seen in Figure 4.33.
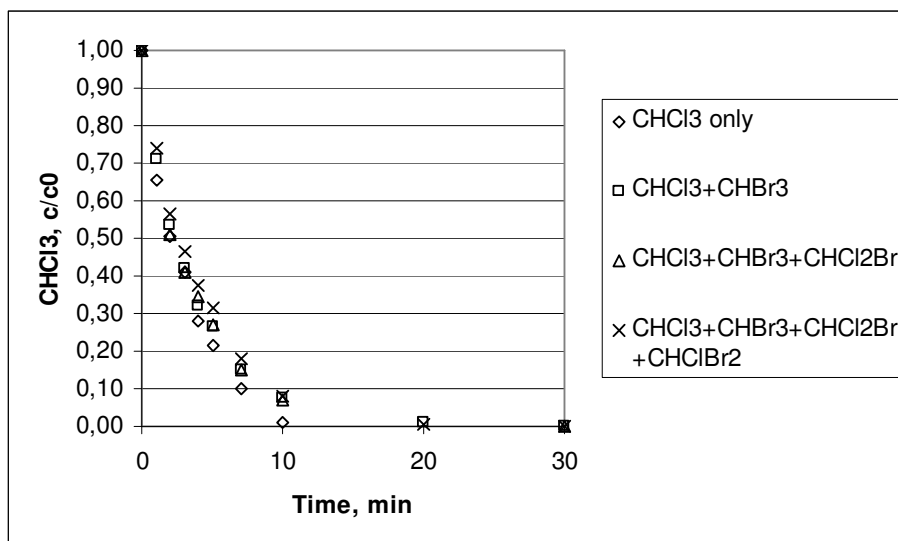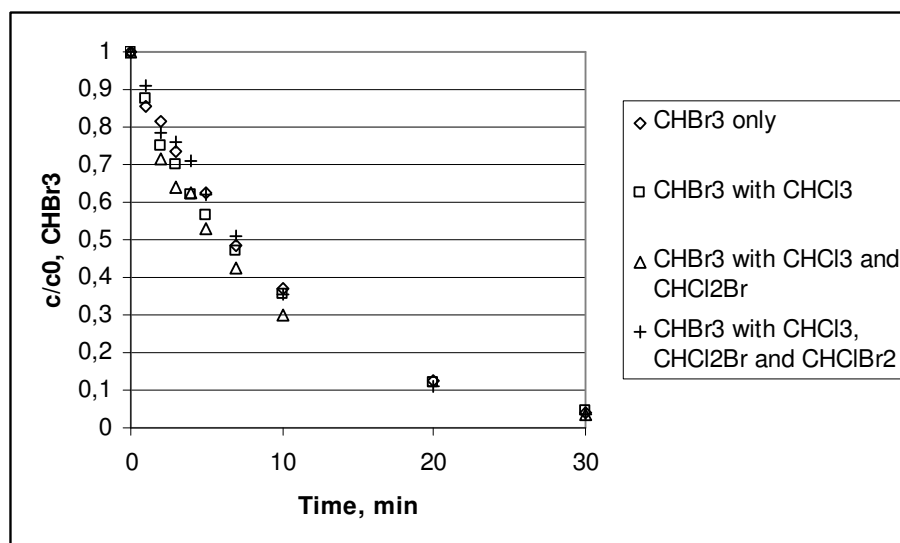
### 4.3. Sonolytical Trihalomethane Removal from Tap Water

Tap water samples with initial THM concentrations of 70 µg/L chloroform, 40 µg/L bromodichloromethane, 56 µg/L dibromochloromethane, and 50 µg/L bromoform, were treated with ultrasound in the batch mode. The samples had alkalinity levels of 65- 70 mg/L as $CaCO_3$ and TOC as 3 mg/L TC and IC as 2 mg/L. The tap water trihalomethanes concentrations measured here are larger than those reported by Toroz and Uyak for the year 2003 (Toroz and Uyak, 2005). The difference can partially be attributed to the sampling conditions, and the time difference between the samplings. It is also possible that part of the difference between our data and those of Toroz and Uyak may be due to instrumental problems encountered in our analytical system. The high baseline level with high noise coupled with a positive drift in the baseline are obvious reasons of high error margins encountered particularly in the analyses of samples with low THM concentrations. Thus, the measurements of our tap water trihalomethane concentrations should be used only for comparison with the rest of the data presented in this dissertation, and not to any exterior source.
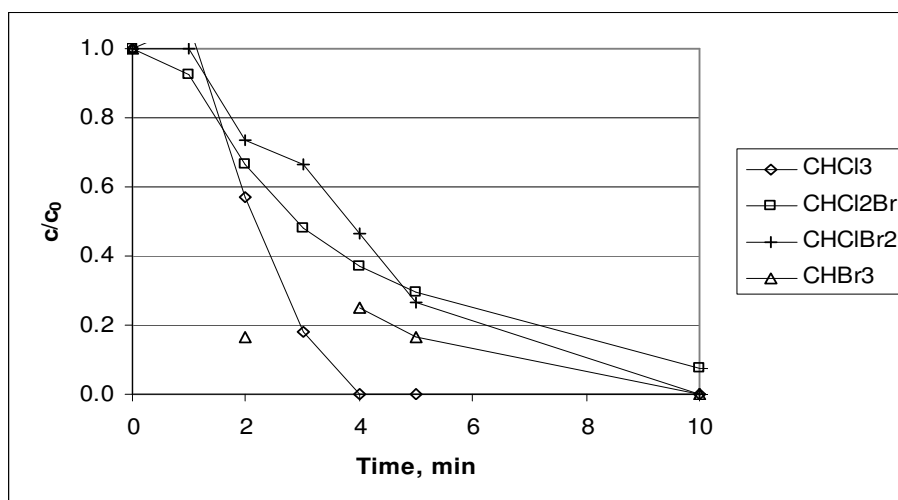


Figure 4.34. Sonochemical removal of trihalomethanes from tap water at 300 kHz with 0.078 W/mL power density

As can be seen in Figure 4.34 chloroform is the fastest removed compound, followed by bromodichloromethane, dibromochloromethane and bromoform. These finding are in agreement with the results obtained with the model studies conducted with

synthetic solutions. Although the low concentrations were removed very quickly, and some of the data were erratic due to analytical problems associated with low concentrations, the observed first order removal rate constants that were calculated as $3.8 \times 10^{-3}$ s$^{-1}$ for chloroform, $3.2 \times 10^{-4}$ s$^{-1}$ for bromodichloromethane, $1.0 \times 10^{-4}$ s$^{-1}$ for dibromochloromethane and $2.0 \times 10^{-3}$ s$^{-1}$ for bromoform.
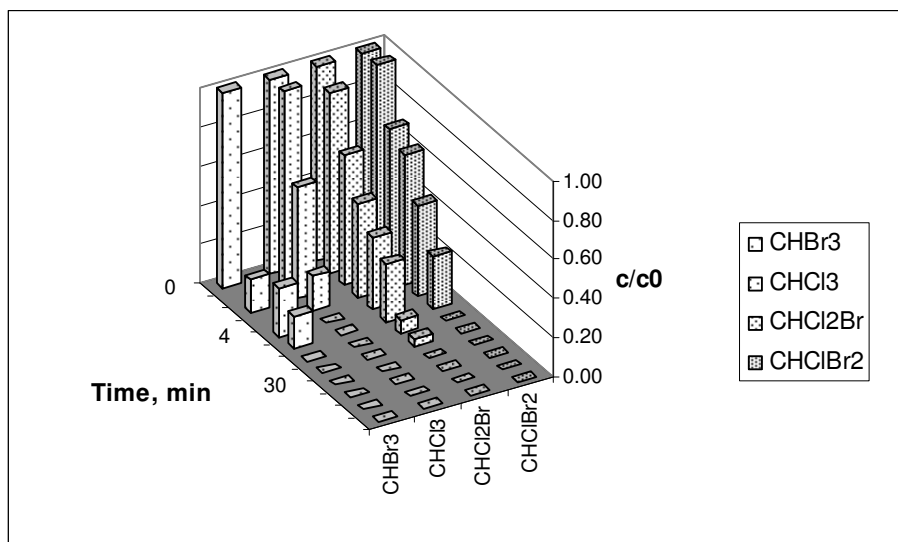


Figure 4.35. The effect of ultrasonic irradiation at 300 kHz with a power density of 0.078 W/mL for 90 min on the trihalomethane concentrations present in Istanbul tap water

In order to observe the effects of long term irradiation, samples of tap water from Istanbul, were treated with 300 kHz for 90 minutes. As can be seen in Figure 4.35, all four trihalomethane species were observed to be completely removed within 30 minutes. The treatment was continued further until the 90th minute to observe if any of the target species re-formed. None of the target species were observed to re-form at any time during 90 minutes irradiation, indicating that all were completely removed at the end of contact.

Tap water samples were also treated with the 20 kHz system at a power density of 0.48 W/mL. The concentrations of the trihalomethanes during the treatment are plotted against irradiation time in Figure 4.36.
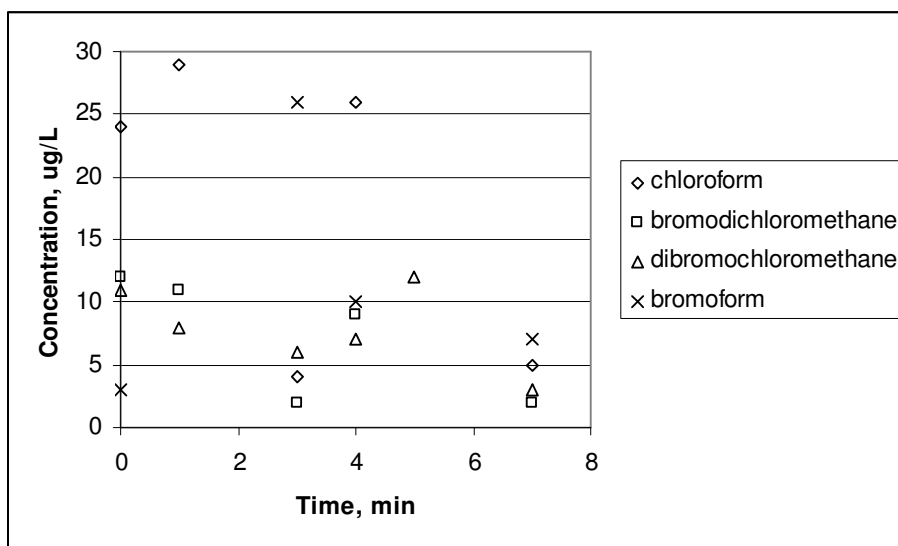
Figure 4.36. Effect of 20 kHz ultrasound (at a power density of 0.48 W/mL) on the THM concentrations in tap water during 7 min. contact time

The fluctuations in the measured concentrations are due to the closeness of the concentration ranges to the detection limit of the analytical system. These fluctuations prohibited the calculation of the reaction rate constants.

As presented in Figure 4.35, and 4.36, concentrations of all trihalomethane species investigated were reduced to below detection limit within 10 minutes of irradiation both at 300 kHz and at 20 kHz. The data demonstrates that trihalomethane species at concentration levels present in tap water are removed quickly with ultrasonic irradiation, establishing this method as a promising treatment of trihalomethanes removal from drinking water, requiring however cost estimation for comparison with other treatment methods.

## 4.4.    Effect of Sonolysis on the Acute Toxicity of Tap Water

The most important concern about application of ultrasonic techniques to drinking water treatment is the scarcity of data on exact reaction pathways, due to the complexity of the reactions involved and the possibility of formation of toxic end products. In order to asses the presence of potential toxic products, Microtox toxicity essay was applied to tap water samples irradiated with ultrasound.

Toxicity of tap water treated with 300 kHz under argon gas for 30 minutes was measured with the Microtox toxicity test. According to the 100% test, a $\Gamma$ % value was calculated for each dilution with the formula:

$$\Gamma \% = I_{tc} / I_t \quad - 1 \tag{4.38}$$

where $I_{tc}$ is the light level (I) at incubation time (t) of the blank control (c)

$I_t$ is the light level (I) at incubation time (t) for various sample concentrations.

The calculated $\Gamma$ % values were plotted versus the sample concentrations on a log-log scale. The EC50 value, which is the concentration where the light emission of the test bacteria is inhibited by 50%, is the concentration where the straight line that passes through the data points intersects with the log gamma value of 1.

For the Equation 4.38 to give positive values, $I_t$ should be smaller than $I_{tc}$, meaning that the added solution needs to be toxic to the test bacteria. However, after 10 minutes of irradiation, including the ten-minutes sample, all the samples actually showed a consistent increase in the light intensity, thus giving negative values to $\Gamma$. The only test sample that gave positive values of $\Gamma$ was tap water. The plot of log $\Gamma$ versus log %tap water is given in Figure 4.37.
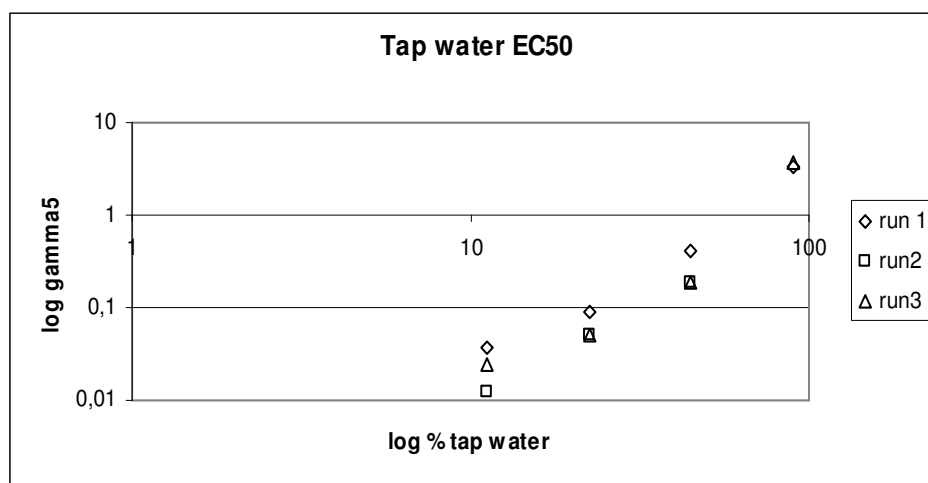
Figure 4.37 The log Γ versus log % tap water graph

In Figure 4.36 the EC50 value (the concentration where the light emission of the test bacteria is inhibited by 50%) of tap water can be seen as the point where the straight line that passes through the data points intersects with the log gamma value of 1. This value is read as 73 %, meaning that the effective concentration of tap water that inhibits 50 % of the light production of the test organisms is 73 % tap water. According to the norm, a sample that causes less than 20 per cent inhibition is considered non-toxic (Gonze et al., 1999).

Hence, effluent samples were found non-toxic. Toxicity of tap water was reduced as a result of sonication. Furthermore, a reduction of toxicity and an increase of the stimulating effect were observed. Ultrasonic irradiation actually reduced the inherent toxicity of tap water due to the presence of free chlorine and the combination of other disinfection by-products. As the test system used is only an acute toxicity test, and does not answer questions about the chronic toxicity potential of the sample tested, the results can be considered encouraging.

# 5. CONCLUSIONS

The investigation of chloroform removal in relation to power density, irradiation frequency, hydrogen peroxide formation rate and initial chloroform concentration in all three systems led to the conclusions of:

i)      At 20 kHz, increased power density or increased initial chloroform concentration does not increase hydrogen peroxide formation rate. Increased chloroform concentration does not increase chloroform removal rate either. However, increased power density increases $CHCl_3$ removal rate, meaning that at this frequency the only factor that causes increase in removal rate is cavitation events. Thus, the primary removal mechanism at this frequency can be deduced as pyrolysis.

ii)      At 300 kHz and 520 kHz increased power density and initial $CHCl_3$ concentration enhances hydrogen peroxide formation. Both of these factors also cause an enhancement of chloroform removal rate. However, the addition of OH radical scavengers to the irradiated medium does not reduce the chloroform removal rate. This positive correlation between the hydrogen peroxide formation and $CHCl_3$ removal could not be proven to point at a cause and effect relationship, but that both phenomena are the results of the same cause, namely the enhancement of cavitation events.

iii)      As pyrolysis is held to be the main sonolytical removal mechanism of chloroform, it comes as a surprise that 20 kHz was the least efficient of the three frequencies investigated. In terms of the observed $CHCl_3$ removal rate per W/mL energy dissipated in the system, 520 kHz is the most efficient system, followed by 300 kHz, and the least efficient system is 20 kHz.

iv)      With its high polytropic ratio, argon would be expected to give the highest pyrolysis temperatures, resulting in the highest $CHCl_3$ removal rates.

However, both air and nitrogen proved to give higher removal rates, suggesting the operation of radical reaction based removal mechanisms inside the cavitation bubbles.

v) The presence of hydroxyl radical scavengers in the medium actually increased the chloroform removal rate at 300 kHz, instead of hindering it.

vi) Combined sonolysis of trihalomethanes at high concentrations showed that the presence of other trihalomethanes in the medium did not affect the removal rates of neither chloroform nor bromoform at the elevated concentrations investigated.

Sonolytical treatment of tap water as collected from a local tap showed that all the target compounds were reduced to below detection limit within 10 minutes, even if reliable rate constants could not be obtained due to the low concentrations and high removal rates involved.

Ultrasonic irradiation appears to be an effective method for the destruction of dilute aqueous solutions of refractory organic contaminants because of the action of localized high concentrations of oxidizing species such as hydroxyl radical and hydrogen peroxide in solution, high localized temperatures and pressures. The simplicity and the flexibility of ultrasonic irradiation along with its high efficiency of THM destruction indicate the potential of a sonochemistry-based process to become a competitive technology with other advanced water treatment technologies.

In all cases, the presence of scavengers was observed to either slightly enhance or not affect sonochemical degradation at the low concentration ranges examined rather than inhibit.

The sonochemical reactions of volatiles in aqueous media are very much concentration dependent. The ultimate way to prove the OH radical induced degradation could be the determination of the intermediates typical for this reaction pathway, provided that they are not produced by pyrolytic reactions. However, due to the low initial

concentrations appropriate for THM removal studies, and presuming that the yield of individual volatile intermediates would be typically in the order of less than 10 per cent (Henglein and Fischer, 1984), analytical methodology could be a major obstacle to prove OH induced radical degradation of THMs in drinking water.

All of the THM concentrations from tap water samples were observed to be completely removed within 10 minutes irradiation at 300 kHz with a power density of 0.078 W/mL, and within 7 minutes irradiation at 20 kHz with a power density of 0.48 W/mL

No increase in the toxicity of the tap water was observed with the acute toxicity test employed. Moreover, the treatment of tap water samples with ultrasound at 300 kHz actually induced a stimulating effect on the metabolic activity of toxicity test organisms with time. However, these data can not be interpreted as a substitute for extensive chronic toxicity tests, which needs to be performed to illuminate the potential effects of ultrasonic treatment of drinking water on human health.

Ultrasonic systems are robust systems that can work under a highly variable range of pollutant loads and environmental conditions. They are simple to use and once established, require minimum skilled worker labor to operate.

# REFERENCES

Abdullah, M.P., Yew, C.H., bin Ramli, M.S., 2003. Formation, Modeling and Validation of Trihalomethanes in Malaysian Drinking Water: A Case Study in the Districts of Tampin, Negeri Semblian and Sabak Bernam, Selangor, Malaysia, Water Research, 37, 4637-4644.

Adin, A., Katzhandler, J., Alkaslassy, D., Rav-Acha, C.H., 1991. Trihalomethane formation in Chlorinated Drinking Water: A Kinetic Model, Water Research, 25, 797-805.

APHA/AWWA/WPCP, 1992. Standard Methods for the Examination of Water and Wastewater, 17th Ed., American Public Health Association, Washington, DC.

Asmus, K.D., Flyunt, R., 2003. Free Radical Mechanisms in Advanced Oxidation Technologies; Degradation of Halogenated Organic Compounds, Proceedings of 3rd International Conference on Oxidation Technologies for Water and Wastewater Treatment, 25-31, Goslar, ISBN 3-89720-655-2.

Beckett, M., Hua, I, 2000. Elucidation of the 1,4-Dioxine Decomposition Pathway at Discrete Ultrasonic Frequencies, Environmental Science and Technology, 3, 3944-3953.

Beilsteins, 1940. Handbuch Der Organischen Chemie, Vierte Auflage, Drittes Erganzungwerk.

Berlan,J., Mason, T.J., 1992. Sonochemistry: From Research Laboratories to Industrial Plants, Ultrasonics, 30, 203-212.

Bhatnagar, A., Cheung, H.M., 1994. Sonochemical Destruction of Chlorinated C1 and C2 Volatile Organic Compounds in Dilute Aqueous Solution, Environmental Science and Technology, 28, 1481-1486.

Biziuk, M., Przyjazny, A., 1996. Methods of Isolation and Determination of Volatile Organohalogen Compounds in Natural and Treated Waters, Journal of Chromatography A, 733, 417-448.

Boyce, S.D., Hornig, J.F., 1983. Reaction Pathways of Trihalomethane Formation from the Halogenation of Dihydroxyaromatic Model Compounds for Humic Acid, Environmental Science and Technology, 17, 202-211.

Buxton, G. V., Greenstock, C. L., Helman, W. P., Ross, A. B., 1988. Critical Review of Rate Constants for Reactions of Hydrated Electrons, Hydrogen Atoms, and Hydroxyl Radicals in Aqueous Solutions, Journal of Physical Chemistry Reference Data, 17, 513-886.

Capar, G., Yetis, U., 2002. Removal of THM Precursors by GAC: Ankara Case Study, Water Research, 36, 1379-1384.

Chemat, F., Teunissen, P.G.M., Chemat, S., Bartels, P.V., 2001. Sono-oxidation Treatment of Humic Substances in Drinking Water, Ultrasonics Sonochemistry, 8, 247-250.

Cheung, H.M., Bhatnagar, A., Jansen, G., 1991. Sonochemical Destruction of Chlorinated Hydrocarbons in Dilute Aqueous Solution, Environmental Science and Technology, 25, 8, 1510-1512.

Courbat, R., Ramseier, S., Walther, J.L., Gaille, P., Jordan, R., Kaiser, H.P., Revelly, P., Stettler, R., von Gunten, U., 1999. Utilisation de l'ozone pour traitement des eaux potables in Suisse, Gas Wasser Abwasser, 79, 843-852.

Dewulf, J., van Langenhove, H., De Visscher, A., Sabbe, S., 2001. Ultrasonic Degradation of Trichloroethylene and Chlorobenzene at Micromolar Concentrations: Kinetics and Modelling, Ultrasonics Sonochemistry, 8, 143-150.

Donnermair, M.M., Blatchley III, E.R., 2003. Disinfection Efficacy of Organic Chloramines, Water Research, 37, 1557-1570.

Duong, H.A., Berg, M., Hoang, M.H., Pham, H.V., Gallard, H., Giger, W., von Gunten, U., 2003. Trihalomethane Formation by Chlorination of Ammonium and Bromide Containing Groundwater in Water Supplies of Hanoi, Vietnam, Water Research, 37, 3242-3252.

El-Shafy, M.A., Grunwald, A., 2000. THM Formation in Water Supply in South Bohemia, Czech Republic, Water Research, 34, 13, 3453-3459.

Faid, F., Contamine, F., Wilhelm, A.M., Delmas, H., 1998. Comparison of Ultrasound Effects in Different Reactors at 20 kHz, Ultrasonics Sonochemistry, 5, 119-124.

Gallard, H., von Gunten, U., 2002. Chlorination of Natural Organic Matter: Kinetics of Chlorination and of THM Formation, Water Research, 36, 65-74.

Garcia-Villanova, R.J., Garcia, C., Gomez, J.A., Garcia, M.P., Ardanuy, R., 1997. Formation, Evolution and Modeling of Trihalomethanes in the Drinking Water of A Town: I. At the Municipal Treatment Utilities, Water Research, 31, 1299-1308.

Gogate, P.R., 2003. Sonochemical Reactors for Waste Water Treatment: Comparison Using Formic Acid Degradation As a Model Reaction, Advances in Environmental Research, 7, 283-299.

Gong, H., Wang, H., You, H., Zou, H., Shen, X., 2005. Molecular Structure of a New Chlorinated Disinfection By-product in Drinking Water, Journal of Molecular Structure, 748, 71-76.

Gonze, E., Fourel, L., Gonthier, Y., Boldo, P., Bernis, A., 1999. Wasterwater Pretreatment with Ultrasonic Irradiation to Reduce Toxicity, Chemical Engineering Journal, 73, 93-100.

Goskonda, S., Catallo, W.J., Junk, T., 2002. Sonochemical Degradation of Aromatic Organic Pollutants, Waste Management, 22, 351-356.

Haag, W.R., Yao, C.C.D., 1992. Rate Constants for Reaction of Hydroxyl Radicals with Several Drinking Water Contaminants, Environmental Science and Technology, 26, 1005-1013.

Henglein, A., Fischer, C.H., 1984. Sonolysis of Chloroform, Ber. Bunsenges. Phys. Chem., 88, 1196-1199.

Hoffmann, M.R., Hua, I., Hochemer, R., 1996. Appication of Ultrasonic Irradiation for the Degradation of Chemical Contaminants in Water, Ultrasonics Sonochemistry, 3, S163-S172.

Hua, I., Hoffmann, M.R., 1996. Kinetics and Mechanism of the Sonolytic Degradation of $CCl_4$: Intermediates and Byproducts, Environmental Science and Technology, 30, 864-871.

Hua, I., Thompson, J.E., 2000. Inactivation of Escherichia Coli by Sonication at Discrete Ultrasonic Frequencies, Water Research, 34, 15, 3888-3893.

Huang, W.J., Fang, G.C., Wang, C.C., 2005. The Determination of Disinfection By-products from Ozonation of Polluted Raw Water, Science of the Total Environment, 345, 261-272.

Ince, N.H., Belen, R., 2001. Aqueous Phase Disinfection with Power Ultrasound: Process Kinetics and Effect of Solid Catalysts, Environmental Science and Technology, 35, 1885-1888.

Ince, N.H., Tezcanli, G., Belen, R.K., Apikyan, I.G., 2000. Ultrasound as a Catalyzer of Aqueous reaction Systems: The State of the Art and Environmental Applications, Applied Catalysis B: Environmental, 766, 1-10.

Ince. N.H., Tezcanli-Guyer, G., 2004. Individual and Combined Effects of Ultrasound. Ozone and UV Irradiation: A Case Study with Textile Dyes, Ultrasonics, 42, 603-609.

Kavanough, M.C., Trussell, A.R., Cromer, J., Trussell, R.R., An Empirical Kinetic Model of THM Formation: Applications to Meet the Proposed THM Standarts, Journal of American Water Works Association, 72, 578-582.

Keck, A., Gilbert, E., Koster, R., 2002. Influence of Particles on Sonochemical reactions in Aqueous Reactions, Ultrasonics, 40, 661-665.

Kıdak. R., 2005. Use of Ultrasound and/or Other Advanced Oxidation Techniques for Environmental Remediation, Ph.D Thesis, Bogazici University. Institute of Environmental Sciences.

Klassen, N.V., Marchington, D., McGowan, H.C.E., 1994. $H_2O_2$ Determination by the $I^{-3}$ Method and by the $KMnO_4$ Titration, Analytical Chemistry 66, 2921-2925.

Kojima, Y., Fujita, T., Ona, E.P., Matsuda, H., Koda, S., Tanahashi, N., Asakura, Y., 2005. Effects of Dissolved Gas Species on Ultrasonic Degradation of (4-chloro-2-methylphenoxy) Acetic Acid (MCPA) in Aqueous Solution, Ultrasonics Sonochemistry, 12, 359-365.

Landi,S., Naccarati, A., Ross, M.K., Hanley, N.M., Dailey. L., Devlin, R.B., Vasquez, M., Pegram, R.A., DeMarini, D.M., 2003. Induction of DNA Strand Breaks by Trihalomethanes in Primary Human Lung Ephitelial Cells, Mutation Research, 538, 41-50.

Larson, R.A, Rockwell, A., 1979. Chloroform and Chlorophenol Production by Decarboxylation of Natural Acids During Aqueous Chlorination, Environmental Science and Technology, 13, 325-329.

Linek, V., Sinkule, J., Janda, V., 1998. Design of Packed Aeration Towers to Strip Volatile Organic Contaminants from Water, Water Research, 32, 1264-1270.

Luche, J.L., Bianchi, C., Chanon, M., Cintas, P., Cordemans, E., Fillion, H., Lepoint, T., Lepoint-Mullie, F., Loupy, A., Mason, T.J., Petrier, C., Ragaini, V., Walton, D., 1998. Synthetic Organic Sonochemistry, Plenum Press, New York, ISBN 0-306-45916-7.

Malliarou, E., Collins, C., Graham, N., Nieuwenhuijsen, M.J., 2005. Haloacetic Acids in Drinking Water in the United Kingdom, Water Research, 39, 2722-2730.

Margulis, M.A., 1995. Sonochemistry and Cavitation, Gordon and Breach Publishers, ISBN 2-88124-849-7.

Mason, T.J., 1990. Chemistry with Ultrasound, Critical Reports on Applied Chemistry Volume 28, Published for the Society of Chemical Industry, Elsevier Applied Science, ISBN 1-85166-422-X.

Mason, T.J., 1999. Sonochemistry: Current Uses and Future Prospects in the Chemical and Processing Industries, Phil. Trans. R.Soc. Lond. A., 357, 355-369.

Mason T.J., and Cordemans, E., 1998. Practical Considerations for Process Optimization, Synthetic Organic Chemistry, ISBN 0-306-45916-7.

Mason, T.J., Lorimer, J.P., 2002. Applied Sonochemistry, Wiley-VCH Verlag GmbH, ISBN 3-527-30205-0.

McCulloch, A., 2003. Chloroform in the Environment: Occurrence, Sources, Sinks and Effects, Chemosphere, 50, 1291-1308.

Meulemans, C.C.E., 1987. Basic Principles of UV-Disinfection of Water, Ozone Science and Engineering, 9, 299-314.

Microbics Corporation, 1992. Microtox Manual, A Toxicity Testing Handbook, Carlsbad, CA.

Morris, J.C., 1975. The Chemistry of Aqueous Chlorine in Relation to Water Chlorination, Proceedings of the Conference on the Environmental Impact of Water Chlorination, 27-41.

Naffrechoux, E., Combet, E., Fanget, B., Petrier, C., 2003. Reduction of Chloroform Formation Potential of Humic Acid by Sonolysis and Ultraviolet Irradiation, Water Research, 37, 1948-1952.

Nagata, Y., Hirai, K., Bandow, H., Maeda, Y., 1996. Decomposition of Hydroxybenzoic and Humic Acids in Water by Ultrasonic Irradiation, Environmental Science and Technology, 30, 1133-1138.

Neppiras, E. A., 1980. Acoustic Cavitation Thresholds and Cyclic Processes, Ultrasonics, 18, 201-209.

Noltingk, B. E., Neppiras, E. A., 1950. Cavitation Induced by Ultrasonics, Proceedings of Physical Society, B63, 674-678.

Norwood, D.L., Johnson, J.D., Christman, R.F., Hass, J.R., Bobenrieth, M.J., 1980. Reactions of Chlorine with Selected Aromatic Models of Aquatic Humic Material, Environmental Science and Technology, 14, 2, 187-190.

OI Analytical, 2002. Model 4560 Sample Concentrator Operator's Manual, Texas, USA.

Peters, D., 2001. Sonolytic Degradation of Volatile Pollutants in Natural Groundwater: Conclusions from a Model Study, Ultrasonics Sonochemistry, 8, 221-226.

Peters, C.J., Young, R.J., Perry, R., 1980. Factors Influencing the Formation of Haloforms in the Chlorination of Humic Materials, Environmental Science and Technology, 14, 1391-1395.

Petrier, C., Francony, A., 1997. Ultrasonic Wastewater Treatment: Incidence of Ultrasonic Frequency on the Rate of Phenol and Carbon Tetrachloride Degradation, Ultrasonics Sonochemistry, 4, 295-300.

Qualls, R.D., Johnson, J.D., 1983. Bioassay and Dose Measurement in UV Disinfection, Applied Environmental Microbiology. 45, 872-877.

Richardson, S.D., Thruston Jr.A.D., Caughran, T.V., Chen, P.H., Collette, T.W., Floyd, T.L., 1999. Identification of New Ozone Disinfection By-products in Drinking Water, Environmental Science and Technology, 33, 3368-3377.

Richardson, S.D., 2003. Disinfection By-products and Other Emerging Contaminants in Drinking Water, Trends in Analytical Chemistry, Vol. 22, No. 10,

Rook J.J., 1974. Formation of Haloforms During Chlorination of Waters, Water Treatment and Examination 23, 234.

Sawyer, C.N., McCarty, P.L., 1978. Chemistry for Environmental Engineering, McGraw-Hill, ISBN 0-07-054971-0.

Shemer, H., Narkis, N., 2004. Mechanisms and Inorganic Byproducts of Trihalomethane Compounds Sonodegradation, Environmental Science and Technology, 38, 4856-4859.

Shemer, H., Narkis, N., 2005a. Sonochemical Removal of Trihalomethanes from Aqueous Solutions, Ultrasonics Sonochemistry, 12, 495-499.

Shemer, H., Narkis, N., 2005b. Trihalomethanes Aqueous Solutions Sono-oxidation, Water Research, 39, 2704-2710.

Shemer, H., Narkis, N., 2005c. Effect of Various Reaction Parameters on THMs Aqueous Sonolysis, Chemosphere, 59, 1317-1321.

Silverstein, RMC, Bassler, GC, Morrill, TC, 1991. Spectrophotometric Identification of Organic Compounds, Wiley, New York, ISBN 0471-63404-2.

Simmons, J.E., Richardson, S.D., Speth, T.F., Miltner, R.J., Rice, G., Schenck, K.M., HunterIII, E.S., Teuschler, L.K., 2002. Development of a Research Strategy for Integrated Technology-Based Toxicological and Chemical Evaluation of Complex Mixtures of

Drinking Water Disinfection By-products, Environmental Health Perspectives, Vol. 110, Suppl. 6, 1013-1024.

Singh, N. P., Graham, M. M., Singh, V., Khan, A. 1995. Induction of DNA Single-strand Breaks in Human Lymphocytes by Low Doses of γ-rays, International Journal of Radiation Biology, 68, 563–569.

Sivakumar, M., Pandit, A.B., 2001. Ultrasound Enhanced Degradation of Rhodamine B: Optimization with Power Density, Ultrasonics Sonochemistry, 8, 233-240.

Snoeyink, V.L., Jenkins, D., 1980. Water Chemistry, Wiley and Sons, ISBN 0-471-05196-9.

Sorlini, S., Collivignarelli, C., 2004. Trihalomethane Formation during Chemical Oxidation with Chlorine, Chlorine Dioxide and Ozone of Ten Italian Natural Waters, Desalination, 176, 103-111.

Stevens, A.A., Slocum, C.J., Seeger, D.R., Robeck, C.B., 1976. Measurement of THM and Precursor Concentration Changes, Journal of American Water Works Association, 68, 546-554.

Suslick, K.S., 1997. Sonoluminescence and Sonochemistry, Proceedings of IEEE Symp. Vol., 1, 523-532.

Suslick, K.S., 1990. Sonochemistry, Science, 247, 1439-1445.

Suslick, K.S., Hammerton, D.A., Cline, R.E. Jr., 1986. The Sonochemical Hot Spot, Journal of American Chemical Society, 108, 5641-5642.

Symons, T.M., Stevens, A.A., 1981. Treatment Techniques for Controlling Trihalomethanes in Drinking Water, EPA/600/2-81/156.

Tang, W.Z., Tassos, S., 1997. Oxidation Kinetics and Mechanisms of Trihalomethanes by Fenton's Reagent, Water Research, 31, 1117-1125.

Tchobanoglous, G, Burton, F.L., 1991. Wastewater Engineering; Treatment, Disposal and Reuse, McGraw-Hill, ISBN 0-07-041690-7.

Tchobanoglous, G., Schroeder, E.D., 1985. Water Quality; Characteristics, Modeling, Modification, Addison Wesley Publishing Company, ISBN 0-201-05433-7.

Tezcanli Güyer. G., 2003. Degradability of Synthetic Dyestuff by Acoustic Cavitation: Impacts of System Conditions and Physical/Chemical Agents, Ph.D Thesis, Bogazici University, Institute of Environmental Sciences.

Thompson, J. A., Blatchley, E. R., 2000. Gamma irradiation for inactivation of C. parvum, E. coli, and Coliphage MS-2, Journal of Environmental Engineering, 126, 761-768

Toroz, I., Uyak, V., 2005. Seasonal Variations of Trihalomethanes (THMs) in Water Distribution Networks of Istanbul City, Desalination, 176, 127-141.

Urano, K., Wada, H., Takemasa, T., 1983. Empirical Rate Equation for Trihalomethane Formation with Chlorination of Humic Substances in Water, Water Research, 17, 1797-1802.

Ullerstam, M., Langer, S., Ljunstrom, E., 2000. Gas Phase Rate Coefficients and Activation Energies for the Reaction of Butanal and 2-methyl-propane with Nitrate Radicals, International Journal of Chemical Kinetics, 32, 294-303.

USEPA (US Environmental Protection Agency), Toxicological Review of Chloroform (CAS No. 67-66-3). In Support of Summary Information on The Integrated Risk Information System (Iris), Report No. EPA/635/R-01/001.

USEPA, 1988. Methods for the Determination of Organic Componds in Drinking Water, EPA/600/4-88/039.

USEPA, 2001. Low Pressure Membrane Filtration for Pathogen Removal: Application, Implementation, and Regulatory Issues, USEPA, Office of Water, EPA 815-C-01-001.

Uyak, V. 2006. Multi-pathway Risk Assessment of Trihalomethanes Exposure in Istanbul Drinking Water Supplies, Environment International, 32, 12-21.

Von Gunten, U., 2003. Ozonation of Drinking Water: Part II. Disinfection and By-product Formation in Presence of Bromide, Iodide or Chlorine, Water Research, 37, 1469-1487.

Wayment, D.G., Casadonte. D.J., 2002. Frequency Effect on the Sonochemical Remediation of Alachlor, Ultrasonics Sonochemistry, 9, 251-257.

Weavers, L.K., Ling, F.H., Hoffmann, M.R., 1998. Aromatic Compound Degradation in Water Using a Combination of Sonolysis and Ozonolysis, Environmental Science and Technology, 32, 2727-2733.

Wegelin, W., Canonica, S., Mechsner, K., Fleischmann, T., Pesaro, F., Metzler, A., 1994. Solar Disinfection: Scope of the Process and Analysis of Radiation Experiments, Aqua, 43, 154-169.

Westerhoff, P., Chao, P., Mash, H., 2004. Reactivity of Natural Organic Matter with Aqueous Chlorine and Bromine, Water Research, 38, 1502-1513.

Williams, D.T., LeBel, G.L., Benoit, F.M., 1997. Disinfection By-products in Canadian Drinking Water, Chemosphere, 34, 299-316.

Yanagida, H., Masubuchi, Y., Minagawa, K., Ogata, T., Takimoto, J., Koyama, K., 1999. A Reaction Kinetics Model of Water Sonolysis in the Presence of a Spin-Trap, Ultrasonics Sonochemistry, 5, 133-139.

Yoo, Y.E., Takenaka, N., Bandow, H., Nagata, Y., Maeda, Y., 1997. Characteristics of Volatile Fatty Acids Degradation in Aqueous Solution by the Action of Ultrasound, Water Research, 31, 1532-1535.